A New Communication Scheme Implying Amplitude Limited Inputs and Signal Dependent Noise: System Design, Information Theoretic Analysis and Channel Coding

by

Ahmad ElMoslimany

A Dissertation Presented in Partial Fulfillment
of the Requirements for the Degree
Doctor of Philosophy

Approved November 2015 by the
Graduate Supervisory Committee:

Tolga M. Duman, Chair
Antonia Papandreou-Suppappola
Cihan Tepedelenlioglu
Oliver Kosut

ARIZONA STATE UNIVERSITY

December 2015

ABSTRACT

I propose a new communications scheme where signature signals are used to carry digital data by suitably modulating the signal parameters with information bits. One possible application for the proposed scheme is in underwater acoustic (UWA) communications; with this motivation, I demonstrate how it can be applied in UWA communications. In order to do that, I exploit existing parameterized models for mammalian sounds by using them as signature signals. Digital data is transmitted by mapping vectors of information bits to a carefully designed set of parameters with values obtained from the biomimetic signal models. To complete the overall system design, I develop appropriate receivers taking into account the specific UWA channel models. I present some numerical results from the analysis of data recorded during the Kauai Acomms MURI 2011 (KAM11) UWA communications experiment.

It is shown that the proposed communication scheme results in approximate channel models with amplitude-limited inputs and signal-dependent additive noise. Motivated by this observation, I study capacity of amplitude-limited channels under different transmission scenarios. Specifically, I consider fading channels, signal-dependent additive Gaussian noise channels, multiple-input multiple-output (MIMO) systems and parallel Gaussian channels under peak power constraints.

I also consider practical channel coding problems for channels with signal-dependent noise. I consider two specific models; signal-dependent additive Gaussian noise channels and Z-channels which serve as binary-input binary-output approximations to the Gaussian case. I propose a new upper bound on the probability of error, and utilize it for design of codes. I illustrate the tightness of the derived bounds and the performance of the designed codes via examples.

To my dear family

ACKNOWLEDGMENTS

First and foremost I wish to thank my advisor and mentor, professor **Tolga M. Duman** for his continuous support of my Ph.D study and related research. His patience, motivation, and immense knowledge are one of the main reasons that helped me in all the time of research and writing of this thesis.

I would like to thank the National Science Foundation for funding parts of this research under the grants NSF-CCF 1117174 and NSF-ECCS 1102357.

Also, I would like also to thank professor **Cihan Tepedelenlioglu**, professor **Antonia Papandreou-Suppappola**, and professor **Oliver Kosut** for being part of my committee, thesis readers. Their invaluable comments were really helpful.

I wish to thank my lab mates **Ahmad Salim**, **Shahrouz Sharifi**, and **Ahmed Ewaisha**, without them I would not have unforgettable memories. We went through a lot of academic and non-academic discussions, they were really inspirational.

I have special friends to thank, friends who were there for me through good and bad times. I cannot imagine my whole life without them, I am really lucky to know them. I will write only their names; my words will not help me writing about them. **AbdelRahman**, **Ehab Alfarkh**, **Omar Habib**, **Ahmed Osama**, **Ahmedin**, **Aziz Abuwandi**, **Mohsen, Shalaan**.

I finish with **Egypt**, where the most basic source of my life energy resides: **my family**. I have an amazing family, unique in many ways. Their support has been unconditional all these years; they have given up many things for me to be here; they have cherished with me every great moment and supported me whenever I needed it. And I need to thank them in Arabic right now ..

أبى و أمى، أكتب إليكما بقلب دامع لإشتياقى لكما و إحتياجى لرؤيتكما بوجوه تعلوها إبتسامة السعاده و الفخر و سلوانى يقينى بفرحتكما الغير متناهية. فى البداية أود أن أعتذر لكما فكلماتى قد لا تسعفنى للتعبير عن جزيل شكرى و عرفانى لفضلكما على. أشكركم بشده، فلولاكم لما أنهيت هذا العمل و ما كنت لأبدأ. أتذكر يا أمى اللحظات التى كنت على شفا أن أتوقف عن إستكمال دراساتى العليا و أتذكر أيضاً رفضك الشديد و معارضتك التى هدتنى لإتخاذ القرار الذى أعتقد أنه القرار الصائب. أشكرك بشده. أبى العزيز، أشكرك على المسانده الدائمه و دعمك و ثقتك الغاليه، فأنت من لم ينسانى فى أجمل لحظات الفرح و أقسى لحظات المرض. أشكركم على تحملكم الصعاب من أجلى و ما أصعب من لحظات فراقكما و أتمنى أن يسعفنى الوقت لأرد لكما الجميل.

أخواتى و أخوانى، إسلام، هشام، دينا، ياسمين، يوسف. أشكركم على ثقتكم، حبكم و دعمكم الدائم لى.

عبد الرحمن، رب أخ لم تلده أمك، فتعريف الصديق ملخصٌ فيك. أشكرك على كل ما قدمته، لم و لن أنسى مساندتك الدائمه و تشجيعك لى من اليوم الأول و ها أنا يا صديقى قد أنهيت ما إتفقنا على إنهائه و لتذكر مقولتى "المصائر المشتركه".

TABLE OF CONTENTS

CHAPTER Page

CHAPTER Page

LIST OF TABLES

LIST OF FIGURES

Figure Page

Figure Page

However, the common flaw among the humans is to see the hardest stuff like the most beautiful things. And most of the people believe that they do not learn anything when they find a clear and simple reason. While they accept the deep and transcendental theories made by the philosophers, even if it was often on basis that was not been sufficiently examined.

Chapter 1

INTRODUCTION

In this dissertation, we propose a new communication scheme where signature signals are used to carry digital data by modulating the parameters of these signals with transmitted bits. For that purpose, we utilize analytical models for certain types of signature signals which are parametrized. Digital data is transmitted by mapping the vectors of information bits to the parameters of these signature signals. At the receiver side, a reverse process is utilized: the parameters of the received signals are estimated, and are demapped back to the information bits.

One possible application for the proposed communication scheme is in underwater acoustic (UWA) communications. There are lot of emerging applications that require UWA communications including offshore oil industry, pollution monitoring, scientific data collection, and military use. However, underwater acoustic communications is considered as one of the most challenging communication environments due to the very highly time-varying nature of the communication medium, large distortions due to extensive multipath spreads, frequency-dependent path loss, time variation of the path propagation which causes Doppler shift and spread, and low propagation speed of the sound in the water [4]. In addition to the average path loss due to spreading and absorption losses, the received power fluctuates as a result of small-scale fading effects due to multipath propagation. UWA channels are often characterized by significant frequency and time selectivity, due to variations in the underwater environment (e.g., surface waves) or due to the relative motion between the transmitter and the receiver. Furthermore, since the speed of the sound in water is low, the transmitted signal may also undergo time-scaling (severe Doppler) effects, due to the fact that the carrier frequencies are in the order of the signal bandwidths

used.

UWA communications have evolved over the years; in earlier UWA communications systems, noncoherent detection is considered in order to overcome the rapid variations in the phase of the channels. For instance, frequency shift keying (FSK) with noncoherent detection is used [5]. Using noncoherent receivers solves the transmitted carrier phase recovery problem, however, it does not solve the intersymbol interference (ISI) problem resulting from long delay spreads. One way to overcome the ISI problem is to insert a long guard period between the adjacent transmitted symbols accounting for the spread of the signal during the transmission. However, long guard periods severely reduce the throughput of the system. Differentially coherent transmission schemes are also considered for use in UWA systems [6]. In differentially coherent systems, the information sequence is used to modulate the phase difference or phase transitions between consecutive symbols and hence we do not have to estimate the absolute phase of the carrier signal. However, differentially coherent modulation systems result in performance degradation [7]. Systems based on coherent modulation are first introduced by Stojanovic, Capitovic and Proakis in [8] which demonstrated for the first time the feasibility of phase coherent communications via a decision feedback equalizer (DFE). To enable coherent transmissions, the DFE coefficients are updated along with the carrier phase by minimizing of the mean square error (MSE) in an adaptive fashion. To guarantee that the receiver would be able to track the rapid phase changes, they used the recursive least square (RLS) algorithm [9] to estimate the filter coefficients, this guarantees a fast convergence.

Recently, orthogonal frequency division multiplexing (OFDM) based multicarrier communication schemes have received great attention in UWA communications as well [10, 11], especially, for applications that require high data rates. For

UWA communications, OFDM trades off ISI with intercarrier interference (ICI) due to the highly time varying nature of the communication medium, see, e.g., [12, 13] and references therein. In the last decade, space-time coding techniques (for multi-input multi-output (MIMO) systems) have also been demonstrated successfully for UWA channels [14–17]. Another fundamental line of research in UWA communications is devoted to the time reversal (TR) techniques [18–25], in which the reciprocity of the UWA channel between the transmitter and the receiver is exploited.

In this dissertation, we utilize analytical models for certain biomimetic signals characterized by certain parameters that distinguish mammalian sound signals. Digital data is transmitted by mapping vectors of information bits to a carefully designed set of parameters with values obtained from the biomimetic signal models. To complete the overall system design, we develop appropriate receivers taking into account the specific UWA channel models. The basic premise is the following: since there will be no artificial embedding of digital data on a (biological) host signal, the transmitted signal mimics a natural sound. Such a scenario may have applications in covert communications with low probability of detection (LPD) and low probability intercept (LPI) characteristics.

In our proposal of using natural sounds for signal transmission, where digital data modulates the parameters of carefully modeled biomimetic signals, our approach provides a way for which signals generated do not sound artificial due to the way in which they are constructed. In other words, signals matched to mammal sounds could be useful for UWA communications even at relatively high transmit power levels. They can also co-exist with other acoustic communication systems without adversely affecting their performance or without being affected by them. Our proposal, as in two very recent papers [26, 27], aims to incorporate biological sounds in UWA

communications systems, however, the specific approach used is completely different.

One of the main challenges that confronts the design of the proposed scheme is the choice of the set of parameters. As we described before, the digital information is transmitted by mapping the transmitted information bits to a carefully designed set of parameters of the biological signals. The problem now lies on the methodology of the design of the signal parameters. Motivated by this problem and using the capacity as the ultimate performance metric, we study the information capacity of the equivalent channel model for the proposed communications scheme. We optimize the input distribution to decide on the specific values of the signal parameters to pick and their probabilities.

As we will see later, an equivalent channel model for the system shows that the estimated values of the parameters can be approximated as the actual transmitted values of the parameters contaminated by signal dependent Gaussian noise. This approximation is based on the asymptotic behavior of the maximum likelihood (ML) estimator which indicates that the estimated parameter—when the length of the received signal is sufficiently large—is distributed according to a Gaussian distribution with mean equal to the true value and variance which can be found from the inverse of the Fisher information matrix which depends on the transmitted signal parameters. Given the fact that the parameters have a specific range that can be used, the capacity optimization problem boils down to the capacity optimization problem of a Gaussian channel with amplitude-limited inputs and signal-dependent noise.

Capacity of Gaussian channels with peak and average power constraints is first studied by Smith [28] where he shows that under these constraints on the input the capacity-achieving distribution is discrete. His approach is based on two propositions: the first one shows that the mutual information function is a strictly concave, weakly

differentiable function of the input probability distribution function, and the space of probability distribution functions is convex and compact in some topology. The second proposition shows that the optimal distribution that achieves the capacity is discrete utilizing ideas from complex analysis. Finding the mass point locations of this discrete distribution and its associated probabilities is done through a numerical convex optimization algorithm, as the problem is reduced to a finite-dimensional problem. Tchamkerten [29] extends Smith's results on channel capacity with amplitude limited inputs to general additive noise channels, and he derives sufficient conditions on the noise probability density functions that guarantee that the capacity-achieving input has a finite number of mass points.

Discrete input distributions show up as the optimal inputs in other scenarios as well. For instance, the authors in [30] study the quadrature Gaussian channel, and they show that a uniform distribution of the phase and discrete distribution of the amplitude achieve the channel capacity. In [31], the authors consider transmission over Rayleigh fading channels where neither the transmitter nor the receiver has the channel state information. They prove that the capacity achieving distribution for average power-constrained inputs is discrete. Also, in [32], the authors study the non-coherent additive white Gaussian noise (AWGN) channels and they show that the optimal distribution is discrete. By characterizing the capacity-achieving distribution, they also compute a tight lower bound on the capacity of the channel based on examination of suboptimal input distributions. In [33], the authors investigate the capacity of Rician fading channels with inputs that have constraints on the second and the forth moments, and the capacity-achieving distribution is shown to be discrete with finite number of mass points. In addition, they study channels with peak power constraints and show that the optimal distribution is discrete as well. Recently, multi-user systems with amplitude-limited inputs have also been considered. The authors

in [34] develop a framework at which the channel capacity is maximized by a unique distribution and this distribution features finite number of mass points, they show that there are many systems that fall within their framework such as parallel Gaussian channels, intensity modulation optical channels, etc. In [35, 36], the authors study the multiple access channel (MAC) with amplitude-constrained inputs. They show that the sum-capacity achieving distribution is discrete. This distribution achieves rates at any of the corner points of the capacity region.

In this dissertation, we study the capacity of several channels that include signal-antenna systems such as fading channels, and signal-dependent Gaussian noise channels. We also study the capacity of multiple-antenna systems that include general multiple-input multiple-output (MIMO) channels and parallel Gaussian channels. Finally, we study the code design problem for signal-dependent Gaussian noise channels and BAC which considered as binary-input binary-output approximation for the signal-dependent Gaussian noise channels.

A BAC and a binary symmetric channel (BSC) are quite different, for instance, the capacity-achieving distribution for a BSC is uniform which is not the case for a BAC. The differences between the BSC and the BAC make the design of channel codes quite distinct. One of the main ideas that has been developed for channel coding over binary asymmetric channels is through the use of a mapper, i.e., a mapper is introduced after a channel encoder designed for a BSC, and at the decoder side, an iterative algorithm that takes the mapper into account is employed [38]. As another approach, in [39], the authors introduce a new class of codes referred as group-theoretic codes, and they prove that this class of codes are able to correct one bit error that may occur during transmission. In [40], a new density evolution technique is derived for optimization of the low density parity check (LDPC) codes.

In [41], the authors propose two methods for code construction; the first one is based on codebook expurgation where the goal is to alter the binary codebook such that the resulting input distribution for the channel becomes nonuniform. The second construction method is based on introducing a mapper after the encoder. This mapper is from a non-binary linear block code into a binary codebook keeping in mind the same objective which is to have a biased (optimal) input distribution. In [42], the authors present new constructions of codes for asymmetric channels for both binary and nonbinary alphabets, based on methods of generalized code concatenation. Recently, different classes of ultra-small finite block-length codes are introduced, called flip codes and weak flip codes [43, 44]. In these papers, the authors introduce another approach to the code design problem referred as the column-based approach. They define set of columns called candidates and the code is constructed by taking combinations of these columns. The authors show the optimality of these codes for the BSC and the Z-channel (binary channel at which one of the cross-over probabilities is zero) when the number of messages is less than four. They also introduce a recursive approach to design codes with large number of messages but the optimality of the modified approach is not established.

In the last part of the dissertation, we focus our study on special classes of codes called ultra-small codes. This class of codes appears in many communication scenarios as viable solutions, e.g., in the initiation of communication links in which we have a small number of messages to be transmitted, also in applications that are so sensitive to delay which do not tolerate transmission of long blocks. Thus, we are interested in using the channel for a limited time, and transmitting all the required information within one signal duration. Considering also the reliability requirements leads to channel codes with a small number of messages and limited block lengths. The study of ultra-small block-codes is interesting not only because of its potential

applications, but also because of their analytical description which is a first step to a better fundamental understanding of optimal nonlinear coding schemes (with ML decoding).

1.1 Contributions of the Dissertation

In Chapter 2, we propose a new communication scheme that uses biological signals to carry the digital information. We show the system model and the receiver design for both AWGN channels and multi-path channels. To validate the proposed communications scheme, we present some numerical results from the analysis of the recorded data during the recent KAM11 experiment. The results show that we can successfully decode the transmitted bits with a relatively low bit error probability under different transmission rates. We also present some numerical examples to show the robustness of the proposed scheme agains interference.

In Chapter 3, we study the capacity of point-to-point amplitude-limited fading channels. We assume that the channel gains are real, have finite support and are known at the receiver. We show that a unique optimal input distribution exists and this optimal distribution is discrete with a finite number of mass points. We prove the result by showing that the conditional mutual information function between the input, output and the channel coefficient is a continuous, strictly concave, and weakly differentiable function of the input distribution. We then we use techniques from complex analysis to establish arguments about the discreteness of the optimal input distribution.

In Chapter 4, we study the capacity of signal-dependent Gaussian channels under amplitude-limited inputs. This model is implied by an equivalent system model to the proposed communication scheme in Chapter 2. This is not the first time signal-dependent noise is considered in the literature as it appears in many communication

scenarios that include optical communications and magnetic recording systems. In a closely related work [34], the authors study the capacity of optical communication channels with intensity modulation for which the noise variance is linearly dependent on the inputs, and show the discreteness of the capacity-achieving distribution. In [66], the authors develop upper and lower bounds on the channel capacity. In this work, we consider an arbitrary noise variance function, and show that the capacity of the signal-dependent Gaussian noise channels with amplitude-limited inputs is achieved by input distribution with a finite number of mass points. We follow similar arguments to the ones followed in Chapter 3; we show that the mutual information is a continuous, concave, and weakly differentiable function of the input distribution, and then use techniques from complex analysis to show that the optimal input distribution has finite number of mass points.

In Chapter 5, we study the capacity of multi-antenna systems with amplitude-limited inputs. Unfortunately, extending the results of Smith to vector random variables is unattainable since the Identity Theorem (one of the main theorems we use to show the discreteness of the capacity-achieving distributions) is only available for one-dimensional functions. Thus, we derive upper and lower bounds on the channel capacity. These bounds are derived for an equivalent channel obtained from the singular value decomposition of the multiple-input multiple-output channel and solving the capacity optimization problem over rectangular regions that inscribe the feasible region (for the upper bound) and rectangular regions that are inscribed by the feasible region (for the lower bound). For the special case of multiple-input single-output (MISO) systems, we are able to compute the capacity as it follows directly from Smith's results by defining an auxiliary variable representing the sum of the channel inputs. We solve the capacity optimization problem between the channel output and this auxiliary variable, and using the solution of this optimization prob-

lem we can generate channel inputs such that the distribution of their sum follows the distribution of the auxiliary random variable. Finally, we study the capacity of parallel Gaussian channels with amplitude-limited and power-limited inputs. We derive analytical bounds on the capacity at low and high noise levels which feature low computational complexity compared to the exact evaluation of the capacity. We then use these upper and lower bound expressions to assign the power for each parallel channel at different noise levels.

Chapter 6 of the dissertation is devoted to the study of the coding problem for signal-dependent Gaussian noise channels, namely we consider practical channel coding problems for the approximate model of the proposed communications scheme in Chapter 2. Specifically, we consider two channel models. The first one uses Gaussian noise channels but with noise variance that depends on the transmitted signal. The second model considers binary asymmetric channels (BACs) which approximate the Gaussian model. We propose a new upper bound on the error probability which is based on Bonferroni type inequalities by considering triplets of pairwise error events. We then use this bound to derive a new metric for designing codes for the Z-channel (a special case of BAC) called the weighted sum Hamming distance. We then use this metric to design specific codes. Our results show that we are able to design codes with low error probabilities for different numbers of messages in the codebook for the case of Z-channels. We also use these codes on signal-dependent Gaussian noise channels, and compare their performance with that of codes designed for BSC.

We finally summarize the contributions of this dissertation in Chapter 7.

Chapter 2

A NEW SIGNALING SCHEME FOR UWA COMMUNICATIONS EXPLOITING BIOLOGICAL SOUNDS

In this chapter, we propose a communication scheme that uses biomimetic signals to transmit digital information. We develop analytical models for certain biomimetic signals and we parametrize them. Digital data is transmitted by mapping vectors of information bits to a carefully designed set of parameters with values obtained from the biomimetic signal models. To complete the overall system design, we develop appropriate receivers taking into account the specific UWA channel models. The basic premise is the following: since there will be no artificial embedding of digital data on a (biological) host signal, the transmitted signal will mimic a natural sound.

As mentioned in Chapter 1, a possible application for the proposed biomimetic communication scheme of this work is for covert UWA communications in which we are interested in low probability of detection (LPD) and/or low probability intercept (LPI). That is, we may be interested in transmitting our signals in such a way that the presence of communication cannot be sensed by eavesdroppers (LPD) and/or cannot be demodulated (LPI) except for intended users. Most existing techniques developed for covert communications rely on spread spectrum ideas. For instance, with the direct sequence spread spectrum (DSSS) techniques, the transmitted signal is spread, using a spreading code, over a certain frequency band such that its power spectral density goes below the noise level which makes it difficult to be detected. At the intended receiver, the spreading code is known, hence the signal is despread and the original transmitted signal is retrieved. The key point in using the DSSS is that as long as the spreading code is long enough, a better performance can be achieved. Different communication schemes have been developed for UWA covert

communications based on spread spectrum techniques [45, 46].

A different approach to provide covertness is based on the use of natural sounds in transmission. The bottlenose dolphin sound signals are used for convert communication, the dolphin whistles are modeled as weighted superpositions of harmonically related sinusoids, and single sinusoidal frequencies are estimated over windowed data; the whistle is assumed to be time-invariant over the window duration [47]. Due to the methodology adopted, the generated signal may sound man-made which may present a problem in using this approach for LPD/LPI communications under water. Two other very recent schemes [26, 27] that use biological sounds for covert communications are presented. In the first one, the authors use dolphin whistles for synchronization purposes, and the time interval between dolphin clicks to convey digital information, while in the second one, DSSS signals which carry digital data are masked with a relatively loud whale sound.

Coming back to our proposal of using natural sounds for signal transmission where digital data is modulated on the parameters of a carefully modelled biological signals, our approach provides a way for which signals generated do not sound artificial due to the way in which they are constructed. In other words, signals matched to mammal sounds could be useful for UWA communications even at relatively high transmit power levels. They can also co-exist with other acoustic communication systems without adversely affecting their performance or without being affected by them. Our proposal, as in two very recent papers [26, 27], aims to incorporate biological sounds in UWA communications systems, however the specific approach used is completely different. A preliminary and brief version of our proposal appeared in the literature [1].

The chapter is organized as follows. In Section 2.1, we develop analytical

models for the biomimetic signals and we provide a parametrization for these models. In Section 2.2, we describe our communication scheme; the signaling scheme, and the receiver structure for additive white Gaussian noise (AWGN) channels and multipath channels, respectively. In Section 2.3, we provide a brief performance analysis for the proposed communication system and derive bounds on error rates. In Section 2.4, we present a detailed set of experimental results demonstrating the feasibility of the proposed communication scheme using data recorded in the KAM11 experiment. We conclude the chapter with a brief summary in Section 2.5.

2.1 Biomimetic Signal Modeling

In this section, we utilize some of the existing models for the biomimetic signals from the literature. The underwater acoustic communications channel has been shown to cause nonlinear time-varying changes to the instantaneous frequency of a waveform. Thus, we define nonlinear frequency-modulated (NFM) signals as [1, 48, 49],

$$s(t;\mathbf{b}) = A\,\alpha(t)\,e^{j2\pi(c\,\xi(t/t_r)+f_0 t)} \tag{2.1}$$

where $\xi(t/t_r)$ is the signal's phase function, f_0 is the carrier frequency, A is the amplitude, $c \in \mathbb{R}$ is the frequency modulation (FM) rate, and $t_r > 0$ is a fixed time constant used for unit normalization. The parameter vector $\mathbf{b}$ of the NFM signal in (1) consists of the FM rate c, amplitude A, phase function $\xi(t/t_r)$ and signal duration T_d. We select $\alpha(t) = \sqrt{|\nu(t)|}$, where $\nu(t)$ is the signal's instantaneous frequency (or derivative of the phase function). Discretizing the real part of the NFM signal using sampling period T_s and $M = \lfloor T_d/T_s \rfloor$ yields

$$s[n;\mathbf{b}] = s(nT_s;\mathbf{b}) \;=\; A\sqrt{|\nu[n]|}\cos(2\pi c\,\xi[n] + 2\pi f_0 T_s n)\,, \quad n \;=\; 0,1,\ldots,M-1\,. \tag{2.2}$$

In Figures 2.1 and 2.2 we show comparison of the spectrogram TFR of an actual long-finned pilot whale whistle and its reconstructed NFM signal with $t_r = 1$.

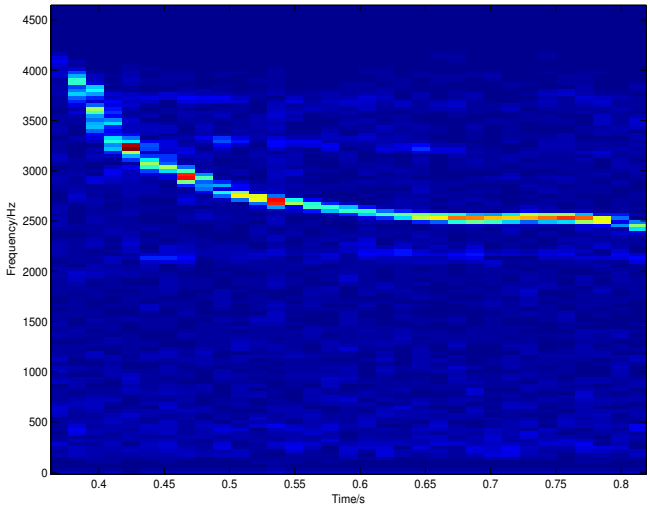

Figure 2.1: Spectrogram TFR of long-finned pilot whale whistle taken from [1].

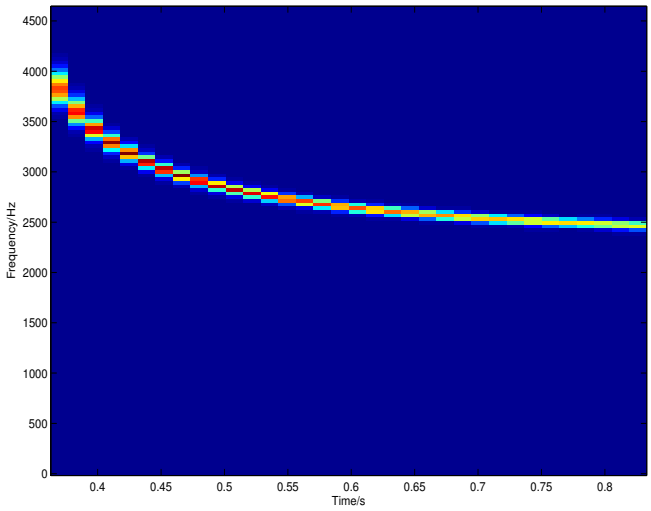

Figure 2.2: Spectrogram TFR of reconstructed noiseless linear FM chirp signal that best matches the time-frequency signature of the whistle taken from [1].

As it can be seen, the time-frequency structure of the whistle and the reconstructed signal are well-matched. Similar results are shown in Figures 2.3 and 2.4 for the whistle of a white-sided dolphin. With models of cetacean mammal sounds developed with appropriate parametrization, we can now propose a new communication scheme

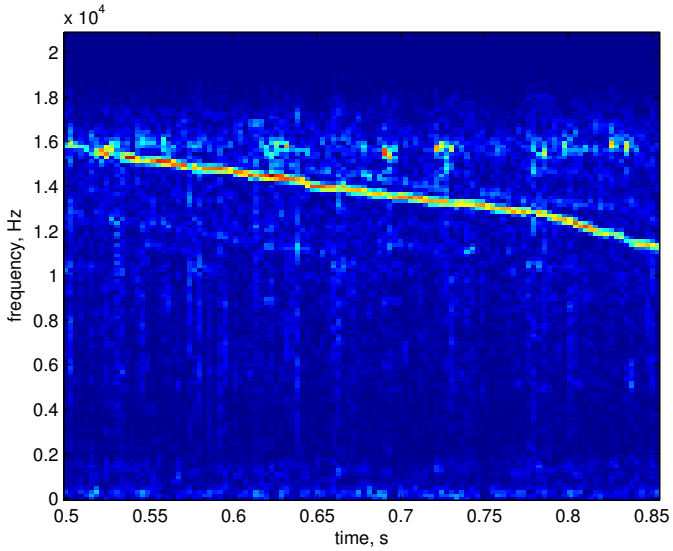

Figure 2.3: Spectrogram TFR of white-sided dolphin whistle taken from [1].

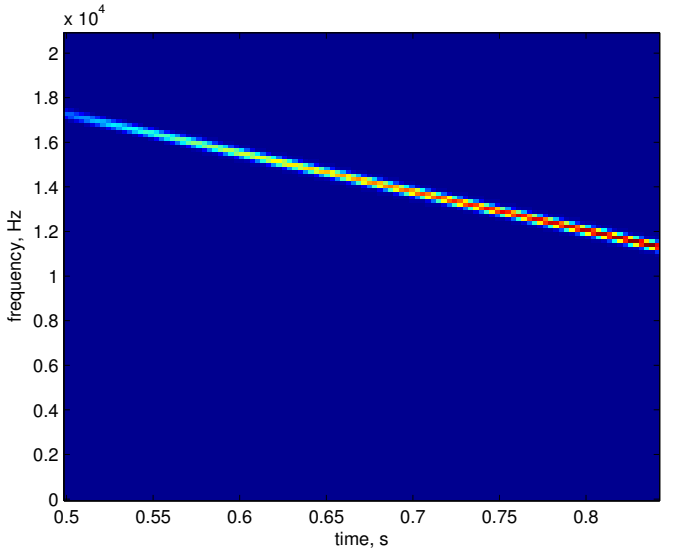

Figure 2.4: Spectrogram TFR of reconstructed noiseless linear FM chirp that best matches the time-frequency structure of the whistle taken from [1].

exploiting such sounds.

2.2 Proposed Communication Scheme

We propose to use a signaling scheme that uses biomimetic signals as the transmission signals that carry digital data. The structure of such signals has been already reviewed in the previous section. Such a communication system may have applications requiring LPI and LPD since these kind of signals sound like other natural sounds that exist in the environment. Specifically, in this paper, we propose to use generalized NFM signals to model the mammal sounds. We first select NFM signals to mimic mammal whistles by matching their TF structures, and then we parametrize this analytical model and we modulate these parameters with our digital data.

The complex envelope of the acoustic NFM signal can be given in the time-domain as

$$\tilde{s}(t;\mathbf{b}) = A\alpha(t)\exp(j2\pi c\xi(t/t_r)), \qquad 0 < t \leq T_d, \tag{2.3}$$

where $\xi(t/t_r)$ is the signal's time-varying phase function (assumed differentiable), and $t_r > 0$ is a normalization time constant. The vector parameter $\mathbf{b}$ contains information about the signal's FM rate $c \in \mathbb{R}$, duration T_d, amplitude $A \in \mathbb{R}$, and phase function $\xi(t/t_r)$. The amplitude modulation $\alpha(t)$ can be changed without affecting the TF of the whistle, and it can be used as another parameter to carry data. As we see from (2.3), we can use the amplitude, the carrier frequency, the chirp rate, and the chirp duration as the parameters that carry our bitstream. At the receiver side, as a practical solution, we develop a maximum likelihood estimator (MLE) to estimate the value of these parameters and decode for the transmitted bits accordingly.

To summarize, a vector $\mathcal{I}$ of information bits will be mapped onto the vector of

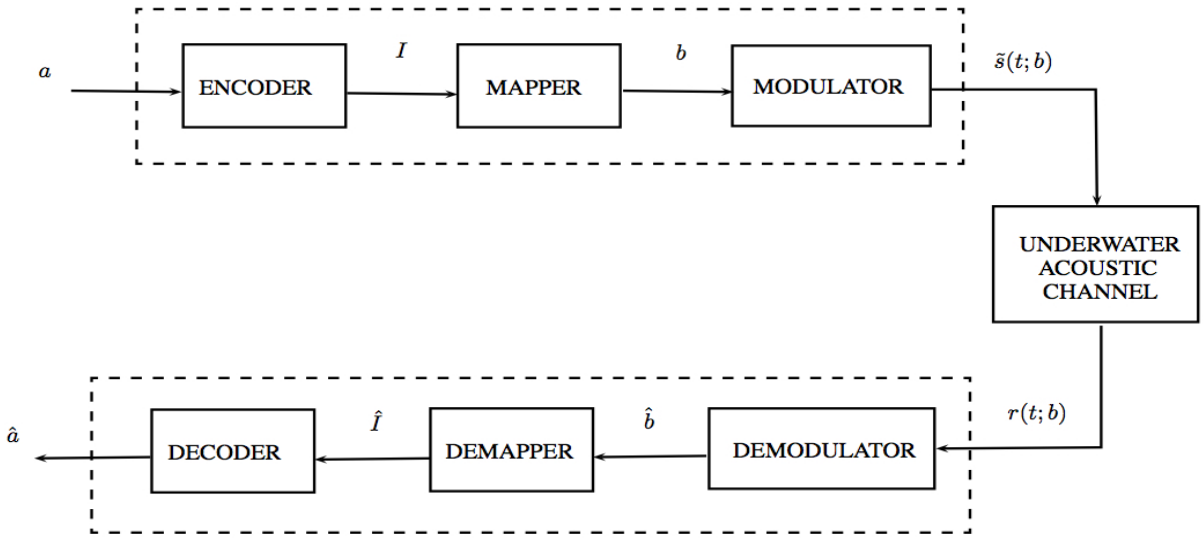

Figure 2.5: Block diagram of the communication system.

parameters $\mathbf{b}$ using a certain mapping rule $f(\mathcal{I})$ that maps between the information bits and the set of signal parameters $\mathcal{C}$. There are several mapping rules that can be considered here, for example, the range of each parameters is divided into 2^n (n is the number of bits) levels then linear mapping is performed between the digital data and the parameter's levels. Then, the acoustic signal $\tilde{s}(t;\mathbf{b})$ is synthesized and transmitted over the channel. At the receiver side, we develop a detector to find an estimate $\hat{\mathbf{b}}$ of the values of these signal parameters. We use a MLE to accomplish this. Finally, a demapping function $f^{-1}(\hat{\mathbf{b}})$ is used to restore the transmitted bits. This process is illustrated using a block diagram shown in Figure 2.5.

2.2.1 Receiver Design for AWGN Channels

In this section, we consider the use of the proposed communication scheme over an AWGN channel. We develop the MLE for the Gaussian channel and we characterize its performance.

We have a sequence of information bits $\mathbf{a}$, we split this information sequence into words each consisting of a given number of bits. We use these consecutive words

to modulate the mammalian sound parameters, i.e., amplitude, phase, and frequency by picking a certain value for these parameters from the set of values specified for each parameter. Upon receiving the signal at the receiver, we find an estimate for the transmitted parameters and demap these estimates into bits according to the demapping rule.

The discrete time version of a real generalized chirp is defined as

$$s[n] = A\sqrt{\nu[n]}\cos\left(2\pi c\xi[n]\right), \qquad n = 0, 1, \ldots, M-1, \tag{2.4}$$

where A is the amplitude of the signal, c is the generalized chirp parameter that controls the shape of the instantaneous frequency, $\xi[n]$ is the frequency modulation function, $\nu[n]$ is the discrete version of the instantaneous frequency $\nu(t) = \frac{d}{dt}\xi(t)$, M is the number of samples that corresponds to the signal duration. We consider the NFM signal in (2.4) as the transmitted chirp signal with parameters A, c, and M that convey the digital bits. The duration of the signal is used as a parameter such that for a fixed interval N, the signal duration varies within this N period. Thus, the received signal can be written as,

$$x[n] = \begin{cases} s[n] + w[n] & \text{if } n = 0, 1, \ldots, M-1, \\ w[n] & \text{if } n = M, \ldots, N-1, \end{cases} \tag{2.5}$$

where $w[n]$ is the AWGN noise with zero mean and variance σ^2.

Before we describe the proposed receiver structure, we note that the optimal solution (to minimize the error probability) is the solution of an $M-$ary hypothesis testing problem where each of the hypotheses corresponds to a particular sequence of bits being packed into the NFM chirp signal. However, the number of bits transmitted with each packet (e.g., dolphin sound) is too many, and hence coming up with the optimal solution becomes problematic (as one would need to consider each of these

M hypotheses, compute their likelihoods and pick the one with the largest value). For instance, when there are 50 bits in a packet, there are a total of 2^{50} different hypotheses making the optimal solution impractical. Therefore, we consider a suboptimal approach to complete the receiver design: using an ML estimator to estimate the signal parameters and then demapping the estimated values into bits.

An MLE [50] of a scalar parameter ϕ is defined as the value of the parameter that maximizes the conditional probability density function (PDF) $p(\mathbf{x};\phi)$ of the sequence $\mathbf{x}$. The maximization is performed over the space constructed by the parameter ϕ. The conditional PDF of the received signal $x[n]$ defined in (2.5) is given by,

$$p(\mathbf{x};A,c,M)=\frac{1}{\left(2\pi\sigma^2\right)^{N/2}}\exp\left[-\frac{1}{2\sigma^2}\left(\sum_{n=0}^{M-1}\left(x[n]-A\sqrt{\nu[n]}\cos\left(2\pi c\xi[n]\right)\right)^2+\sum_{n=M}^{N-1}\left(x[n]\right)^2\right)\right].$$

Thus the ML estimate of the parameters A, c, and M is,

$$\begin{bmatrix}\hat{c}\\ \hat{M}\\ \hat{A}\end{bmatrix}=\underset{\substack{c,M,A\\ c_1\le c\le c_2\\ M_1\le M\le M_2\\ A_1\le A\le A_2}}{\arg\max}\ \frac{1}{\left(2\pi\sigma^2\right)^{N/2}}\exp\left[-\frac{1}{2\sigma^2}\left(\sum_{n=0}^{M-1}\left(x[n]-A\sqrt{\nu[n]}\cos\left(2\pi c\xi[n]\right)\right)^2+\sum_{n=M}^{N-1}\left(x[n]\right)^2\right)\right], \tag{2.6}$$

which is equivalent to

$$\begin{bmatrix}\hat{c}\\ \hat{M}\\ \hat{A}\end{bmatrix}=\underset{\substack{c,M,A\\ c_1\le c\le c_2\\ M_1\le M\le M_2\\ A_1\le A\le A_2}}{\arg\min}\ \left\{\sum_{n=0}^{M-1}\left(x[n]-A\sqrt{\nu[n]}\cos\left(2\pi c\xi[n]\right)\right)^2+\sum_{n=M}^{N-1}\left(x[n]\right)^2\right\}. \tag{2.7}$$

This problem can be reformulated as follows;

$$\begin{bmatrix} \hat{c} \\ \hat{M} \\ \hat{A} \end{bmatrix} = \underset{M, M_1 \leq M \leq M_2}{\arg\min} \left\{ \underbrace{\begin{array}{c} \min \\ {\scriptstyle c, A} \\ {\scriptstyle c_1 \leq c \leq c_2} \\ {\scriptstyle A_1 \leq A \leq A_2} \end{array} \sum_{n=0}^{M-1} \left(x[n] - A\sqrt{\nu[n]} \cos\left(2\pi c \xi[n]\right) \right)^2}_{\text{separate optimization problem}} + \sum_{n=M}^{N-1} \left(x[n]\right)^2 \right\}. \tag{2.8}$$

Thus, for a fixed value of M we can separate the problem into two consecutive problems, one optimizes over the chirp duration and the other optimizes over the other parameters (the chirp rate c and amplitude A), for a specific chirp duration. Therefore, the optimal solution (for the estimation problem) can be obtained by considering all possible values of the signal duration (determined from the particular mapping from bits to parameters adopted), performing the inner optimization for each of these values, and picking the most likely result as the optimal estimates for the three parameters embedded into the signal. Each of the inner optimization problems (optimization of A and c for a given M) involve (as we will see shortly) a one-dimensional grid search which may be costly. Therefore, to reduce the computational burden of the algorithm we propose the following: estimate the A and c values based on the lowest possible value for the signal duration (hence it is guaranteed that the actual signal is present in this window), and then use these estimates search over the parameter M (going over all possibilities). We adopt the latter simplification in our results section. There is another suboptimal solution that can be considered to solve the optimization problem in (2.8) using a simple energy detector followed by a decoder that estimates the other parameters, in other words, changing the order at which the parameters are estimated. Our experimental results show that there is no

significant difference on the system performance by changing the order at which the parameters get estimated, i.e., both simplifications result in similar performance.

For a given chirp duration $\tilde{M}$, we define $r[n] = \sqrt{\nu[n]}\cos\left(2\pi c\xi[n]\right)$, $n = 0, \ldots, \tilde{M}-1$, and the vector of parameters θ

$$\theta = \begin{bmatrix} A \\ c \end{bmatrix}. \tag{2.9}$$

The cost function $g(A, c; \tilde{M})$ is defined as

$$g(A, c; \tilde{M}) = \sum_{n=0}^{\tilde{M}-1} \left(x[n] - A\sqrt{\nu[n]}\cos\left(2\pi c\xi[n]\right)\right)^2 \tag{2.10}$$

$$= \sum_{n=0}^{\tilde{M}-1} \left(x[n] - Ar[n]\right)^2. \tag{2.11}$$

Thus, the solution to the maximum likelihood estimation problem is reduced to

$$\hat{\theta} = \underset{\substack{c,A \\ c_1 \le c \le c_2 \\ A_1 \le A \le A_2}}{\arg\min}\ g(A, c; \tilde{M}). \tag{2.12}$$

To estimate the parameters A and c we need to do a two-dimensional grid search over the given range of both parameters. However, this two-dimensional search can be reduced to a one-dimensional search instead as we are able to find a closed form expression for the optimal estimator of the amplitude given any value of c. That is, for each value of c, the optimal amplitude parameter value can be found by solving the following capacity optimization problem,

$$\hat{A} = \underset{A: A_1 \le A \le A_2}{\arg\min} \sum_{n=0}^{\tilde{M}-1} \left(x[n] - Ar[n]\right)^2. \tag{2.13}$$

the Lagrangian is given by,

$$L(A, \lambda_1, \lambda_2) = \sum_{n=0}^{\tilde{M}-1} \left(x[n] - Ar[n]\right)^2 + \lambda_1(A - A_2) - \lambda_2(A - A_1). \tag{2.14}$$

The resulting KKT conditions are then

$$-2\sum_{n=0}^{\tilde{M}-1}\left(x[n]-Ar[n]\right)r[n]+\lambda_1-\lambda_2=0, \tag{2.15}$$

$$\lambda_1\geq 0,\quad \lambda_2\geq 0,\quad \lambda_1(A-A_1)=0,\quad \lambda_2(A-A_2)=0. \tag{2.16}$$

Define $\hat{A}=\arg\min_{A}\sum_{n=0}^{\tilde{M}-1}\left(x[n]-Ar[n]\right)^2$, thus, an optimal solution for the problem is

$$A^*=\begin{cases}\hat{A} & \text{if } A_1\leq\hat{A}\leq A_2,\\ A_1 & \text{if } \hat{A}<A_1,\\ A_2 & \text{if } \hat{A}>A_2.\end{cases} \tag{2.17}$$

We now study the asymptotic behavior of the MLE for the parameters A and c. Under certain regularity conditions [51], the maximum likelihood estimator has asymptotically (as the number of samples become large) a Gaussian distribution with mean being the true mean and variance-covariance matrix given by the inverse of the Fisher information matrix [50]. These regularity conditions include the following: the true parameter value must be interior to the parameter space, the log-likelihood function must be twice differentiable, the second derivatives must be bounded, the expected value of the log-likelihood function equals zero when the values of the parameters are taken as the true values. It is straightforward to show that the MLE of the vector θ in our case satisfies these conditions, and hence for large number of samples, the estimated vector of parameters $\hat{\theta}$ has a Gaussian distribution

$$\hat{\theta}\sim\mathcal{N}\left(\theta, I(\theta)^{-1}\right), \tag{2.18}$$

where $I(\theta)^{-1}$ is the Fisher Information matrix derived in Appendix A.

2.2.2 Receiver Design for Time-Varying Multipath Channels

We now consider the case of transmission over a time and frequency dispersive channel, which is typical in UWA communications. In this case, the discrete time received

signal can be written as

$$x[n] = \begin{cases} \sum_{l=0}^{L-1} h_l[n]s[n-l] + w[n] & \text{if } n = 0, 1, \ldots, M-1, \ldots, M+L-2 \\ w[n] & \text{if } n = M+L-1, \ldots, N-1, \end{cases} \tag{2.19}$$

where $w[n]$ is an AWGN, and $h_l[n]$ is the time varying channel coefficient at the lth delay pin and the nth instant. We assume that the receiver has an estimate for these channel coefficients. In practice the time varying channel taps can be estimated with some accuracy using known transmitted bits (pilot bits). To accomplish this, we can use one of the common channel estimation techniques for UWA channels, e.g. the matching pursuit (MP) [52, 53] or basis pursuit (BP) [54] algorithms.

The PDF of the received signal for a given set of parameters A, c and M is given by

$$p(\mathbf{x}; A, c, M) = \frac{1}{(2\pi\sigma^2)^{N/2}} \exp\left[-\frac{1}{2\sigma^2}\left(\sum_{n=0}^{M-1}\left(x[n] - A\sum_{l=0}^{L-1} h_l[n]r[n-l]\right)^2 + \sum_{n=M}^{N-1}(x[n])^2\right)\right]. \tag{2.20}$$

Thus, the MLE problem can be written as,

$$\begin{bmatrix} \hat{c} \\ \hat{M} \\ \hat{A} \end{bmatrix} = \underset{\substack{c,M,A \\ c_1 \le c \le c_2 \\ M_1 \le M \le M_2 \\ A_1 \le A \le A_2}}{\arg\max} \frac{1}{(2\pi\sigma^2)^{N/2}} \exp\left[-\frac{1}{2\sigma^2}\left(\sum_{n=0}^{M-1}\left(x[n] - A\sum_{l=0}^{L-1} h_l[n]r[n-l]\right)^2 + \sum_{n=M}^{N-1}(x[n])^2\right)\right]. \tag{2.21}$$

where $r[n]$ is as defined before, $r[n] = \sqrt{\nu[n]}\cos\left(2\pi c\xi[n]\right), \qquad n = 0, \ldots, M-1.$

Let us define $u[n] = \sum_{l=0}^{L-1} h_l[n]r[n-l],\ n = 0, \ldots, M$. Thus, the maximization

defined before is equivalent to

$$\begin{bmatrix} \hat{c} \\ \hat{M} \\ \hat{A} \end{bmatrix} = \underset{\substack{c,M,A \\ c_1 \le c \le c_2 \\ M_1 \le M \le M_2 \\ A_1 \le A \le A_2}}{\arg\min} \left\{ \sum_{n=0}^{M-1} \left(x[n] - Au[n]\right)^2 + \sum_{n=M}^{N-1} \left(x[n]\right)^2 \right\}, \tag{2.22}$$

which can be reformulated as

$$\begin{bmatrix} \hat{c} \\ \hat{M} \\ \hat{A} \end{bmatrix} = \underset{M: M_1 \le M \le M_2}{\arg\min} \left\{ \underbrace{\min_{c,A} \sum_{n=0}^{M-1} \left(x[n] - Au[n]\right)^2}_{\text{separate optimization problem}} + \sum_{n=M}^{N-1} \left(x[n]\right)^2 \right\}. \tag{2.23}$$

To perform the inner optimization for each value of M, as in the previous case, we perform a one-dimensional grid search (over the parameter c) instead of the two-dimensional grid search over the two parameters A and c since we are able to find the optimal estimator for the amplitude given the value of c. For a given value of the signal duration and the c value, the optimal solution for the amplitude estimate is

$$\hat{A} = \frac{\sum_{n=0}^{\hat{M}} x[n]u[n]}{\sum_{n=0}^{\hat{M}} u^2[n]}, \tag{2.24}$$

Therefore, the optimal MLE can be obtained similar to the one in the previous section. As an alternative, to simplify the solution, we can estimate the parameters A and c for the lowest possible value of the signal duration, and then search over the possible signal durations using these estimated quantities. This is the approach adopted in the examples section.

As in the previous subsection the asymptotic distribution of the ML estimated vector $\hat{\theta}$ is Gaussian with mean equal to the true mean and covariance matrix given by the inverse of the Fisher information matrix, i.e.,

$$\hat{\theta} \sim \mathcal{N}\left(\theta, I(\theta)^{-1}\right), \tag{2.25}$$

where $I(\theta)^{-1}$ is the Fisher Information matrix derived in Appendix B.

2.3 Error Probability Analysis

In the previous section, we have argued that the estimated parameter vector in our digital communication system can be modeled as

$$\hat{\theta} = \theta + \rho, \tag{2.26}$$

where $\hat{\theta}$ is a vector of the estimated parameters, θ is a vector of the actual the parameter values, and ρ is a Gaussian distributed noise vector with zero mean and covariance matrix given by the inverse of the Fisher information matrix as shown before. This is a common channel model, and there are many standard techniques that can be used to analyze the bit error probability (BEP) of the proposed system. For instance, we can resort to the union bound on the BEP.

In our proposed communication scheme, the acoustic signal that is being transmitted has n parameters that convey the digital bits; these signal parameters take values from their given range. Thus every transmitted acoustic signal is synthesized by picking a combination from these parameters. An equivalent model for the system is derived from the analysis of the asymptotic ML estimator of the signal parameters in (2.18). In this equivalent model the received signal can be represented as an n-dimensional vector of parameters that are transmitted over an additive colored Gaussian noise. Hence we can use noise whitening and apply the standard union bound to estimate the error rates.

We now give a specific (toy) example to demonstrate the performance of the proposed communication system. We use a hyperbolic chirp signal with two param-

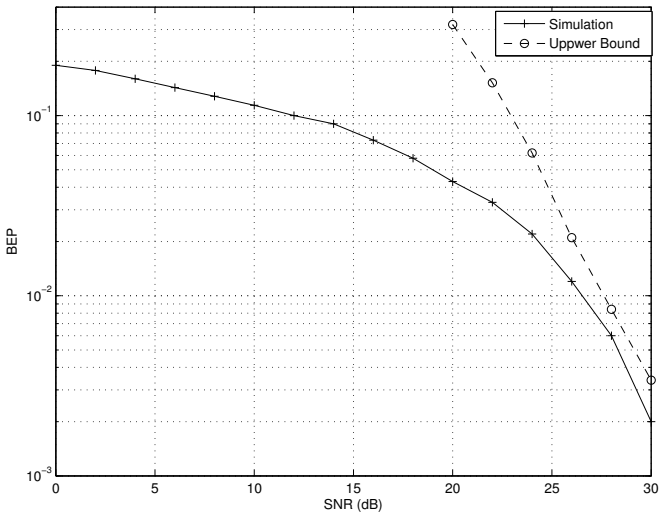

Figure 2.6: Simulated BEP and union bound.

eters used for the modulation purposes; namely the amplitude A and the chirp rate c. We transmit the signal $x(t)$

$$x(t) = A\sqrt{v(t)}\cos(2\pi c\xi(t)), \quad 0 < t < T, \tag{2.27}$$

where $\xi(t) = \ln(t)$ and $v(t) = \frac{d\eta(t)}{dt} = \frac{1}{t}$. In this example, T is the signal duration taken as 10 ms, A, and c are the parameters that are used to carry the information bits. The value of the parameter A ranges between 1 and 8, and c ranges between 20 kHz and 22 kHz. Each parameter is quantized into five bits. Thus, the size of the two-dimensional signal constellation is 1024 points. Figure 2.6 shows the BEP of the proposed communication scheme, using Monte Carlo simulations, and the union bound computed using the approach in the previous paragraph. It is clear that the union bound on the BEP matches the BEP computed from the simulations well for high SNR.

2.4 Experimental Results

We now provide some experimental results for the proposed communication system based on measurements taken at the recent KAM11 experiment [2].

2.4.1 KAM11 Experiment

The KAM11 experiment was conducted in shallow water off the western coast of Kauai, Hawaii, at the Pacific Missile Range Facility (PMRF) during the period 23 June and 12 July 2011. The bathymetry of the operation area is shown in Figure 2.7. We consider a fixed-source scenario at which there is no intentional motion between the transmitter and the receiver. The positions of the adopted transmitters and receivers are illustrated in Figs. 2.8 and 2.9. An 8-element vertical-array source was deployed with an inter-element separation of 7.5 m and an aperture of 52.5 m. The top element was at a nominal depth of 30 m, and the bottom element was not anchored to the sea floor. At the receiver side, a 16-element vertical array was deployed at a distance of 3 km from the source. The inter-element spacing was 3.75 m, with the top element deployed at a nominal depth of 35.5 m.

The transmitted signal is a linear phase chirp signal $x(t)$, given by

$$x(t) = A\cos\left(2\pi f_0 t + 2\pi c t^2\right), \qquad 0 < t < T \tag{2.28}$$

where A is the amplitude of the chirp signal, f_0 is the center frequency, c is the chirp rate, and T is the signal duration. The amplitude was then between 0.5 and 1; the center frequency was between 22 kHz and 26 kHz; the chirp rate was changed between 2 kHz and 10 kHz, and the signal duration was selected from 100 ms and 200 ms. Each parameter is quantized into four to ten bits to obtain different transmission rates.

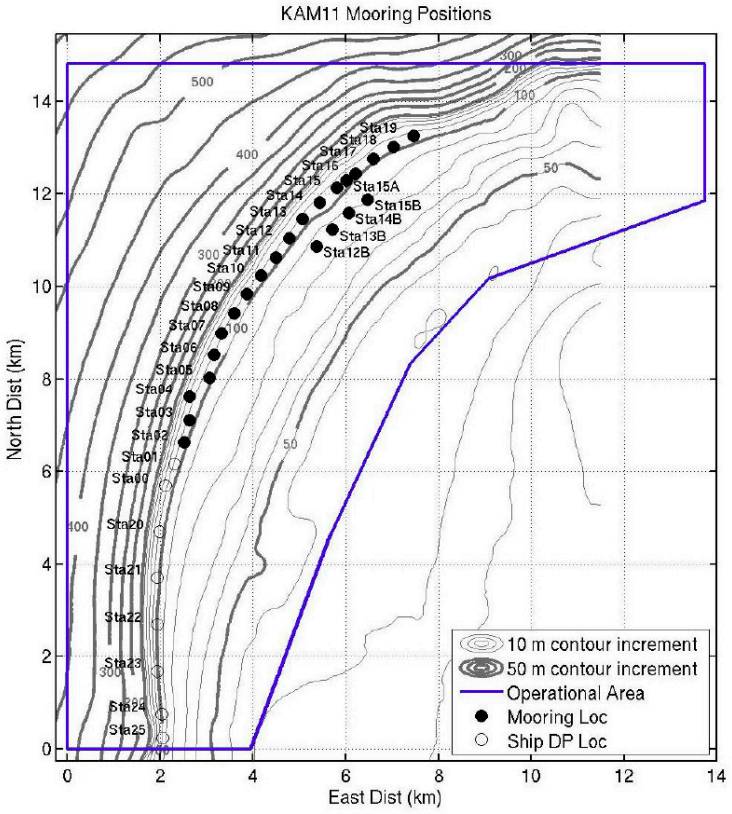

Figure 2.7: The operation area in the KAM11 (taken from [2]).

Every recoding consists of seven transmission frames (sometimes, called subgroups) where each subgroup corresponds to a different transmission rate. These different rates are attained from the fact that we map each parameter to different number of bits, e.g., in the first subgroup the parameters are mapped to four bits, in the second subgroup the parameters are mapped to five bits, etc. In each subgroup, we transmit 30 consecutive chirp sequences separated by a 60 ms guard period. Thus, the transmission rates that correspond to these subgroups are 107 bps, 127 bps, 147 bps, 167 bps, 187 bps, 207 bps, and 227 bps, respectively. In Section 2.4.4, we will present decoding results obtained for these different rates using different receiver combining techniques.

During the experiment, the transmitter/receiver separation was about 3 km.

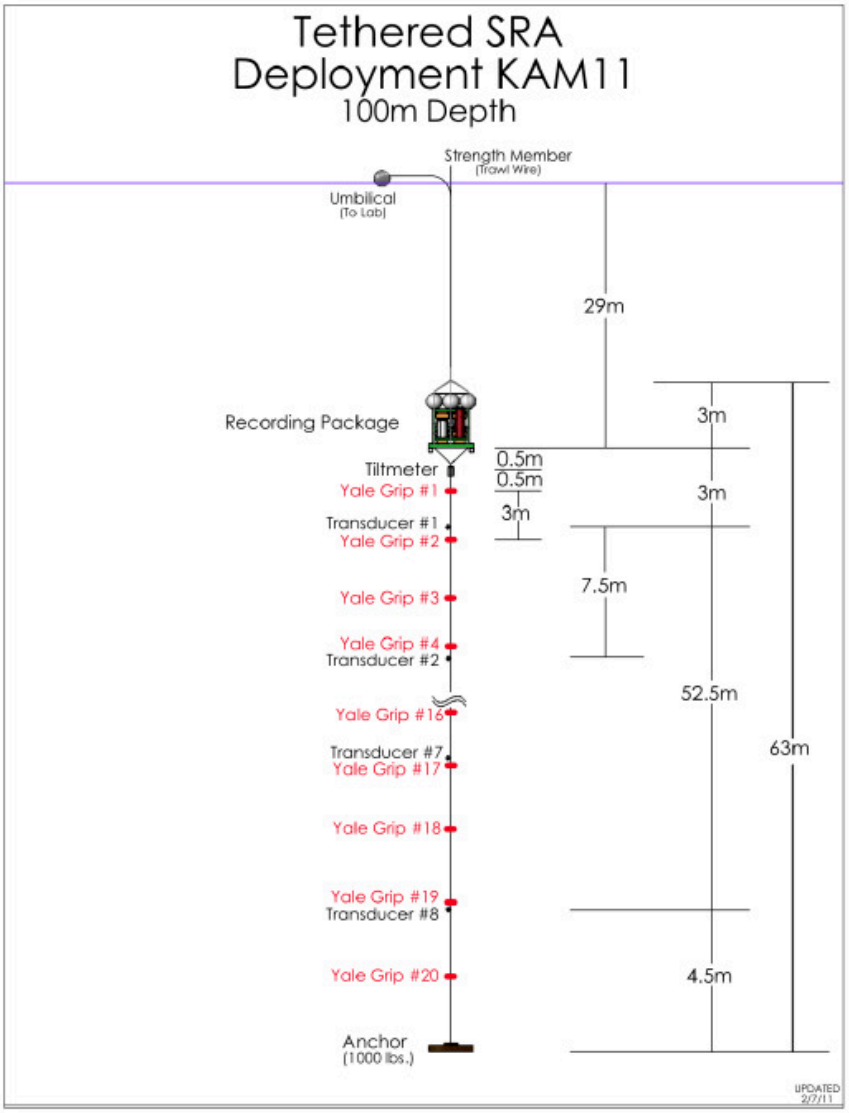

Figure 2.8: The positions of the adopted transmitters (taken from [2]).

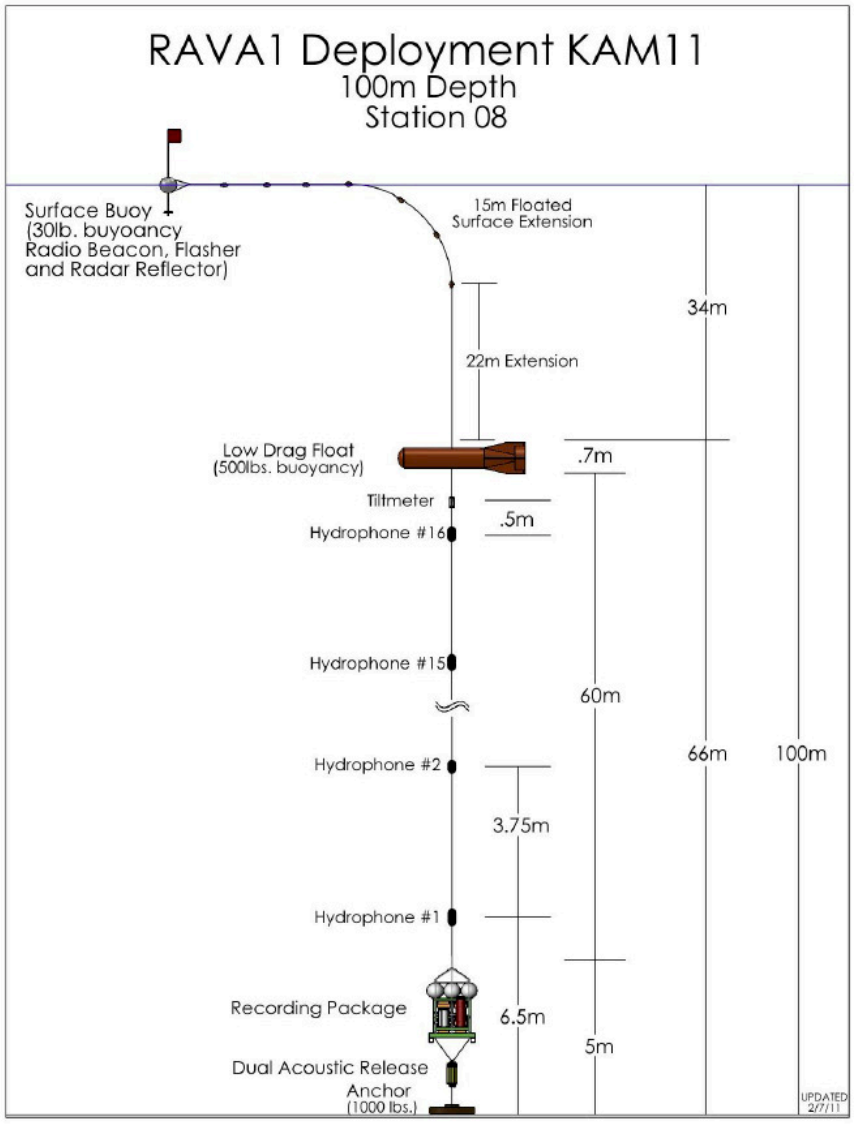

Figure 2.9: The positions of the adopted receivers (taken from [2]).

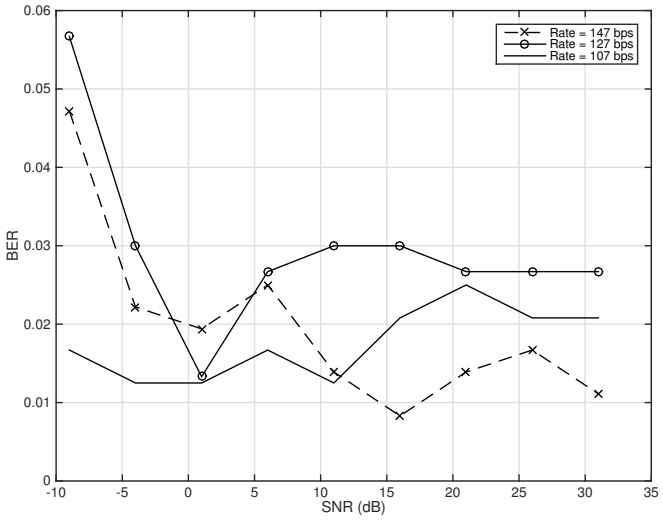

Figure 2.10: BER as a function of the SNR (emulated by adding Gaussian noise on the recorded data).

Defining the SNR at the receiver as the ratio between the signal power and the noise power after the amplifier and the bandpass digital filter, the corresponding SNR during the transmission is estimated to be around 11 dB. Since the SNR observed during the experiment was relatively high, we also consider decoding of the experimental data at lower SNRs by adding artificial (Gaussian) noise to the observations. Figure 2.10 shows the bit error rate (BER) versus the SNR for different transmission rates which are obtained by using majority voting combining technique (will be discussed later in more details) across the 16-antenna elements. It is clear that it is possible to decode the transmitted data with a reasonable BEP even at very low SNR values.

2.4.2 Channel Estimation

For the channel estimation purposes, we use the transmitted chirp signals as the channel probes as well. We employ the MP algorithm [53] to find an estimate of the channel coefficients. The MP algorithm is based on synthesizing a signal dictionary that consists of the transmitted signal and delayed versions of this signal. Since the

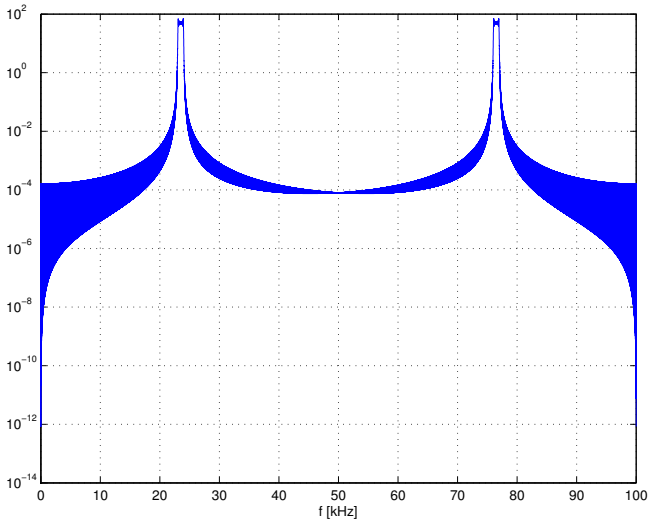

Figure 2.11: Power spectral density function of a chirp signal.

power spectral density of chirp signals is not close to being white, a resolution issue appears in the channel estimation process as the chirp cannot resolve all the arrivals that lie in a certain time interval. Nevertheless, we are constrained to using these signals as channel probes as no other signals were transmitted during the experiment. As an example, Figure 2.11 shows the power spectral density of a chirp signal. In other words, we cannot use a dictionary with a high resolution, and we have to settle for a coarse channel estimate. Even with this coarse channel estimate, we will be able to report acceptable raw error probabilities hence this is not a major issue.

For the MP algorithm due to the correlation structure of the transmitted signal, we use a dictionary that allows us to resolve only paths within 1 ms separation. The stopping criteria we set for the MP algorithm is the number of resolvable paths identified. We stop the algorithm when the number of resolvable paths equals 20 which means that we are able to span a delay spread of about 20 ms.

As an example, Figure 2.12 shows the time varying channel impulse response

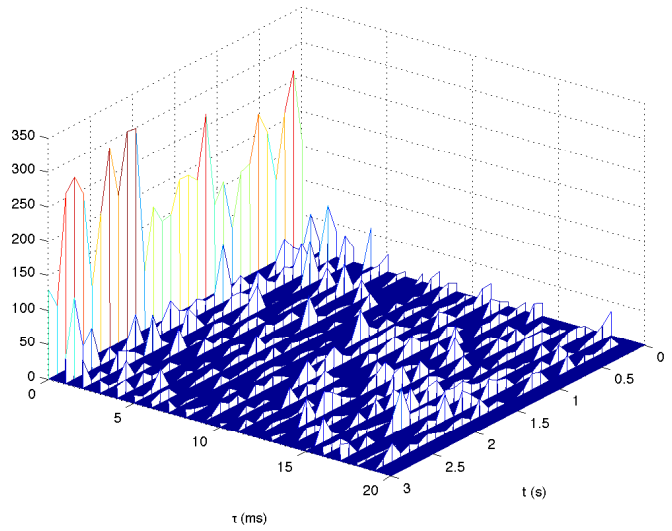

Figure 2.12: Channel impulse response for 30 consecutive chirps at the first receive element (these estimates have been computed from the data recorded on July 2nd, 2011 at 3:24 during the KAM11 experiment)

which is computed over a duration equals to the duration spanned by 30 adjacent chirp signals. These channel responses correspond to the channel between the transmitter and the first receive element. From these figures we can notice that the channel does not significantly change from signal block to the other. The reason that we observe a slowly varying channel is due to our channel estimator being a coarse one. The channel in KAM 2011 at a finer resolution changes more significantly as reported in [2]. For instance, we see from Figure 14(b) on page 34 and Figure 15(b) on page 35 in [2] that the change in the channel taps within a second or less is due to slight change in the arrival time – which is not being resolved in our channel estimates (being obtained from chirp signals as opposed to OFDM or other probe signals with a high resolution). This observation (on the estimated channel being slowly varying) will help us in the decoding process as we will see later.

2.4.3 Receiver Structure

The receiver has 16 elements, therefore it is possible to use receive diversity to enhance the performance of the system. During our investigations, we explore different combining techniques that can be used. The decoding process works as follows: we use the MLE to find estimates of the signal parameters at each receive element, then we decode these parameters into bits according to the mapping rule used at the transmitter side. Then, we apply a diversity combining technique to combine the decoded bits across all the receive elements. In the following subsections, we summarize the different combining techniques we use.

2.4.3.1 Majority Voting Combining

In the majority voting (MV) combining technique, the final decision is made by the majority voting rule. In other words, the final decision is said to be "1" if more than half of the receive elements decide for "1" and vice versa.

2.4.3.2 Weighted Sum Combining

In weighted sum (WS) combining schemes, the overall rule is based on weighting each receive element with a certain weight based on the reliability of its decision. We propose to use two different weighting schemes based on the model of the decoded bits. The first model is derived from the asymptotic behavior of the MLE. We know that the PDF of the estimated parameters is Gaussian with means equal the true value and the variance computed from the inverse of the Fisher information matrix. So, for the ith receive element we have

$$\eta_i \sim \mathcal{N}(\eta_0, I_i(\eta_0)^{-1}), \tag{2.29}$$

where η_0 is the true value. In our case, the vector of parameters η is given by,

$$\eta = \begin{bmatrix} C \\ F_0 \end{bmatrix}. \tag{2.30}$$

Thus MLE of the mean η_0 is,

$$\hat{\eta}_0 = \left(\sum_{i=0}^{N_r-1} I_i(\hat{\eta}_i) \right)^{-1} \sum_{i=0}^{N_r-1} I_i(\hat{\eta}_i)\eta_i, \tag{2.31}$$

where N_r is the number of the receive elements at the receiver, and $\hat{\eta}_i$ is the estimate of the vector of parameters η at the ith receiver element.

The second WS combining technique we use is based on the classical maximum ratio combining (MRC) model. In this scheme, the output bit from the ith receive element is modeled as

$$d^{(i)} = \alpha^{(i)}q + n^{(i)}, \tag{2.32}$$

where q is the original transmitted bit, $\alpha^{(i)}$ is the ℓ^2-norm of the estimated channel vector $\mathbf{h}^{(i)}$ at the ith receive element, and $n^{(i)}$ is the additive noise at the ith receive element. Thus, the weight of the output bit at the ith receive element is

$$\gamma_i = \frac{|\alpha^{(i)}|^2}{\hat{\sigma_i}^2}, \tag{2.33}$$

where $\hat{\sigma_i}^2$ is the noise variance at the ith receive element. We measure the noise variance from the silence period that exist between the transmission blocks using

$$\hat{\sigma}^2 = \frac{1}{N_s} \sum_{n=0}^{N_s-1} x[n]^2, \tag{2.34}$$

where N_s is the length of the silence period, and $x[n]$ is the received signal at the nth instant. We define the vector $\boldsymbol{\gamma} = [\gamma_1, \gamma_2, \ldots, \gamma_{N_r}]^T$ and we combine the soft values of the bits as follows

$$d_{combined} = \frac{1}{||\boldsymbol{\gamma}||_1}\boldsymbol{\gamma}^T\mathbf{d}, \tag{2.35}$$

where $||\cdot||_1$ denotes ℓ_1-norm. This combined value $d_{combined}$ is used with a threshold to make the final decision, the value of this threshold is $\frac{1}{2}$ as we assume the same a priori probabilities for "0" and "1".

2.4.3.3 *Selection Combining*

The last combining technique used is the selection combining (SC). In this case, we perform the selection based on the two models described before. For the first model, we select the decision made by the receive element that has the lowest noise variance. For the chirp rate c we choose the decision made by the element l_c which is given by,

$$l_c = \arg\min_i \sigma^2_{c^{(i)}}, \tag{2.36}$$

and for the frequency f_0 we choose the decision made by the element l_{f_0} which is given by,

$$l_{f_0} = \arg\min_i \sigma^2_{f_0^{(i)}}. \tag{2.37}$$

2.4.4 Decoding Results

We now present bit error rate results for our proposed communication scheme. At the receiver, a chirp signal block is used to estimate the channel; then this channel estimate is used to decode the next block, and so on. We can justify this from Figure 2.12 that shows that the channel impulses responses separated by a chirp duration are close to each other and the channel does not change significantly from one signal block to the other. We use the 16 receive elements at the receiver to decode the chirp parameters. Table 2.1 shows the uncoded error probability of the chirp parameters for the three combining techniques described before. We show the error probability results for nineteen different recordings. The results correspond to a transmission rate of 107bps. These recordings were taken on July 2nd, 2011 at 3:24, 5:24, 7:24, 9:24, 11:24, 13:24, 15:24, 17:24, 19:24, 21:24, and 23:24, respectively, and on

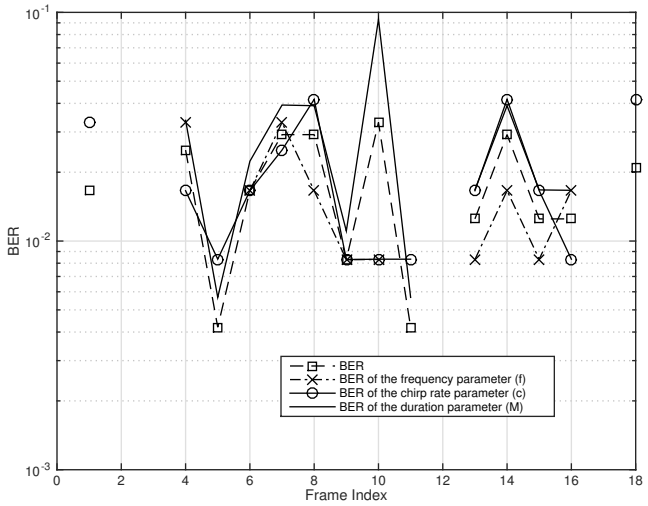

Figure 2.13: The BER for different parameters. "Blank space" means that no error for that frame is observed. The average error rate of the frequency parameter is 0.92%, the average error rate of the chirp rate parameter is 1.62%, and the average BER of the signal duration parameter is 2.17%.

July 3rd 2011 at 3:24, 5:24, 7:24, 9:24, 11:24, 13:24, 17:24, 21:24, 23:24, respectively. As another example, Table 2.2 shows the error probability for different transmission rates using the majority voting combining technique. Figure 2.13 shows the BER for different parameters separately.

From the decoding results, it is clear that we are able to decode the signal parameters successfully with a good BER. Our results indicate that the amplitude and the signal duration parameters are more vulnerable to errors than the frequency and chirp rate which is expected since the UWA channel is highly dispersive and it affects the amplitude and the signal duration than the other parameters. Also, the WS technique with the Gaussian model shows an average BER better than the other combining techniques. However, sometimes the MV shows a better BER than the WS. We have observed that the SC technique shows the worst performance among all the techniques (we did not show the resulting decoding error for that technique).

Env.	MV	WS, 1st model	WS, 2nd model
1	1.67%	2.5%	1.67%
2	0%	0%	0.83%
3	0%	1.25%	2.5%
4	2.5%	2.08%	3.33%
5	0.42%	2.08%	1.25%
6	1.67%	2.5%	1.67%
7	2.92%	3.33%	3.75%
8	2.92%	2.5%	1.67%
9	0.83%	0.42%	0.83%
10	3.33%	3.33%	3.75%
11	0.42%	1.25%	1.25%
12	0%	0%	0.42%
13	1.25%	0%	0.42%
14	2.92%	2.92%	4.17%
15	1.25%	0.42%	1.25%
16	1.25%	4.17%	3.33%
17	0%	0%	0%
18	2.08%	1.25%	1.67%
19	0%	0%	0%

Table 2.1: The uncoded error probability of the chirp parameters at rate equals to 107 bps. The table shows the uncoded BER for the three combining techniques, majority voting, weighted sum (two versions).

Rate (bps)	107	127	147	167	187	207	227
Env. 1	1.67%	3.67%	2.22%	1.67%	5.63%	8.15%	13.5%
Env. 2	0%	0%	1.94%	2.86%	4.37%	8.33%	11.67%
Env. 3	0%	2%	1.11%	0.71%	6.54%	7.41%	13%
Env. 4	2.5%	7%	1.11%	1.9%	7.71%	8.33%	13.5%

Table 2.2: Error probability for different transmission rates using the MV combining technique.

Also, by comparing the two models of the WS technique we can notice that the first model (the Gaussian one) shows a better average performance than the other model.

From the decoding results of different transmission rates we can notice that for lower data rates, the BER is not monotonically increasing with the rate. However, for higher rates, the BER states to follow a monotonically increasing behavior (increasing the rate results on increasing the BER) as it is expected.

Although it is not our major focus, we would also like to comment on the data rates obtained in our work compared to some other work reported on covert UWA communications. In [46], the authors present results from the SPACE'08 experiment during which DSSS technique was used for data transmission (to provide covertness). The transmitter/receiver separations in this experiment are 60 m, 200 m, and 1 km. The transmit bandwidth is 7.8125 kHz that leads to a payload data rate of 156.25 bps. In this paper, we have demonstrated successful decoding results up to 207 bps over a bandwdith of 10 kHz with a transmitter/receiver separation of about 3 km (significantly longer than the ones in [46]). In [26], the authors use the duration between dolphin clicks to convey digital bits. In their work, the data rate obtained is 37 bps with transmitter/receiver separation of about 2 km, which is a lower rate than what we have demonstrated over a longer transmitter/receiver separation in this paper. We further note that we were not very aggressive in selecting the transmission rates; we anticipate that it would have been possible to pack more bits and decode them successfully, or even use other set of parameters (using a different chirp signal) to carry more bits.

2.4.5 Interference Analysis

In this subsection, we study the effect of the coexisting other mammalian sounds on the system performance. We conduct our study by simple method of emulation for the

	f_0	c	T
SINR = 8dB	25kHz	2kHz	260msec
SINR = 4dB	25kHz	2kHz	260msec

Table 2.3: Signal parameters of the hyperbolic interfering signal.

KAM11 experiment. Specifically, we generate synthesized mammalian sounds using the signal models described in Section 2.1 and add it to the recorded data during the KAM11 experiment. For that purpose, we assume the following: the received does not know the existence of the interference and we use the decoder described in Section 2.4.3, the parameters of the interfering signal is random but fixed for during the experiment. We consider two interference scenarios cause by two different sound signals. The first one is the hyperbolic signal which is given by

$$i[nT_s] = A\sqrt{c/nT_s}\cos(2\pi c \ln nT_s + 2\pi f_0 nT_s). \tag{2.38}$$

Table 2.3 shows the signal parameters that have been used in the emulation. The parameters are chosen such that the interfering signal is located in the same frequency band of the transmitted signal with the maximum spread over this band and there is severe interference. Figure 2.14 shows the BER for different values of signal-to-interference plus noise ratios (SINRs). The figure shows that the BER changes by no more than 1%.

The second interference model we consider is the logarithmic signal which is given by

$$i[nT_s] = A\sqrt{c\ln nT_s}\cos(2\pi cnT_s(\ln nT_s - 1) + 2\pi f_0 nT_s), \tag{2.39}$$

Table 2.4 shows the signal parameters that have been used in the emulation. Figure 2.15 shows the resulting BER. From 2.14 and 2.15 we can notice that the proposed scheme shows an immunity against interference from coexisting signals.

	f_0	c	T
SINR = 9dB	25kHz	500Hz	260msec
SINR = 6dB	25kHz	500Hz	260msec

Table 2.4: Signal parameters of the logarithmic interfering signal.

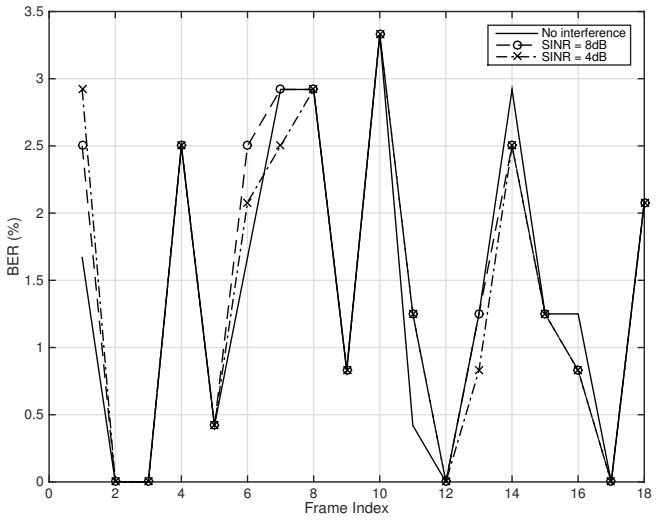

Figure 2.14: BERs for different values of SINRs, the interfering signal is hyperbolic.

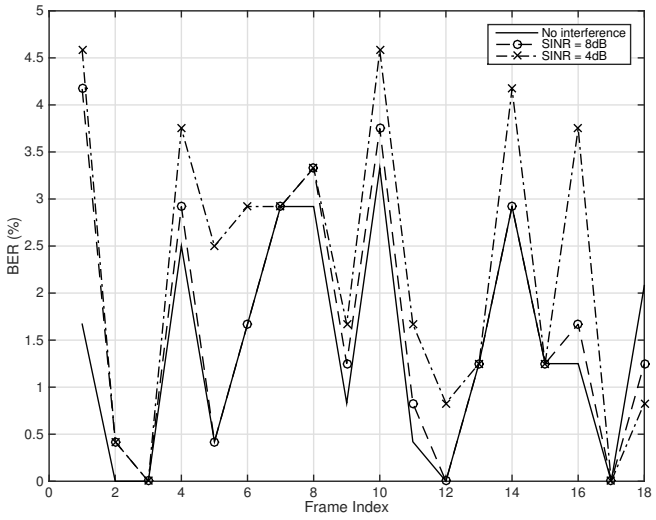

Figure 2.15: BERs for different values of SINRs, the interfering signal is logarithmic.

2.5 Chapter Summary

In this chapter, we have proposed a new communications scheme which uses signature signals to carry digital data through a mapping of information bits into the parameters characterizing them. At the receiver side, a decoder is developed which estimates the parameters of the signal used, and demaps these estimates back to bits. We show how this communications scheme can be applied in a UWA communications setting. We utilize existing parametrized biomimetic signals as signature signals, and design decoders that take into account the UWA channel conditions. We then derive an equivalent approximate channel model for the proposed communications scheme which implies a channel modeled with amplitude limited inputs and additive noise which is signal-dependent. We demonstrate the viability of the proposed communication scheme via some experimental results recorded at the Kauai Acomms MURI 2011 experiment.

Chapter 3

CAPACITY OF FADING CHANNELS WITH PEAK-POWER CONSTRAINED INPUTS

Information transfer over fading channels is one of the major challenges that confronts communication over wireless channels. The knowledge of the channel capacity and optimal input distribution is of crucial importance and plays a fundamental role in the design of channel codes. In this chapter, motivated by the amplitude-limited channel models implied by the proposed communications scheme in Chapter 2, we consider fading channels with amplitude limited inputs and channel gain with arbitrary distribution and finite support. We compute the capacity of fading channels under peak power constraint where the channel state information is only available at the receiver side.

Smith in [28] studies the capacity of scalar Gaussian channel under peak and average power constraints. He shows that there is a unique optimal distribution that maximizes the mutual information function and this distribution has a finite number of mass points. His results are based on two propositions. In the first proposition he shows that the mutual information function is a continuous function of the distribution, and it is strictly concave and weakly differentiable. Combining these characteristics of the mutual information function for such a channel leads to proving the existence of a unique optimal input distribution. In the second proposition, he uses techniques from measure theory and complex analysis to establish that this capacity-achieving distribution has a finite number of mass points.

The capacity of fading channels with amplitude-limited inputs has been studied previously in the literature for certain fading distributions and different input constraints. For instance, in [31] the authors consider transmission over Rayleigh

fading channels where neither the transmitter nor the receiver has the channel state information. They prove that the capacity-achieving distribution for average power-constrained inputs is discrete. Their approach is based on the following: they show that the capacity optimization problem is a convex optimization problem and hence there is a unique distribution that maximizes the mutual information function. Then, they use the KKT conditions to derive conditions on the optimal input distribution. They establish the discreteness of the optimal distribution by arriving at contradictions using techniques from complex analysis and measure theory. In fact, their proof shares the same spirit with that of Smith's for a standard AWGN channel in [28].

In [33], the authors investigate the capacity of Rician fading channels with inputs having constraints on the second and the fourth moments. The capacity-achieving distribution is shown to be discrete with a finite number of mass points. They also study channels with peak power constraints and show that the optimal distribution is discrete as well. In a closely related work [34], the authors generalize the previous results, and show that any conditionally Gaussian channel with amplitude-limited inputs has a discrete input distribution that achieves the capacity. By conditionally Gaussian channels, the authors refer to the distribution of the channel output conditioned on the channel input. The uniqueness of the capacity-achieving distribution is a result of the strict convexity of the capacity optimization problem. The discreteness of the optimal distribution is shown for conditionally Gaussian channels. In their work, the authors show that when the set of points of increase is a collection of concentric shells and bounded, it is sparse (has a finite number of mass points) if and only if its number of shells is finite.

In this chapter, we consider fading channels with amplitude-limited inputs with a well-behaved probability density function for the fading gain. We assume that

the channel gains are real, have finite support and are known at the receiver. We show that the capacity achieving distribution for a general fading model is discrete with a finite number of mass points. Note that the channel model under consideration does not fall within the framework of conditionally Gaussian channel studied in [34]. We also illustrate our findings in some examples.

The chapter is organized as follows. In Section 3.1, we present the fading channel model under consideration at which the transmitted signal is exposed to fading that follows an arbitrary probability density function with a finite support. In Section 3.2, we show that the capacity is maximized by a unique distribution. To do this, we prove that the mutual information is continuous, strictly concave, and weakly differentiable function of the input distribution. Then, we show, in Section 3.3, that this input distribution is discrete using techniques from complex analysis. In Section 3.4, we present numerical examples to illustrate our findings, and conclude the chapter in Section 5.6 with a summary.

3.1 Channel Model and Definitions

The received signal Y is given by

$$Y = \alpha X + N \tag{3.1}$$

where X is the channel input that is amplitude-constrained to $[-A,\ A]$, i.e., it has a probability distribution function $F_X(x)$ that belongs to the class of probability distribution functions $\mathcal{F}_X$ such that for any $F_X \in \mathcal{F}_X$, $F_X(x) = 0$ for any $x < -A$ and $F_X(x) = 1$ for any $x > A$. The channel coefficient α is the fading channel coefficient that has a probability distribution function $F_\alpha(u)$, we assume that the channel coefficient α has a finite support, i.e., $\alpha \in [0, u_0]$ for some $u_0 < \infty$. The noise N is Gaussian, i.e., $N \sim \mathcal{N}(0, \sigma^2)$, and it is independent for different uses of the channel. We assume that the input X and the fading coefficient α are independent.

The probability density function of the denoted output is given by

$$f_Y(y; F_X) = \int_0^{u_0} \int_{-A}^{A} P_N(y - ux) dF_X(x) dF_\alpha(u), \tag{3.2}$$

where $P_N(y - ux) = f_{Y|X,\alpha}(y|x, u)$ is the probability density function of the channel output Y conditioned on specific values of X and α, and $f_Y(y; F_X)$ is the probability density function of the channel output Y when the input has a probability distribution function F_X. The existence of $f_Y(y; F_X)$ is guaranteed by the existence of P_N which can be verified by computing the probability distribution function of the output

$$\begin{aligned} F_Y(y; F_X) &= \int_0^{u_0} \int_{-A}^{A} F_N(y - ux) dF_X(x) dF_\alpha(u), \\ &= \int_0^{u_0} \int_{-A}^{A} \int_{-\infty}^{y} P_N(y' - ux) dy' dF_X(x) dF_\alpha(u), \\ &= \int_{-\infty}^{y} \int_0^{u_0} \int_{-A}^{A} P_N(y' - ux) dF_X(x) dF_\alpha(u) dy' \\ &= \int_{-\infty}^{y} f_Y(y'; F_X) dy', \end{aligned}$$

where the interchange of the order of the integration is justified by the Fubini's Theorem because the probability density function of the noise P_N is non-negative and integrable.

In the following, we derive bounds on the probability density function of the noise function $P_N(y - ux)$ and the conditional probability density function $f_{Y|\alpha}(y|u)$ for later use. It is straightforward to show that, for $u > 0$, the probability density function is bounded as follows

$$q(y, u) \leq P_N(y - ux) \leq Q(y, u), \tag{3.3}$$

where

$$q(y, u) = \begin{cases} k_1 \exp(-k_2(y - uA)^2) & \text{if } y \leq 0, \\ k_1 \exp(-k_2(y + uA)^2) & \text{if } y > 0, \end{cases} \tag{3.4}$$

and

$$Q(y,u) = \begin{cases} k_3 \exp(-k_4(y+uA)^2) & \text{if } y \leq -A, \\ k_3 & \text{if } y \in [-A, A], \\ k_3 \exp(-k_4(y-uA)^2) & \text{if } y > A, \end{cases} \tag{3.5}$$

for some finite and positive k_1, k_2, k_3, and k_4. As a result, the conditional probability density function $f_{Y|\alpha}(y|u)$ can be bounded as well

$$\gamma(y,u) \leq f_{Y|\alpha}(y|u) \leq \Gamma(y,u), \tag{3.6}$$

where

$$\gamma(y,u) = q(y,u), \tag{3.7}$$

and

$$\Gamma(y,u) = Q(y,u). \tag{3.8}$$

Thus, we can use the Fubini's theorem to interchange the order of integration which can be justified by using (3.6) such that

$$\begin{aligned} f_Y(y; F_X) &= \int_0^{u_0} \int_{-A}^{A} P_N(y-ux) dF_X(x) dF_\alpha(u), \\ &\leq k_3 \int_{-A}^{A} \int_0^{u_0} dF_\alpha(u) dF_X(x), \\ &= k_3, \\ &< \infty. \end{aligned}$$

Thus,

$$\begin{aligned} f_Y(y; F_X) &= \int_0^{u_0} \int_{-A}^{A} P_N(y-ux) dF_X(x) dF_\alpha(u), \\ &= \int_{-A}^{A} \int_0^{u_0} P_N(y-ux) dF_\alpha(u) dF_X(x). \end{aligned}$$

The average mutual information between the input, output conditioned on the channel is defined as [55, 56]

$$I_{F_X}(X;Y|\alpha) \triangleq \int_0^{u_0} I_{F_X}(X;Y|\alpha=u)dF_\alpha(u) \tag{3.9}$$

where

$$I_{F_X}(X;Y|\alpha=u) \triangleq \int_{-\infty}^{\infty}\int_{-A}^{A} P_N(y-ux)\log\left(\frac{P_N(y-ux)}{f_{Y|\alpha}(y|u;F_X)}\right)dF_X(x)dy \tag{3.10}$$

We define the conditional entropy $H_{F_X}(Y|\alpha)$ as

$$H_{F_X}(Y|\alpha) \triangleq -\int_0^{u_0}\int_{-\infty}^{\infty} f_{Y|\alpha}(y|u;F_X)\log f_{Y|\alpha}(y|u;F_X)dF_\alpha(u)dy. \tag{3.11}$$

For noise with finite variance and bounded density function, the conditional mutual information function can be written as,

$$I_{F_X}(X;Y|\alpha) = H_{F_X}(Y|\alpha) - D, \tag{3.12}$$

where D is the noise entropy which is defined as

$$D \triangleq -\int_{-\infty}^{\infty} P_N(z)\log P_N(z)dz. \tag{3.13}$$

For a Gaussian channel of mean 0 and variance σ^2, the noise entropy is

$$D = \frac{1}{2}\log\left(2\pi e\sigma^2\right). \tag{3.14}$$

The channel capacity is defined as

$$C = \max_{F_X\in\mathcal{F}_X} I_{F_X}(X;Y|\alpha). \tag{3.15}$$

We define the conditional mutual information density $i_F(x|\alpha=u)$ conditioned on a specific value of α, and the conditional entropy density $h_F(x|\alpha=u)$ conditioned on a specific value of α as

$$i_{F_X}(x|\alpha=u) \triangleq \int_{-\infty}^{\infty} P_N(y-ux)\log\frac{P_N(y-ux)}{f_{Y|\alpha}(y|u;F_X)}dy, \tag{3.16}$$

$$h_{F_X}(x|\alpha=u) \triangleq -\int_{-\infty}^{\infty} P_N(y-ux)\log f_{Y|\alpha}(y|u;F_X)dy. \tag{3.17}$$

Thus, the following equation holds

$$i_{F_X}(x|\alpha = u) = h_{F_X}(x|\alpha = u) - D. \tag{3.18}$$

Define the conditional mutual information density $i_{F_X}(x|\alpha)$ and the conditional entropy density as $h_{F_X}(x|\alpha)$

$$i_{F_X}(x|\alpha) \triangleq \int_0^{u_0} i_{F_X}(x|\alpha = u) dF_\alpha(u), \tag{3.19}$$

$$h_{F_X}(x|\alpha) \triangleq \int_0^{u_0} h_{F_X}(x|\alpha = u) dF_\alpha(u). \tag{3.20}$$

Thus, the following equations hold

$$i_{F_X}(x|\alpha) = h_{F_X}(x|\alpha) - D, \tag{3.21}$$

$$I_{F_X}(X;Y|\alpha) = \int_{-A}^{A} i_{F_X}(x|\alpha) dF_X(x), \tag{3.22}$$

$$H_{F_X}(Y|\alpha) = \int_{-A}^{A} h_{F_X}(x|\alpha) dF_X(x). \tag{3.23}$$

These equations hold by the definition of the information density and the definition of the entropy density.

Lemma 3.1.1. *The entropy density $h_{F_X}(x|\alpha)$ and the the mutual information density $i_{F_X}(x|\alpha)$ are finite.*

Proof. It is sufficient to show the finiteness of $H_{F_X}(Y|\alpha)$ as the difference between $I_{F_X}(X;Y|\alpha)$ and $H_{F_X}(Y|\alpha)$ is just a constant. In order to show the finiteness of $H_{F_X}(Y|\alpha)$, we show the finiteness of $h_{F_X}(x|\alpha)$ and hence conclude the finiteness of

$H_{F_X}(Y|\alpha)$. $\forall x \in [-A, A]$, we have

$$\begin{aligned}
|h_{F_X}(x|\alpha)| &= \left| \int_0^{u_0} h_{F_X}(x|\alpha = u) dF_\alpha(u) \right| \\
&\leq \int_0^{u_0} \int_{-\infty}^{\infty} \left| P_N(y - ux) \log(f_{Y|\alpha}(y|u; F_X)) \right| dF_\alpha(u) dy \\
&\leq \int_0^{u_0} \int_{-\infty}^{\infty} P_N(y - ux)[-\log(f_{Y|\alpha}(y|u; F_X)) + 2|\log(k_3)|] dF_\alpha(u) dy \\
&\leq \int_0^{u_0} \int_{-\infty}^{\infty} Q(y, u)[-\log(q(y, u)) + 2|\log(k_3)|] dF_\alpha(u) dy \\
&= 2 \int_0^{u_0} \int_0^{\infty} (-Q(y, u) \log(q(y, u)) + 2Q(y, u)|\log(k_3)|) \, dF_\alpha(u) dy.
\end{aligned}$$

It is easy to show that $\int_0^{u_0} \int_0^{\infty} 2Q(y, u)|\log(k_3)|) dF_\alpha(u) dy < \infty$, e.g., similar to the arguments in [35]. Hence, $h_{F_X}(x|\alpha)$ is finite, and $|h_{F_X}(x|\alpha)| \leq k$, for some $k < \infty$. This implies

$$\begin{aligned}
H_{F_X}(Y|\alpha) &= \int_{-A}^{A} h_{F_X}(x|\alpha) dF_X(x), \\
&\leq k \int_{-A}^{A} dF_X(x), \\
&< \infty,
\end{aligned}$$

that is, $I_{F_X}(X; Y|\alpha)$ and $H_{F_X}(Y|\alpha)$ are both finite. □

3.2 Capacity Optimization Problem

In this sub-section, we show that the mutual information is a strictly concave function, weakly differentiable, and continuous function of the input distribution. In order to show the concavity of the mutual information, we use Ash's Lemma [57] to bound the mutual information. The weak differentiability is shown by following similar line of arguments as in [28]. Continuity of the mutual information is shown using the Helly-Bray Theorem.

3.2.1 The Mutual Information is a Continuous Function of the Distribution

The conditional mutual information is

$$I_{F_X}(X;Y|\alpha) = H_{F_X}(Y|\alpha) - D, \tag{3.24}$$

and the conditional entropy is

$$H_{F_X}(Y|\alpha) = \int_0^{u_0} H_{F_X}(Y|\alpha = u) dF_\alpha(u). \tag{3.25}$$

Thus, if we can show that $H_{F_X}(Y|\alpha = u)$ is a continuous function of the input distribution, we can invoke the Dominated Convergence Theorem to conclude the continuity of $H_{F_X}(Y|\alpha)$.

Let us fix a sequence $\{F_X^{(n)}(x)\}_{n\geq 1}$ in $\mathcal{F}_X$ such that $F_X^{(n)}(x) \to F_X(x)$ for some $F_X \in \mathcal{F}_X$.

$$\begin{aligned}
\lim_{n\to\infty} f_{Y|\alpha}(y|u;F_X^{(n)}) &= \lim_{n\to\infty} \int_{-A}^{A} P_N(y-ux) dF_X^{(n)}(x), \\
&\overset{(a)}{=} \int_{-A}^{A} P_N(y-ux) dF_X(x), \\
&= f_Y(y;F_X),
\end{aligned}$$

where (a) follows by the Helly-Bray Theorem [58]. Then,

$$\lim_{n\to\infty} f_{Y|\alpha}(y|u;F_X^{(n)}) \log\left(f_{Y|\alpha}(y|u;F_X^{(n)})\right) = f_{Y|\alpha}(y|u;F_X) \log\left(f_{Y|\alpha}(y|u;F_X)\right). \tag{3.26}$$

On the other hand, from (3.6),

$$\left| -f_{Y|\alpha}(y|u;F_X^{(n)}) \log\left(f_{Y|\alpha}(y|u;F_X^{(n)})\right) \right| \leq \Gamma(y,u) \left[-\log(\gamma(y,u)) + 2|\log(k_3)| \right], \tag{3.27}$$

and hence we can easily verify that

$$\left| \int_{-\infty}^{\infty} f_{Y|\alpha}(y|u;F_X) \log\left(f_{Y|\alpha}(y|u;F_X)\right) dy \right| < \infty. \tag{3.28}$$

Thus, by applying the Dominated Convergence Theorem, we can conclude that the function $H_{F_X}(Y|\alpha)$ is continuous function of the input distribution and hence $I_{F_X}(X;Y|\alpha)$ is a continuous function of $F_X(x)$ as well.

3.2.2 The Mutual Information Function is a Strictly Concave Function of the Input Distribution

We have

$$I_{F_X}(Y;X|\alpha) = H_{F_X}(Y|\alpha) - D. \tag{3.29}$$

Hence, it is enough to show that the conditional entropy $H_{F_X}(Y|\alpha)$ is strictly concave function of the distribution to conclude the strict concavity of the mutual information function. The conditional entropy is given by

$$H_{F_X}(Y|\alpha) = \int_0^{u_0} H_{F_X}(Y|\alpha = u) dF_\alpha(u). \tag{3.30}$$

To show the strict concavity of the conditional entropy, we first show that $H_{F_X}(Y|\alpha = u)$ is strictly concave for every u in the support of the random variable α by considering

$$Y = uX + N. \tag{3.31}$$

for a fixed u. For $u > 0$, we define a new random variable $Y' = \frac{Y}{u}$, and hence

$$Y' = X + \frac{N}{u}. \tag{3.32}$$

This equivalent model is the same as the scalar Gaussian channel model studied by Smith in [28], however, the noise variance for our case is $\frac{\sigma^2}{u^2}$. The strict concavity applies immediately using his results and we conclude the strict concavity of the conditional output entropy since positive weighted sum of strictly concave function is strictly concave [59]. For the case of $u = 0$, the received signal $Y = N$ and hence the conditional mutual information $I_{F_X}(X;Y|\alpha = 0) = 0$

3.2.3 The Mutual Information is a Weakly Differentiable Function

Lemma 3.2.1. *The mutual information function $I(X;Y|\alpha)$ is a weakly differentiable function and its weak derivative is*

$$I'_{F_1,F_2}(X;Y|\alpha) = \int_{-A}^{A} i_{F_1}(x|\alpha)dF_2(x) - I_{F_1}(X;Y|\alpha). \tag{3.33}$$

Proof. The weak derivative is defined as [60]

$$\begin{aligned} I'_{F_1,F_2}(X;Y|\alpha) &= \lim_{\theta\to 0} \frac{I_{(1-\theta)F_1+\theta F_2}(X;Y|\alpha) - I_{F_1}(X;Y|\alpha)}{\theta} \\ &= \lim_{\theta\to 0} \int_0^{u_0} \frac{I_{(1-\theta)F_1+\theta F_2}(X;Y|\alpha=u) - I_{F_1}(X;Y|\alpha=u)}{\theta} dF_\alpha(u), \\ &= \lim_{\theta\to 0} \int_0^{u_0} \frac{H_{(1-\theta)F_1+\theta F_2}(Y|\alpha=u) - H_{F_1}(Y|\alpha=u)}{\theta} dF_\alpha(u). \end{aligned}$$

Let us define $F_\theta \triangleq (1-\theta)F_1 + \theta F_2$ and

$$J(\theta, F_1, F2) \triangleq \int_0^{u_0} \frac{H_{F_\theta}(Y|\alpha=u) - H_{F_1}(Y|\alpha=u)}{\theta} dF_\alpha(u). \tag{3.34}$$

Noting that

$$f_{Y|\alpha}(y|\alpha=u;F_\theta) = f_{Y|\alpha}(y|\alpha=u;F_1) + \theta\left(f_{Y|\alpha}(y|\alpha=u;F_2) - f_{Y|\alpha}(y|\alpha=u;F_1)\right), \tag{3.35}$$

we can write

$$\begin{aligned} J(\theta,F_1,F_2) &= -\frac{1}{\theta}\int_0^{u_0}\int_{-\infty}^{\infty} f_{Y|\alpha}(y|\alpha=u;F_\theta)\log\left(f_{Y|\alpha}(y|\alpha=u;F_\theta)\right) dy dF_\alpha(u) \\ &\quad +\frac{1}{\theta}\int_0^{u_0}\int_{-\infty}^{\infty} f_{Y|\alpha}(y|\alpha=u;F_1)\log\left(f_{Y|\alpha}(y|\alpha=u;F_1)\right) dy dF_\alpha(u) \\ &= -\int_0^{u_0}\int_{-\infty}^{\infty} \frac{f_{Y|\alpha}(y|\alpha=u;F_1)}{\theta} \\ &\quad \log\left(f_{Y|\alpha}(y|\alpha=u;F_1) + \theta\left(f_{Y|\alpha}(y|\alpha=u;F_2) - f_{Y|\alpha}(y|\alpha=u;F_1)\right)\right) dy dF_\alpha(u) \\ &\quad -\int_0^{u_0}\int_{-\infty}^{\infty} \left(f_{Y|\alpha}(y|\alpha=u;F_2) - f_{Y|\alpha}(y|\alpha=u;F_1)\right) \\ &\quad \log\left(f_{Y|\alpha}(y|\alpha=u;F_1) + \theta\left(f_{Y|\alpha}(y|\alpha=u;F_2) - f_{Y|\alpha}(y|\alpha=u;F_1)\right)\right) dy dF_\alpha(u) \\ &\quad +\int_0^{u_0}\int_{-\infty}^{\infty} \frac{f_{Y|\alpha}(y|\alpha=u;F_1)}{\theta}\log\left(f_{Y|\alpha}(y|\alpha=u;F_1)\right) dy dF_\alpha(u) \end{aligned}$$

From Taylor expansion (similar to [28, 35]) we have

$$\begin{aligned}
&\log\left(f_{Y|\alpha}(y|\alpha=u;F_1)+\theta\left(f_{Y|\alpha}(y|\alpha=u;F_2)-f_{Y|\alpha}(y|\alpha=u;F_1)\right)\right)\\
&\quad=\log\left(f_{Y|\alpha}(y|\alpha=u;F_1)\right)+\theta\left(\frac{f_{Y|\alpha}(y|\alpha=u;F_2)-f_{Y|\alpha}(y|\alpha=u;F_1)}{f_{Y|\alpha}(y|\alpha=u;F_1)}\right)\\
&\qquad-\frac{\theta^2}{2}\left(\frac{f_{Y|\alpha}(y|\alpha=u;F_2)-f_{Y|\alpha}(y|\alpha=u;F_1)}{f_{Y|\alpha}(y|\alpha=u;F_1)+\epsilon\theta\left(f_{Y|\alpha}(y|\alpha=u;F_2)-f_{Y|\alpha}(y|\alpha=u;F_1)\right)}\right)^2
\end{aligned}$$

for some $\epsilon\in[0,1]$. Rewriting (3.36) using the previous expansion gives us

$$\begin{aligned}
&J(\theta,F_1,F_2)+\int_0^{u_0}\int_{-\infty}^{\infty}\left(f_{Y|\alpha}(y|\alpha=u;F_2)-f_{Y|\alpha}(y|\alpha=u;F_1)\right)\log\left(f_{Y|\alpha}(y|\alpha=u;F_1)\right)dydu\\
&=\theta\int_0^{u_0}\int_{-\infty}^{\infty}\left(\frac{\left(f_{Y|\alpha}(y|\alpha=u;F_2)-f_{Y|\alpha}(y|\alpha=u;F_1)\right)^2\left(f_{Y|\alpha}(y|\alpha=u;F_1)+\theta\left(f_{Y|\alpha}(y|\alpha=u;F_2)-f_{Y|\alpha}(y|\alpha=u;F_1)\right)\right)}{2\left(f_{Y|\alpha}(y|\alpha=u;F_1)+\epsilon\theta\left(f_{Y|\alpha}(y|\alpha=u;F_2)-f_{Y|\alpha}(y|\alpha=u;F_1)\right)\right)^2}\right.\\
&\qquad\left.-\frac{\left(f_{Y|\alpha}(y|\alpha=u;F_2)-f_{Y|\alpha}(y|\alpha=u;F_1)\right)^2}{f_{Y|\alpha}(y|\alpha=u;F_1)}\right)dydF_\alpha(u)\qquad(3.36)
\end{aligned}$$

$$\begin{aligned}
&J(\theta,F_1,F_2)+\int_0^{u_0}\int_{-\infty}^{\infty}\left(f_{Y|\alpha}(y|\alpha=u;F_2)-f_{Y|\alpha}(y|\alpha=u;F_1)\right)\log\left(f_{Y|\alpha}(y|\alpha=u;F_1)\right)dydF_\alpha(u)\\
&\qquad=\theta\int_0^{u_0}\int_{-\infty}^{\infty}\eta(y,u)dydF_\alpha(u),
\end{aligned}$$

where $\eta(y,u)$ is the integrand in (3.36). Using exact line of arguments as in [28, 35], and using Lemma 3.1.1 to show the finiteness of $\int_0^{u_0}\int_{-\infty}^{\infty}\eta(y,u)dydF_\alpha(u)$, we obtain

$$\begin{aligned}
\lim_{\theta\to0}J(\theta,F_1,F_2) &= -\int_0^{u_0}\int_{-\infty}^{\infty}\left(f_{Y|\alpha}(y|\alpha=u;F_2)-f_{Y|\alpha}(y|\alpha=u;F_1)\right)\log\left(f_{Y|\alpha}(y|\alpha=u;F_1)\right)dydF_\alpha(u)\\
&= -\int_0^{u_0}\int_{-\infty}^{\infty}f_{Y|\alpha}(y|\alpha=u;F_2)\log\left(f_{Y|\alpha}(y|\alpha=u;F_1)\right)dydF_\alpha(u)-H_{F_1}(y|\alpha)\\
&= \int_{-A}^{A}h_{F_1}(x|\alpha)dF_2(x)-H_{F_1}(y|\alpha).
\end{aligned}$$

As a result, the weak derivative is

$$\begin{aligned}
I'_{F_1,F_2}(X;Y|\alpha) &= \int_0^{u_0}\left(\int_{-A}^{A}i_{F_1}(x|\alpha=u)dF_2(x)-I_{F_1}(X;Y|\alpha=u)\right)dF_\alpha(u),\\
&= \int_{-A}^{A}i_{F_1}(x|\alpha)dF_2(x)-I_{F_1}(X;Y|\alpha).\qquad(3.37)
\end{aligned}$$

□

Theorem 3.2.2. *C, the capacity of the channel, is achieved by a unique probability distribution function F_0 in $\mathcal{F}_X$, i.e.,*

$$C \triangleq \max_{F_X in \mathcal{F}_X} I(X;Y|\alpha) \tag{3.38}$$

for some unique F_0 in $\mathcal{F}_X$.

Proof. The space $\mathcal{F}_X$ is convex and compact in some topology [61]. We showed that the function $I : \mathcal{F}_X \to \mathcal{R}$ is strictly concave, continuous, and weakly differentiable in $\mathcal{F}_X$ which concludes the proof of the theorem. □

Corollary 3.2.3. *There exists an optimal $F_0 \in \mathcal{F}_X$ which satisfies*

$$\int_{-A}^{A} i_{F_0}(x|\alpha) dF(x) - I_{F_0}(X;Y|\alpha) \leq 0 \tag{3.39}$$

Also,

$$i_{F_0}(x|\alpha) \leq I_{F_0}(X;Y|\alpha), \qquad \forall x \in [-A, A], \tag{3.40}$$

$$i_{F_0}(x|\alpha) = I_{F_0}(X;Y|\alpha), \qquad \forall x \in E_0, \tag{3.41}$$

where E_0 is the set of points of increase of the probability distribution function F_X.

Proof. The proof follows from similar lines of reasoning as in [28]. Assume that F_0 is optimal but the first equation is not true. Then there exists $X_1 \in [-A, A]$ such that $i_{F_0}(x|\alpha) > I_{F_0}(X;Y|\alpha)$. Let $F_x(x) \triangleq \mathbf{U}(x - x_1)$. Then,

$$\int_{-A}^{A} i_{F_0}(x|\alpha) dF_1(x) = i_{F_0}(x_1|\alpha) > I_{F_0}(X;Y|\alpha). \tag{3.42}$$

This contradicts the results of Theorem 3.2.2. Thus, the first equation is valid, i.e.,

$$i_{F_0}(x|\alpha) \leq I_{F_0}(X;Y|\alpha), \qquad \forall x \in [-A, A]. \tag{3.43}$$

Now, assume that the second equality is not valid. Define E' as a subset of E_0 with positive measure,

$$\int_{E'} dF_0(x) = \delta > 0, \tag{3.44}$$

and

$$i_{F_0}(x|\alpha) < I_{F_0}(X;Y|\alpha), \quad \forall x \in [-A, A]. \tag{3.45}$$

Since

$$\int_{E_0 - E'} dF_0(x) = 1 - \delta \tag{3.46}$$

and

$$i_{F_0}(x|\alpha) = I_{F_0}(X;Y|\alpha) \quad \text{on } E_0 - E' \tag{3.47}$$

then

$$\begin{aligned} I_{F_0}(X;Y|\alpha) &= \int_{E_0} i_{F_0}(x|\alpha) dF_0(x) \\ &= \int_{E'} i_{F_0}(x|\alpha) dF_0(x) + \int_{E_0 - E'} i_{F_0}(x|\alpha) dF_0(x) \\ &< \delta I_{F_0}(X;Y|\alpha) + (1-\delta) I_{F_0}(X;Y|\alpha) \\ &= I_{F_0}(X;Y|\alpha) \end{aligned}$$

which is a contradiction. Thus, the second statement holds. □

3.3 Discreteness of the Optimal Distribution

In this subsection, we prove that the optimal distribution that maximizes the mutual information function is discrete with a finite number of mass points. The proof is based on contradiction arguments as in [28] by assuming that the set E_0 has an infinite number of mass points, and since the set E_0 is bounded, we can use Bolzano Weierstrass to argue that the set E_0 has a limit point. Then, we extend the conditional entropy function to the complex and show its analyticity on an open connected set in the complex plane (including the real line). By doing so, we can use the Identity

Theorem to establish contradiction arguments that lead to the impossibility of the set E_0 to have infinite number of points.

We extend the conditional entropy density $h_{F_0}(x|\alpha)$ to the complex plane. The conditional entropy density is given by

$$h_{F_0}(x|\alpha) = \int_0^{u_0} h_{F_0}(x|\alpha = u) dF_\alpha(u). \tag{3.48}$$

We first extend $h_{F_0}(x|\alpha = u)$ to the complex plane. For any $z = \eta + i\zeta \in \mathbb{C}$ and $u \in [0,\ u_0]$,

$$\begin{aligned}
|h_{F_X}(z|\alpha = u)| &\leq \int_{-\infty}^{\infty} |P_N(y - uz)| |\log f_{Y|\alpha}(y|u; F_X)| dy, \\
&= \int_{-\infty}^{\infty} \frac{1}{\sqrt{2\pi\sigma^2}} \left| \exp\left(\frac{-(y-uz)^2}{2\pi\sigma^2} \right) \right| |\log f_{Y|\alpha}(y|u; F_X)| dy, \\
&\leq \int_{-\infty}^{\infty} \frac{1}{\sqrt{2\pi\sigma^2}} \left| \exp\left(\frac{-(y-u\eta - iu\zeta)^2}{2\pi\sigma^2} \right) \right| [-\log(\gamma(y,u)) + 2|\log(k_3)|] dy, \\
&\leq \frac{1}{\sqrt{2\pi\sigma^2}} \exp\left(\frac{u\zeta^2}{2\sigma^2} \right) \int_{-\infty}^{\infty} \left| \exp\left(\frac{-(y-u\eta)^2}{2\pi\sigma^2} \right) \right| \\
&\qquad \left[\log(k_1) + k_2 |(y-uz)^2| + 2|\log(k_3)| \right] dy, \\
&\leq \frac{1}{\sqrt{2\pi\sigma^2}} \exp\left(\frac{u\zeta^2}{2\sigma^2} \right) \int_{-\infty}^{\infty} |P_N(y-u\eta)| \left[\log(k_1) + k_2 |(y-uz)^2| + 2|\log(k_3)| \right] dy, \\
&< \infty,
\end{aligned}$$

which is finite for any $|z| \leq \infty$. Thus, the extension of $h_{F_X}(z|\alpha = u)$ is well defined. The existence of the extension of $h_{F_0}(z|\alpha)$ is shown by defining M_u

$$M_u = \max_{u \in [0,\ u_0]} |h_{F_X}(z|\alpha = u)|. \tag{3.49}$$

Note that the M_u exists and attained since the conditional entropy $|h_{F_X}(z|\alpha = u)|$ is bounded and the support of α is compact.

Thus,

$$\begin{aligned}
|h_{F_0}(z|\alpha)| &= \left| \int_0^{u_0} h_{F_X}(z|\alpha = u) dF_\alpha(u) \right|, \\
&\leq \int_0^{u_0} |h_{F_X}(z|\alpha = u)| \, dF_\alpha(u), \\
&\leq M_u \int_0^{u_0} dF_\alpha(u), \\
&= M_u, \\
&< \infty,
\end{aligned}$$

and hence $h_{F_0}(z|\alpha)$ has an extension to the complex plane.

Since the probability density function of the noise $P_N(y - uz)$ is analytic, i.e., using Morera's theorem we can write

$$\oint_\omega P_N(z) dz = 0, \tag{3.50}$$

where ω is a closed contour on the complex plane. As a result, to show the analyticity of the of the conditional entropy density we need to show that the integration of the conditional entropy over a closed contour is zero. This can be shown as follows:

$$\begin{aligned}
\oint_\omega h_{F_X}(z|\alpha) dz &= -\oint_\omega \int_0^{u_0} \int_{-\infty}^{\infty} P_N(y - uz) \log(f_{Y|\alpha}(y|u; F_X)) du dy dz, \\
&\stackrel{a}{=} \int_0^{u_0} \int_{-\infty}^{\infty} \log(f_{Y|\alpha}(y|u; F_X)) \oint_\omega P_N(y - uz) dz du dy, \\
&= 0,
\end{aligned}$$

where in (a) we used Fubini's Theorem to change the order of integrations which can be justified by recalling that the inner integration is the conditional entropy density $|h_{F_X}(z|\alpha)|$ which was shown to be finite in (3.49). Now let us define M_ω as

$$M_\omega = \max_{z \in \omega} |h_{F_X}(z|\alpha)|, \tag{3.51}$$

M_ω exists since the conditional entropy $|h_{F_X}(z|\alpha)|$ is bounded and the contour ω is closed. Hence

$$\begin{aligned}
\left|\oint_\omega h_{F_X}(z|\alpha)dz\right| &= \left|\oint_\omega \int_0^{u_0}\int_{-\infty}^{\infty} P_N(y-uz)\log(f_{Y|\alpha}(y|u;F_X))dudydz\right|, \\
&\leq \oint_\omega \left|\int_{-\infty}^{\infty}\int_0^{u_0} P_N(y-uz)\log(f_{Y|\alpha}(y|u;F_X))dudy\right| dz, \\
&\leq \oint_\omega M_\omega dz, \\
&\leq M_\omega l_\omega, \\
&< \infty,
\end{aligned}$$

where l_ω is the length of ω which is finite as ω is a closed contour.

It is now straightforward to establish that the extension of the marginal density $i_{F_0}(z|\alpha)$ is well defined (since its difference with the entropy density is a constant). Also it is analytic on some open connected set $\mathcal{D} \subset \mathbb{C}$ including the real line.

To show that E_0 should have a finite number of mass points let us define the function $g(x,u) = i_{F_0}(x|\alpha = u) - I_{F_0}(X;Y|\alpha = u)$. The optimality condition is $\int_0^{u_0} g(x,u)dF_\alpha(u) = 0$. Thus,

$$\int_0^{u_0} \left(i_{F_0}(x|\alpha = u) - I_{F_0}(X;Y|\alpha = u)\right) dF_\alpha(u) = 0, \tag{3.52}$$

$$\int_0^{u_0} \left(-\int_{-\infty}^{\infty} P_N(y-ux)\log f_{y|\alpha}(y|u)dy - \frac{1}{2}\log(2\pi\sigma^2) - I_{F_0}(X;Y|\alpha = u)\right) dF_\alpha(u) = 0. \tag{3.53}$$

We note that the lower bound of the integration can be changed to 0^+ instead of 0; that is because if $u = 0$, $i_{F_0}(x|\alpha = u) = I_{F_0}(X;Y|\alpha = u) = 0$. Let us define $L(u) = I_{F_0}(X;Y|\alpha = u) + \frac{1}{2}\log(2\pi\sigma^2)$ and $\rho(y,u) \triangleq \log f_{y|\alpha}(y|u) + L(u)$. Define

$$\Omega_u^+ = \{y : \rho(y,u) \geq 0\}, \text{ and } \Omega_u^- = \{y : \rho(y,u) < 0\}. \tag{3.54}$$

Then,

$$\int_0^{u_0} \left[\int_{\Omega_u^+} P_N(y-ux)\rho(y,u)dy + \int_{\Omega_u^-} P_N(y-ux)\rho(y,u)dy\right] dF_\alpha(u) = 0. \tag{3.55}$$

For the set Ω_u^+, we have $\rho(y,u) \leq \log(\Gamma(y,u)) + L(u) \leq \log(k_3) + L(u)$, hence, $k_3(u) > 2^{-L(u)}$. Choose a constant l such that $l > 2uA + \sqrt{\frac{\log(k_3(u))+L(u)}{k_4 \log(e)}}$. Therefore, for very large values of x and $u > 0$

$$\begin{aligned}\int_{\Omega_u^+} P_N(y-ux)\rho(y,u)dy &\leq \int_{-l}^{l} P_N(y-ux)\rho(y,u)dy, \\ &\leq (\log(k_3(u)) + L(u)) \int_{-l}^{l} Q(y-ux)dy, \end{aligned} \tag{3.56}$$

which can be made arbitrary small by choosing large values for x, i.e.,

$$\int_{\Omega_u^+} P_N(y-ux)\rho(y,u)dy \leq 0. \tag{3.57}$$

On the other hand,

$$\begin{aligned}\int_{\Omega_u^-} P_N(y-ux)\rho(y,u)dy &\leq \int_{l}^{\infty} P_N(y-ux)\rho(y,u)dy, \\ &\leq \int_{l}^{\infty} P_N(y-ux)\left[\log(\Gamma(y,u)) + L(u)\right]dy, \\ &\overset{(a)}{<} \int_{x-A}^{x+A} q(A,u)\left[\log(\Gamma(x+A,u)) + L(u)\right]dy, \\ &< 2Aq(A,u)\left[\log(\Gamma(x+A,u)) + L(u)\right], \\ &< 0, \end{aligned} \tag{3.58}$$

where (a) follows from (4.4) and the fact that the integrable function is monotone in y. Let us define $M(x)$ as

$$M(x) = \max_{u\in[0,u_0]} g(x,u). \tag{3.59}$$

First we note that $M(x)$ is attainable for some $u \in [0,\ u_0]$ since the function $g(x,u)$ is continuous, and defined over a compact set. We also note from (3.56) and (3.58)

that $M(x) < 0$. As a result, we have

$$\begin{aligned}\int_0^{u_0} g(x,u)dF_\alpha(u) &\leq \int_0^{u_0} M(x)dF_\alpha(u),\\ &= M(x)\int_0^{u_0} dF_\alpha(u),\\ &= M(x),\\ &< 0,\end{aligned}$$

which contradicts with the optimality condition in (3.55), hence the set E_0 cannot have infinite number of mass points concluding the proof of the desired result.

3.4 Numerical Example

In order to exemplify our findings, we present the following numerical example. We consider a fading channel for which the channel coefficient α follows a truncated Rayleigh distribution, i.e., the probability density function of the channel coefficient is given by

$$f_\alpha(u) = \frac{4u}{1-\exp(-32)}\exp(-2u^2), \quad u \in [0,\ 4]. \tag{3.60}$$

We take a noise variance of 1.5, and an amplitude constraint of $A = 3$. We compute the capacity-achieving distribution by following an iterative algorithm similar to the one in [28] that starts by assuming that the input distribution has only two points and keep changing the number of points and computing the associated probabilities until the optimality conditions are satisfied. Figure 3.1 shows the resulting optimal input distribution for the example above.

We also compare the capacity of the truncated Rayleigh fading channel, with the same fading distribution, for two different input constraints: the first one is the peak-power constrained inputs and the second one is the average power constrained inputs. Both capacities are plotted in Figure 3.2 which shows that constraining the peak power reduces the channel capacity compared to constraining the average power.

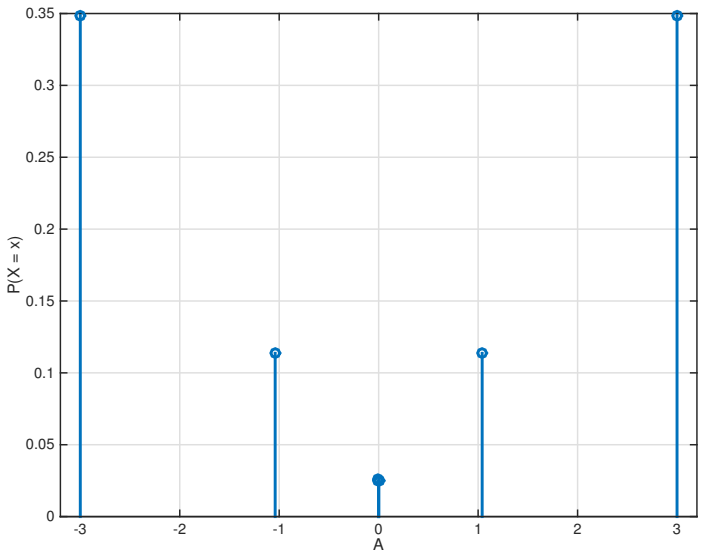

Figure 3.1: The optimal input distribution of a truncated Rayleigh fading channel with variance 1.5 and amplitude constraint equals to three.

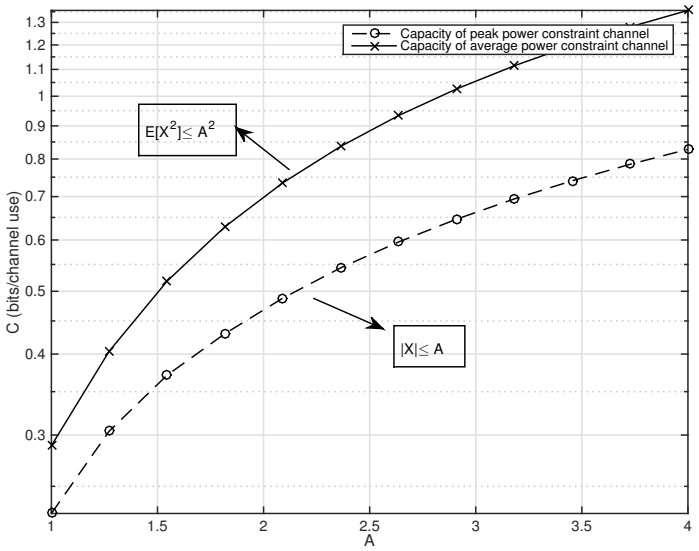

Figure 3.2: The capacity of the Rayleigh fading channel vs the amplitude constraint A.

3.5 Chapter Summary

In this chapter, we study the capacity of fading channels where the channel gain which is available at the receiver follows an arbitrary distribution with finite support. We show that the channel capacity is achieved by a unique optimal distribution and this distribution is discrete with a finite number of mass points, and we illustrate our findings via some numerical examples.

Chapter 4

CAPACITY OF AMPLITUDE-LIMITED AWGN CHANNELS WITH SIGNAL-DEPENDENT NOISE

The proposed communication scheme in Chapter 2 implies that the approximate channel model is a Gaussian channel with signal-dependent noise and amplitude-limited inputs. This motivates us to study the capacity of channels with signal-dependent additive Gaussian noise under peak power constraints. Such channel models appear in other applications as well. For instance, it appears in magnetic recording for which the media noise affects the reading and recording on the disk due to the jitter in the read head [62, 63]. As another example, this model is also suitable in free space optical communications where message bits are encoded and then modulated to create coded symbols which are transmitted via a laser beam through the optical channel. At the receiver side, the received optical signal is detected by avalanche photodiodes that convert it to an electrical signal. The photo detection process introduces extra noise to the system, this noise is modeled as signal-dependent noise. An existing channel model for the photo detection process in the optical communication is the Poisson channel model [64] at which the number of photons has a Poisson distribution with rate that depends on the current input. An approximate model is presented in [65] in which the the added noise to the transmitted signal is a signal-dependent Gaussian noise with variance related to the system parameter and the input signal.

Finding the capacity of signal-dependent additive Gaussian noise channels is of significant interest to facilitate a through understanding of the system proposed in Chapter 2. Motivated by this and other applications, in this chapter, we consider a Gaussian channel with signal-dependent noise with amplitude-limited inputs. We investigate the capacity of such channels and the capacity-achieving distributions.

Certain aspects of the problem of finding the capacity of signal-dependent Gaussian noise channels with amplitude-limited inputs has been studied in the previous literature. For example, Moser in [66] derives upper and lower bounds on the capacity of certain channels with input-dependent Gaussian noise. The upper bound relies on a dual expression for channel capacity and a new notion called the capacity-achieving input distributions that escape to infinity. The lower bound is based on a lower bound on the differential entropy of the channel output in terms of the differential entropy of the input.

Tchamkerten in [29] generalizes Smith's results in [28] for channels with additive noise which is not necessarily Gaussian. He shows that the capacity-achieving distributions of certain class of additive channels (that satisfy some regularity conditions) are discrete as well. Discrete distributions appear as optimal inputs in other cases too. As an example, quadrature Gaussian channels have been studied in [30], where the authors show that the capacity-achieving distribution has a uniformly distributed phase and discrete distribution of the amplitude. In [32], the authors study non-coherent AWGN channels and prove that the optimal input distribution is discrete, and they compute tight lower bounds on the capacity of the channel based on examination of some suboptimal input distributions. The authors in [35, 36] study the capacity of the multiple access channel (MAC) with amplitude-constrained inputs. They show that the sum-capacity achieving distribution is discrete. This distribution achieves rates at any of the corner points of the capacity region. In Chapter 3, we compute the capacity of fading channels under peak power constraints, and show that the capacity-achieving distribution is discrete even when the receiver has access to the channel state information.

In this chapter, we show that under some technical conditions and for well-

behaved noise, the capacity of signal-dependent Gaussian noise with arbitrary noise variance is achieved by a discrete input distribution. We follow similar arguments as in [35, 61], and show that the mutual information function is concave, continuous, and weakly differentiable over a compact and convex space of distributions. Then, we show that for well-behaved noise variance functions, the capacity is achieved by a discrete input distribution.

The chapter is organized as follows: In Section 4.1, we present the specific channel model under consideration where the additive noise is Gaussian with variance that depends on the transmitted signal. In Section 4.2, we show that the there is an input distribution that maximizes the mutual information by proving that the capacity is a continuous, concave function of the distribution, and weakly differentiable function. Then, in Section 4.3, we show that under some technical conditions on the noise variance, the input distribution is discrete using techniques from complex analysis. In Section 4.4, we present numerical examples for two models that exist in the literature; the first one is an optical communication based on intensity modulation which introduced by Moser in [66] and the second one is an example from magnetic recording channels. We finally conclude the chapter in Section 4.5 with a summary.

4.1 Channel Model

The received signal Y is given by

$$Y = X + N(X) + Z \tag{4.1}$$

where X is the channel input, $N(X)$ is the noise, and Y is the output random variable. We assume that the random variable X has an amplitude-constraint such that $|X| \leq A$ for some $A > 0$. Let $\mathcal{F}_X$ denote the corresponding class of distribution functions F_X; i.e., F_X in $\mathcal{F}_X$ implies $F_X(x) = 0$ for all $x < -A$ and $F_X(x) = 1$ for all $x \geq A$. $N(X)$ is an additive Gaussian noise, that depends on the transmitted signal X, with

zero mean and variance $\sigma_n^2(x)$ when $X = x$. We define $\sigma_n^2(x) = \sigma_n^2(A)$ for all $x \geq A$, and $\sigma_n^2(x) = \sigma_n^2(-A)$ for all $x \leq -A$ without loss of generality. We assume that $\sigma_n^2(x)$ is a bounded, continuous, and differentiable function of the input x. We note that if $\sigma_n^2(x) = 0$, then $N(X) = 0,\ \forall x \in [-A,\ \ A]$. Z is an independent additive Gaussian noise with variance σ_z^2.

The existence of $f_Y(y; F_X)$ is guaranteed by the boundedness and integrability of the noise function P_N, i.e.,

$$f_Y(y; F_X) = \int_{-A}^{A} P_N(y - x, x) dF_X(x). \tag{4.2}$$

The probability density function of the output $f_Y(y; F_X)$ can be bounded by

$$\gamma(y) \leq f_Y(y; F_x) \leq \Gamma(y), \tag{4.3}$$

where

$$\begin{aligned} \gamma(y) &= \min_{x \in [-A,A]} P_N(y - x, x) \\ &= \min_{x \in [-A,A]} \frac{1}{\sqrt{2\pi(\sigma_z^2 + \sigma_n^2(x))}} \exp\left[-\frac{(y-x)^2}{2(\sigma_z^2 + \sigma_n^2(x))} \right]. \\ &= k_1 e^{-k_2 (y - x_0)^2} \end{aligned}$$

where $x_0 = \arg\min_{x \in [-A,A]} P_N(y - x, x)$ and

$$\Gamma(y) = \max_{x \in [-A,A]} k \exp - \frac{(y-x)^2}{2(\sigma_z^2 + \sigma_n^2(x))}, \tag{4.4}$$

where k is defined as $k \triangleq \max_{x \in [-A,A]} \frac{1}{\sqrt{2\pi(\sigma_z^2 + \sigma_n^2(x))}}$; we clearly have $k < \infty$.

For a given distribution function F_X on the channel input X the average mutual information between X and Y will be denoted by $I_F(X; Y)$ and will be written as $I(F_X)$. The output entropy $H_F(Y)$ will be denoted as $H(F_X)$, and the conditional

entropy is denoted as $H_F(Y|X)$. The conditional entropy $H_F(Y|X)$ is given by

$$\begin{aligned} H_F(Y|X) &= \int_{-A}^{A} H(Y|X=x)dF(x), \\ &= \int_{-A}^{A} \frac{1}{2}\log(2\pi e(\sigma_n^2(x)+\sigma_z^2)dF(x), \\ &= \int_{-A}^{A} \frac{1}{2}\log(2\pi e\sigma_z^2)dF(x) + \frac{1}{2}\int_{-A}^{A} \log\left(1+\frac{\sigma_n^2(x)}{\sigma_z^2}\right)dF(x), \\ &= \frac{1}{2}\log(2\pi e\sigma_z^2) + \frac{1}{2}\mathbf{E}[\log(\sigma^2(X))], \end{aligned} \tag{4.5}$$

where $\sigma^2(x) = 1 + \frac{\sigma_n^2(x)}{\sigma_z^2}$. We note that the function $\sigma^2(x)$ is continuous and bounded and greater than or equal to one, hence the expectation $\frac{1}{2}\mathbf{E}[\log(\sigma^2(X))]$ exists. Thus, the average mutual information between the random variables X and Y is

$$I(F_X) = H(F_X) - D - \frac{1}{2}\mathbf{E}_F[\log(\sigma^2(X))], \tag{4.6}$$

where $D = \frac{1}{2}\log(2\pi e\sigma_z^2)$.

We define the mutual information density $i_F(x)$ and the entropy density $h_F(x)$ as

$$i_{F_X}(x) \triangleq \int_{-\infty}^{\infty} P_N(y-x,x)\log\frac{P_N(y-x,x)}{f_Y(y;F_x)}dy, \tag{4.7}$$

$$h_{F_X}(x) \triangleq -\int_{-\infty}^{\infty} P_N(y-x,x)\log f_Y(y;F_x)dy. \tag{4.8}$$

Thus, the following equation holds

$$i_{F_X}(x) = h_{F_X}(x) - \frac{1}{2}\log(\sigma^2(x)) - D. \tag{4.9}$$

The capacity $C(A)$ of such channel is defined as the maximum of the mutual information over the space of the probability distribution functions which is given by:

$$C(A) = \max_{F_X \text{ in } \mathcal{F}_\mathcal{X}} I(F_X). \tag{4.10}$$

4.2 Capacity Optimization Problem

In this section, we present our results on the capacity optimization problem of signal-dependent Gaussian channels with amplitude-limited inputs. Our results show that there is an optimal distribution that maximizes the mutual information and this distribution is discrete under certain technical conditions. To accomplish this, we first show that the mutual information is a concave function and hence an optimal distribution exists, and then we derive conditions on the optimal distribution using the Karush-Kuhn-Tucker (KKT) conditions. Finally, we investigate this optimal distribution using techniques from the real analysis, and we show that under some technical conditions on the function that relates the noise variance to the input signal the capacity-achieving distribution is discrete with a finite number of mass points. Our result is given in the following theorem:

Theorem 4.2.1. *C is achieved by a random variable, denoted by X_0 with probability distribution function $F_0 \in \mathcal{F}_X$, i.e.,*

$$C = \max_{F_X \in \mathcal{F}_X} I(F_X) = I(F_0) \tag{4.11}$$

for some $F_0 \in \mathcal{F}_X$. A necessary and sufficient condition for F_0 to achieve capacity is

$$i_{F_0}(x) \leq I(F_0), \quad \forall x \in [-A, A]. \tag{4.12}$$

Furthermore, this distribution is discrete and consists of finite number of mass points if some technical conditions on $\sigma^2(X)$ hold.

Proof. To prove the theorem, it is sufficient to show that the $\mathcal{F}_X$ is convex and compact in some topology, and that the mutual information $I(X;Y) : \mathcal{F}_X \to \mathbb{R}$ is a continuous, concave function, and weakly differentiable. Thus, invoking the KKT Theorem results in sufficient and necessary conditions for the optimal input probability distribution.

For the functional space $\mathcal{F}_X$, convexity and compactness follow by following similar arguments as in [61]. For the mutual information function, we first show that it is a continuous function using Helly-Bray Theorem [58]. Then, we show that it is concave in the input distribution. Finally, weak differentiability is shown by following similar line of arguments as in [61].

The discreteness of the input distribution is established using Bolzano-Weierstrass and the Identity Theorems that lead to contradiction arguments which conclude the discreteness of the input distribution. In the following subsections, we present the details of the proof. □

As described before the mutual information function is given by

$$I(F_X) = H(F_X) - D - \frac{1}{2}\mathbf{E}_F[\log(\sigma^2(X))]. \tag{4.13}$$

Hence, clearly, we note that the main difference between this work and the work in [61] is the existence of the expectation term $\frac{1}{2}\mathbf{E}_F[\log(\sigma^2(X))]$ and the difference in the form of $H(F_X)$ in the mutual information function. The objective of this work boils down to studying the effects of these on the concavity of the mutual information, its weak differentiability, and discreteness of the capacity-achieving distribution.

4.2.1 The Mutual Information is a Continuous Function of the Distribution

Let us fix a sequence $\{F_X^{(n)}(x)\}_{n\geq 1}$ in $\mathcal{F}_X$ such that $F_X^{(n)}(x) \to F_X$ for some $F_X \in \mathcal{F}_X$. Since the noise variance function $\sigma^2(X)$ continuous by assumption, $P_N(\cdot)$ is bounded and continuous as well. As a result

$$\begin{aligned}
\lim_{n\to\infty} f_Y(y; F_X^{(n)}) &= \lim_{n\to\infty} \int_{-A}^{A} P_N(y-x, x) dF_X^{(n)}(x), \\
&\overset{(a)}{=} \int_{-A}^{A} P_N(y-x, x) dF_X(x), \\
&= f_Y(y; F_X),
\end{aligned}$$

where (a) follows by the Helly-Bray Theorem [58]. Then,

$$\lim_{n\to\infty} f_Y(y; F_X^{(n)}) \log\left(f_Y(y; F_X^{(n)})\right) = f_Y(y; F_X) \log\left(f_Y(y; F_X)\right). \tag{4.14}$$

On the other hand, from (4.4),

$$\left|-f_Y(y; F_X^{(n)}) \log\left(f_Y(y; F_X^{(n)})\right)\right| \leq \Gamma(y)[-\log(\gamma(y)) + 2\left|\log(k)\right|], \tag{4.15}$$

and hence we can easily verify that

$$\left|\int_{-\infty}^{\infty} f_Y(y; F_X) \log\left(f_Y(y; F_X)\right) dy\right| < \infty. \tag{4.16}$$

Thus, by applying the Dominated Convergence Theorem, we have

$$\begin{aligned}\lim_{n\to\infty} \int_{-\infty}^{\infty} f_Y(y; F_X^{(n)}) \log\left(f_Y(y; F_X^{(n)})\right) dy &= \int_{-\infty}^{\infty} \lim_{n\to\infty} f_Y(y; F_X^{(n)}) \log\left(f_Y(y; F_X^{(n)})\right) dy, \\ &= \int_{-\infty}^{\infty} f_Y(y; F_X) \log\left(f_Y(y; F_X)\right) dy.\end{aligned}$$

We can conclude that the function $H(F_X)$ is a continuous function of the distribution. The continuity of $\mathbf{E}_F[\log(\sigma^2(X))]$ is straightforward and follows by another application of the Dominated Convergence Theorem (since $\sigma^2(X) \geq 1$ and it is bounded from above).

4.2.2 Concavity of the Mutual Information Function

The mutual information function is given by

$$I(F_X) = H(F_X) - D - \frac{1}{2}\mathbf{E}_{F_X}[\log(\sigma^2(X))]. \tag{4.17}$$

Since $\sigma^2(x)$ is bounded, we can write $0 \leq \log(\sigma^2(x)) \leq M_0$, where $M_0 < \infty$. Thus, we have,

$$\begin{aligned}\mathbf{E}_{F_X}[\log(\sigma^2(X))] &= \int_{-A}^{A} \log(\sigma^2(x)) dF_X(x), \\ &\leq M_0 \int_{-A}^{A} dF_X(x), \\ &= M_0, \\ &< \infty.\end{aligned}$$

The concavity of the output entropy $H(F_X)$ can be shown by considering the input distribution function $F_\theta = \theta F_1 + (1-\theta)F_2$. We can write

$$\begin{aligned} f_Y(y;F_\theta) &= \int_{-A}^{A} P_N(y-x,x)dF_\theta(x), \\ &= \theta\int_{-A}^{A} P_N(y-x,x)dF_1(x) + (1-\theta)\int_{-A}^{A} P_N(y-x,x)dF_2(x), \\ &= \theta f_Y(y;F_1) + (1-\theta)f_Y(y;F_2). \end{aligned}$$

To show the concavity of the entropy function we will use Ash's Lemma [57] to bound the entropy which applies due to its finiteness, i.e.,

$$\begin{aligned} |H(F_X)| &= \left| -\int_{-\infty}^{\infty} f_Y(y;F_X)\log\left(f_Y(y;F_X)\right)dy \right|, \\ &\leq \int_{-\infty}^{\infty} |f_Y(y;F_X)|\,|\log\left(f_Y(y;F_X)\right)|\,dy, \\ &\leq \int_{-\infty}^{\infty} \Gamma(y)\left[-\log(\gamma(y)) + 2|\log k_1|\right]dy, \\ &< \infty. \end{aligned}$$

Hence, the output entropies corresponding to the input distribution functions F_1 and F_2, respectively, are

$$H(F_1) \leq -\int_{-\infty}^{\infty} f_Y(y;F_1)\log\left(f_Y(y;F_\theta)\right)dy, \tag{4.18}$$

and

$$H(F_2) \leq -\int_{-\infty}^{\infty} f_Y(y;F_2)\log\left(f_Y(y;F_\theta)\right)dy. \tag{4.19}$$

As a result, the output entropy corresponding to the input distribution F_θ is

$$\begin{aligned} H(F_\theta) &= -\theta\int_{-\infty}^{\infty} f_Y(y;F_1)\log\left(f_Y(y;F_\theta)\right)dy - (1-\theta)\int_{-\infty}^{\infty} f_Y(y;F_2)\log\left(f_Y(y;F_\theta)\right)dy, \\ &\geq \theta H(F_1) + (1-\theta)H(F_2). \end{aligned}$$

Thus, $H(F_X)$ is a concave function of the input distribution function. For the mutual

information, we can write

$$\begin{aligned} I(\theta F_1 + (1-\theta)F_2) &= H(\theta F_1 + (1-\theta)F_2) - D - \frac{1}{2}\int_{-A}^{A} \log(\sigma^2(x))\,(\theta dF_1 + (1-\theta)dF_2)\,, \\ &\geq \theta H(F_1) - \theta \textstyle\int_{-A}^{A} \log(\sigma^2(x)) dF_1 - \theta D + (1-\theta)H(F_2) - (1-\theta)\int_{-A}^{A} \log(\sigma^2(x)) dF_2 - (1-\theta)D, \\ &= \theta I(F_1) + (1-\theta) I(F_2). \end{aligned}$$

Hence, the function $I(F_X)$ is a concave function of the input distribution.

4.2.3 The Mutual Information Function $I(F_X)$ Is Weakly Differentiable

For arbitrary F_1, F_2, $\theta \in [0,1]$, defining $F_\theta = (1-\theta)F_1 + \theta F_2$, we have

$$I(F_\theta) = H(F_\theta) - D - \frac{1}{2}\mathbf{E}_{F_\theta}[(\log(\sigma^2(X))]. \tag{4.20}$$

Define $J(\theta, F_1, F_2) = \frac{I(F_\theta) - I(F_1)}{\theta}$, we can write

$$\begin{aligned} J(\theta, F_1, F_2) &= \frac{H(F_\theta) - H(F_1)}{\theta} - \frac{1}{2}\frac{\mathbf{E}_{F_\theta}[\log(\sigma^2(X))] - \mathbf{E}_{F_1}[\log(\sigma^2(X))]}{\theta}, \\ &= \frac{H(F_\theta) - H(F_1)}{\theta} - \frac{1}{2}\left(\mathbf{E}_{F_2}[(\log(\sigma^2(X))] - \mathbf{E}_{F_1}[\log(\sigma^2(X))]\right). \end{aligned}$$

We then have

$$\begin{aligned} I'_{F1}(F_2) &= \lim_{\theta\to 0} J(\theta, F_1, F_2) &(4.21)\\ &= \lim_{\theta\to 0}\left[\frac{H(F_\theta) - H(F_1)}{\theta}\right] - \frac{1}{2}\left(\mathbf{E}_{F_2}[\log(\sigma^2(X))] - \mathbf{E}_{F_1}[\log(\sigma^2(X))]\right). &(4.22)\end{aligned}$$

Following similar arguments as in Smith [28], we obtain

$$\lim_{\theta\to 0}\frac{H(F_\theta) - H(F_1)}{\theta} = \int_{-A}^{A} h(x; F_1) dF_2(x) - H(F_1) \tag{4.23}$$

$$I'_{F_1}(F_2) = \int_{-A}^{A}\left(h(x;F_1) - \frac{1}{2}\log(\sigma^2(x))\right) dF_2(x) - H(F_1) - \frac{1}{2}\mathbf{E}_{F_1}[(\log(\sigma^2(X))]. \tag{4.24}$$

Thus,

$$I'_{F_1}(F_2) = \int_{-A}^{A} i(x; F_1) dF_2 - I(F_1). \tag{4.25}$$

As a result of this theorem and similar to what is done in [28], we can show that the following conditions are sufficient and necessary conditions on the optimal distribution F_0:

$$i(x;F_0) - I(F_0) \leq 0, \qquad \forall x \in [-A, A], \tag{4.26}$$

$$i(x;F_0) - I(F_0) = 0, \qquad \forall x \in E_0, \tag{4.27}$$

where E_0 is the set of points of increase of F_0.

We have shown that there is an optimal distribution that maximizes the mutual information. In the next subsection, we show that under certain technical conditions on the noise function, the capacity-achieving distribution of the signal-dependent AWGN channel is discrete with finite number of mass points.

4.3 The Capacity-Achieving Distribution is Discrete

We first assume the following: the logarithm of the noise variance function $\log(\sigma^2(x))$ can be extended to an open connected set in the complex plane containing the real line $\mathbb{R}$ (possible excluding certain branch points denoted by the set Ψ). We also assume that the function $\log(\sigma^2(z))$ is analytic over some open connected set $\mathcal{D} \in \mathbb{C}$ on the complex domain[1].

We define the extension of the noise variance function on the real line as follows:

$$\sigma_r^2(x) = \begin{cases} \sigma^2(-A) & \text{if } x < -A, \\ \sigma^2(x) & \text{if } x \in [-A, A], \\ \sigma^2(A) & \text{if } x > A. \end{cases} \tag{4.28}$$

From the optimality condition,

$$i_{F_X}(x) = h_{F_X}(x) - \frac{1}{2}\log(\sigma^2(x)) - D, \quad \forall x \in E_0 \tag{4.29}$$

[1]The function $log(\sigma^2(z))$ is defined over an open connected set on the complex plane except branch cuts that can be defined such that they do not include the entire real line.

First, we extend the function $i_{F_X}(x)$ to the complex plane. In order to do so, we show that the entropy can be extended to the complex plane as shown in Appendix C and D. The discreteness of the optimal distribution can be established through the following contradiction arguments.

- We assume that the set E_0 contains infinite number of mass points.
- Since E_0 is a bounded set, then any sequence in E_0 has a limit point (Bolzano-Weierstrass Theorem).
- The functions $h_{F_0}(z)$, and $I(F_0) + \frac{1}{2}\log(\sigma^2(z)) + D$ are analytic on some open connected set $\mathcal{D}$ in the complex plane $\mathbb{C}$ that includes the real line $\mathbb{R}$ except the set of branch points Ψ. Using the Identity Theorem, we conclude that this equality holds on an open connected set in the complex plane, i.e.,

$$h_{F_0}(z) = I(F_0) + \frac{1}{2}\log(\sigma^2(z)) + D, \quad \forall z \in \mathcal{D}. \tag{4.30}$$

- This implies that $h_{F_0}(x) = I(F_0) + \frac{1}{2}\log(\sigma^2(x)) + D$ on the entire real line except the branch points of $\log(\sigma^2(z))$ which leads to a contradiction when x is sufficiently large. We note that the branch points of the function $\log(\sigma^2(z))$ are only located in the region between $[-A, A]$ because out of this region the noise variance is defined to be constant and strictly greater than one.

  A contradiction can be established by following similar line of arguments as in [35]. From the optimality condition we have

$$h_{F_0}(x) - I(F_0) - \frac{1}{2}\log(\sigma_r^2(x)) - D = 0, \quad \forall x \in \mathbb{R} - \Psi. \tag{4.31}$$

  We note that $\sigma^2(x) \geq 1$, and hence $\log(\sigma^2(x)) \geq 0$. Let us define $L \triangleq I(F_0) + D + \frac{1}{2}\log(\sigma^2(A))$ and $\rho(y) \triangleq \log(f_Y(y; F_0)) + L + \frac{1}{2}\log(\sigma^2(A))$. For sufficiently

large values of x, i.e., $x > A$, we have

$$h_{F_x}(x) - I(F_X) - \frac{1}{2}\log(\sigma^2(A)) - D = 0, \quad \forall x > A, \tag{4.32}$$

which can be written as

$$\int_{-\infty}^{\infty} P_N(y-x,x)\left[\log(f_Y(y;F_0)) - \frac{1}{2}\log(\sigma^2(A)) - D\right]dy = 0, \quad \forall x > A, \tag{4.33}$$

and

$$P_N(y-x,x) = P_N^*(y-x) = \frac{1}{\sqrt{2\pi(\sigma_z^2+\sigma_n^2(A))}}\exp\left(-\frac{(y-x)^2}{2(\sigma_z^2+\sigma_n^2(A))}\right), \ \forall x > A. \tag{4.34}$$

We define

$$\Omega^+ \triangleq \{y : \rho(y) \geq 0\}, \text{ and } \Omega^- \triangleq \{y : \rho(y) < 0\}. \tag{4.35}$$

Then,

$$\int_{\Omega^+} P_N(y-x,x)\rho(y)dy + \int_{\Omega^-} P_N(y-x,x)\rho(y)dy = 0. \tag{4.36}$$

By (4.4), we get $\rho(y) \leq \log(\Gamma(y)) + L + \frac{1}{2}\log(\sigma^2(A)) \leq \log(k) + L + \frac{1}{2}\log(\sigma^2(A))$, for any $y \in \mathbb{R}$, and $x > A$. From, (4.36) we choose $k > 2^{-(L+\frac{1}{2}\log(\sigma^2(A)))}$. Choose a constant l such that $l > A - \frac{1}{\pi k^2}\log(k)$. Using (4.4), one has $\Omega^+ \subseteq [-l, l]$. Therefore,

$$\begin{aligned}
\int_{\Omega^+} P_N(y-x,x)\rho(y)dy &\leq \int_{-l}^{l} P_N^*(y-x,x)\rho(y)dy, \\
&\leq \left(\log(k) + L + \frac{1}{2}\log(\sigma^2(A))\right)\int_{-l}^{l} P_N^*(y-x)dy, \quad (4.37) \\
&\leq 0, \quad (4.38)
\end{aligned}$$

which can be arbitrarily small by choosing x large enough due to the behavior of the noise probability density function. On the other hand, for $x > A + l$, we

have

$$\begin{aligned}
\int_{\Omega^-} P_N(y-x,x)\rho(y)dy &\leq \int_l^{\infty} P_N(y-x,x)\rho(y)dy, \\
&\leq \int_l^{\infty} P_N(y-x,x)\left[\log(\Gamma(y)) + L + \frac{1}{2}\log(\sigma^2(A))\right]dy, \\
&\overset{(a)}{<} \int_{x-A}^{x+A} q(A,x)\left[\log(\Gamma(x+A)) + L + \frac{1}{2}\log(\sigma^2(A))\right]dy \\
&< 2Aq(A,x)\left[\log(\Gamma(x+A)) + L + \frac{1}{2}\log(\sigma^2(A))\right] \\
&< 0
\end{aligned}$$

where (a) follows from (4.4) and the fact that the integrable function is monotone in y. By combining (4.38) and (4.39), we can establish that (4.31) does not hold for large values of x and hence there is contradiction and the set E_0 cannot have an infinite number of mass points. Hence the proof is complete.

4.4 Numerical Examples

In this section, we present two examples that show the capacity for some signal-dependent noise Gaussian channels with amplitude-limited inputs. The first model we consider is the optical communication channel based on intensity modulation which has been studied in detail by Moser in [66]. The received signal Y is given by,

$$Y = x + \sqrt{x}Z_1 + Z_0, \tag{4.39}$$

where $x \geq 0$ denotes the channel input $Z_0 \sim \mathcal{N}(0,\sigma^2)$ is a zero-mean, variance σ^2 Gaussian random variable describing the input-independent noise and $Z_1 \sim \mathcal{N}(0,\varsigma\sigma^2)$ is a zero-mean, variance $\varsigma\sigma^2$ Gaussian random variable describing the input-dependent noise. Here Z_0 and Z_1 are assumed to be independent. The parameter $\sigma^2 > 0$ describes the strength of the input-independent noise, while $\varsigma > 0$ is the ratio of the input-dependent noise variance to the input-independent noise. Thus, $\sigma^2(x) = 1+\varsigma x$. In [66], Moser derives an approximation for the channel capacity at small signal-to-

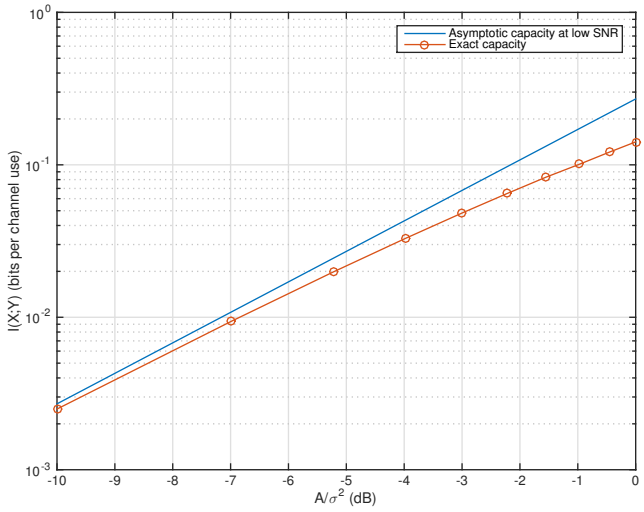

Figure 4.1: Asymptotic capacity of intensity modulated optical channel at low values of SNRs.

noise ratios (SNRs) and a universal lower bound for any amplitude value and an upper bound that is valid only at high SNRs.

The function $\log(\sigma^2(z)) = \log(1+\varsigma z)$ has a branch point at $z = -\frac{1}{\varsigma}$ and hence we can define a branch cut as the line connecting the two points $\{(-\frac{1}{\varsigma}, 0), (-\frac{1}{\varsigma}, \tilde{\infty})\}$, where $\tilde{\infty}$ represents the complex infinity. The, the extension of the function $\sigma^2(x)$ is well defined on the whole complex plane except the line connecting the two points $\{(-\frac{1}{\varsigma}, 0), (-\frac{1}{\varsigma}, \tilde{\infty})\}$.

Figure 4.1 shows the capacity of the above optical channel model at low SNRs along with the approximate formula for the capacity derived in [66]. Figure 4.3 shows the capacity of intensity modulated optical channel along with a universal lower bound derived by Moser in his work in [66] and an upper bound that is valid only at high SNR values.

As a second illustration, we present another example in which the signal-dependent noise appears as the dominating noise, i.e., in magnetic recording systems

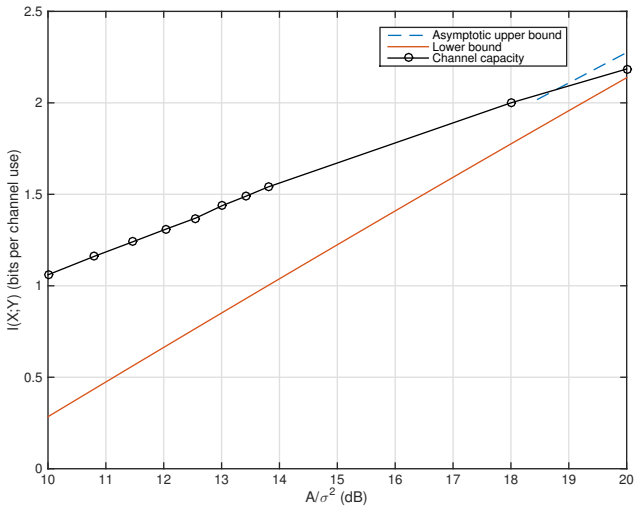

Figure 4.2: The capacity of intensity modulated optical channel along with an upper and lower bound on it.

where the media noise is strongly signal-dependent and is modeled as Gaussian noise with variance $\sigma^2(x) = 1 + \sqrt{1 - x^2}$, where the input signal $|x| < 1$ [3]. The extension of the function $\log(\sigma^2(x))$ to the complex plane $\log(1 + \sqrt{1 - z^2})$ has two branch points, $(1, 0)$, $(-1, 0)$, the branch cuts can be chosen such that they do not include other parts of the real line as, for instance, as the lines connecting $\{(1, 0), (1, \tilde{\infty})\}$ and $\{(-1, 0), (-1, \tilde{\infty})\}$. Figure 4.3 shows the capacity of this magnetic recording system along with a lower bound on it. The lower bound is computed based on an evaluation of the mutual information with a suboptimal input distribution. We observe that the capacity calculated is much higher than the mutual information evaluated with the specific truncated Gaussian distributions.

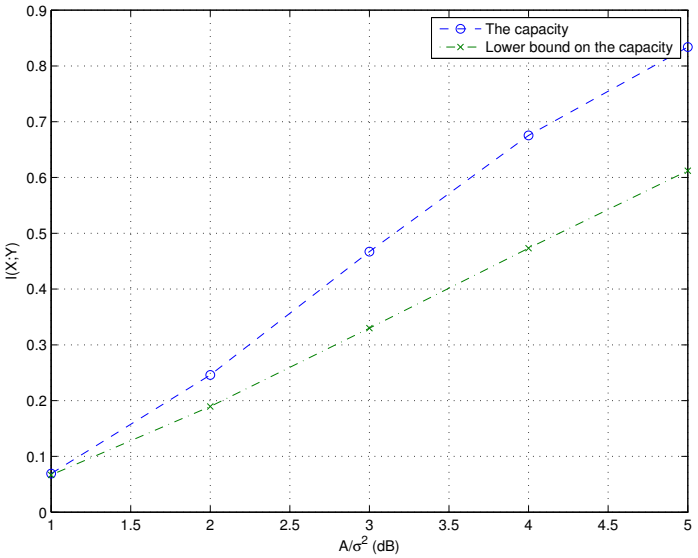

Figure 4.3: The capacity of the magnetic recording system modeled as in [3].

4.5 Chapter Summary

In this chapter, we studied the capacity of Gaussian channels with signal-dependent noise and peak power constrained inputs. We show that under some technical conditions on the noise variance functions, the capacity achieving distribution is discrete with a finite number of mass points. We developed the results by showing that the mutual information is a continuous, concave, and weakly differentiable function of the input distribution. We used some theorems and arguments from the complex analysis to conclude the discreteness of the optimal input distribution. We have also presented numerical examples using channel models that appear in optical communication and magnetic recording systems.

Chapter 5

MULTIPLE-ANTENNA SYSTEMS WITH AMPLITUDE-LIMITED INPUTS

Motivated by the equivalent system model proposed in Chapter 2, we now study the capacity of mutiple-antenna systems under peak power constraints. In Chapters 3 and 4, we have studied the capacity of single-antenna fading channels under peak power constraints, and the capacity of scalar Gaussian channel with signal-dependent noise. We now turn our attention to the case of mutiple-antenna systems and parallel Gaussian channels.

Capacity of multi-input channels with amplitude-limited inputs has been considered recently, but in a different communication scenario. Specifically, the authors in [35, 36] study the capacity of the multiple access channel (MAC) with amplitude-constrained inputs. They show that the sum-capacity achieving distribution is discrete. This distribution achieves rates at any of the corner points of the capacity region. We note, however, that these results are not applicable to the problem at hand, i.e., on the problem of capacity of MIMO channels with amplitude-limited inputs.

In the first part of the chapter, we study the capacity of MIMO systems. For the special case of multiple-input single-output (MISO) channels, it is easy to argue that the capacity achieving distribution exists and it is discrete. However, there is no uniqueness result as the capacity-optimization problem boils down to an optimization problem that aims to choose a distribution for the sum of the channel inputs which maximizes the mutual information. Hence, different marginal distributions for the inputs can be chosen such that the distribution of their sum is the same as the distribution that results from the solution of the optimization problem. However, for the case of MIMO communications showing the discreteness of the capacity-achieving

distribution does not seem possible by adopting the existing techniques. The reason behind this non-viability is that the discreteness of the capacity-achieving distribution is proved through some arguments based on the Identity Theorem in complex analysis [67]. However, the Identity Theorem is only available for one-dimensional functions and there is no equivalent result for the multi-dimensional case. More precisely, we can show that there is a unique optimal distribution that maximizes the mutual information function. However, we are not be able to provide any characterization for that distribution, hence finding the capacity-achieving distribution does not seem feasible. Therefore, we direct our attention to computation of bounds on the capacity, that is, we derive upper and lower bounds on the capacity of MIMO systems. The bounds rely on transforming the coupled MIMO channel into decoupled (independent) channels with coupled inputs, and then relaxing the constraint imposed on these inputs or restricting them further. In our study, we consider the 2×2 MIMO case in detail and simply note that extending the results for arbitrary number of antennas is possible.

In the second part of the chapter, we investigate the capacity of parallel Gaussian channels under peak and average power constraints. It is straightforward to show that the capacity achieving distribution is discrete as this can be implied directly from Smith's results. Also, the authors in [34] show (through a different approach) that the capacity-achieving distribution is discrete. However, there is no-closed form expression and finding the capacity achieving distribution requires numerical computations with high complexity particularly when the number of parallel channels is large. With this motivation, we consider the behavior of such channels asymptotically in the low and high signal-to-noise ratio (SNR) regimes. Our approach is based on the following: in the very high noise variance regime, the capacity-achieving distribution consists only of two points, hence using the data processing inequality the problem

boils down to be finding the capacity of (parallel) binary channels, and in the low noise variance regime, the capacity-achieving distribution can be approximated by a continuous distribution. We provide the optimal power assignment for the case of N-parallel channels case; by adopting a technique from the calculus of variations to show that the capacity-achieving distribution in the very low noise variance regime is a Gaussian-like distribution with a truncated domain.

The chapter is organized as follows. In Section 5.1, we describe the channel model for a general MIMO system. In Section 5.2, we compute the capacity of MISO systems, and we show that the capacity-achieving distribution is discrete. In Section 5.3, we use singular value decomposition to decouple the system into parallel independent channels. Then, we propose the upper and lower bounds by relaxing the input constraints of the new optimization problem. Finally, we describe an alternative lower bounding approach. In Section 5.4, we study the capacity of the parallel Gaussian channels under peak and average power constraints. In Section 5.5, we present numerical examples to demonstrate our findings, and conclude the chapter with a summary in Section 5.6.

5.1 System Models

We consider a MIMO system where the received signal $\mathbf{y}$ is written as

$$\mathbf{y} = \mathbf{H}\mathbf{x} + \mathbf{z}, \tag{5.1}$$

where $\mathbf{H}$ is an $N_r \times N_t$ channel matrix, N_r is the number of receive elements, and N_t is the number of transmit elements. The channel matrix $\mathbf{H}$ is assumed to be deterministic. The vector $\mathbf{z}$ denotes an AWGN vector whose elements are independent and identically distributed (i.i.d.) and each is $z_i \sim \mathcal{N}(0, \sigma^2)$, where σ^2 is the noise variance. We assume that the channel inputs and outputs, the channel matrix and noise terms are all real valued to simplify the exposition of the results.

For much of the results on the MIMO communications, we consider the case of a 2×2 MIMO system with $N_r = 2$ and $N_t = 2$. Hence, the channel input $\mathbf{x}$ has a two-dimensional joint distribution $f(x_1, x_2)$ and the channel inputs are amplitude limited as $|X_1| \leq A_{x_1}$ and $|X_2| \leq A_{x_2}$. As the channel under consideration is deterministic, we assume that it is known both at the transmitter and the receiver. The capacity of the 2×2 MIMO system is the maximum of the mutual information between the input and the output of the channel under the given input constraints, i.e.,

$$C = \max_{f(x_1,x_2):|X_1|\leq A_{x_1},|X_2|\leq A_{x_2}} I(Y_1, Y_2; X_1, X_2). \tag{5.2}$$

The main issue in solving this optimization problem using Smith's original approach is that the Identity Theorem used in characterizing the capacity achieving distribution is only applicable for one-dimensional functions.

For the parallel Gaussian channels, we have a set of N Gaussian channels with outputs given by

$$y_i = x_i + z_i, \quad \forall i = 1, 2, \cdots, N, \tag{5.3}$$

where $|x_i| \leq A_i$, and z_i is an AWGN with zero mean and variance σ_i^2. For N parallel Gaussian channels, the mutual information between the input vector $\mathbf{X}$ and the output vector $\mathbf{Y}$ is given by

$$I(X_1, X_2, \cdots, X_N; Y_1, Y_2, \cdots, Y_N) = h(Y_1, Y_2, , \cdots, Y_N) - \sum_{i=1}^{N} h(Z_i), \tag{5.4}$$

where $h(Z_i)$ is the entropy of the Gaussian noise random variable Z_i which is given by $h(Z_i) = \frac{1}{2}\log(2\pi e\sigma^2)$. The optimal input distribution for the N parallel Gaussian channels under peak and average power constraints has been shown in to be discrete and independent of each other [34]. Hence,

$$I(X_1, X_2, \cdots, X_N; Y_1, Y_2, \cdots, Y_N) = \sum_{i=1}^{N} h(Y_i) - \sum_{i=1}^{N} h(Z_i). \tag{5.5}$$

The channel capacity is then

$$C = \max_{\substack{f(x_1,x_2,\cdots,x_N):|X_i|\leq A_i,\\ \sum_i X_i^2 \leq P_0}} \sum_{i=1}^{N} h(Y_i) - \sum_{i=1}^{N} h(Z_i). \tag{5.6}$$

5.2 Capacity of MISO Systems with Amplitude-Limited Inputs

Since there is only one receive antenna in this case, the received signal y can be written as

$$y = h_1 x_1 + h_2 x_2 + z. \tag{5.7}$$

Define an auxiliary variable u such that $u = h_1 x_1 + h_2 x_2$. Since x_1 and x_2 are amplitude-limited, u will also be amplitude limited, i.e.,

$$-|h_1|A_{x_1} - |h_2|A_{x_2} \leq u \leq |h_1|A_{x_1} + |h_2|A_{x_2}. \tag{5.8}$$

Thus, the received signal y can be written as $y = u + z$, and the problem boils down to the classical point-to-point scalar problem that has been investigated by Smith. Hence, the distribution of the auxiliary random variable U that achieves the capacity is discrete, i.e.,

$$f_U(u) = \sum_{i=0}^{N-1} p(u_i)\delta(u - u_i) \tag{5.9}$$

where the number of mass points N are to be determined numerically by solving the capacity optimization problem using the algorithm given in [28]. The specific channel inputs x_1 and x_2 can be arbitrarily generated such that their weighted sum (weighted by the channel coefficients) follows the optimal probability mass function of the random variable U.

5.3 Bounds on the Capacity of 2×2 MIMO Systems with Amplitude-Limited Inputs

For a 2×2 MIMO system, we obtain an equivalent model via the singular value decomposition of the channel matrix $\mathbf{H}$, i.e., $\mathbf{H} = \mathbf{U}\Omega\mathbf{W}^H$. That is,

$$\tilde{\mathbf{y}} = \Omega\tilde{\mathbf{x}} + \tilde{\mathbf{z}}, \tag{5.10}$$

where $\tilde{\mathbf{y}} = \mathbf{U}^H\mathbf{y}$, $\tilde{\mathbf{x}} = \mathbf{W}^H\mathbf{x}$, and $\tilde{\mathbf{z}} = \mathbf{U}^H\mathbf{z}$, where $\mathbf{U}$ and $\mathbf{W}$ are unitary matrices. Define $\mathbf{V} = \mathbf{W}^H$. Since the amplitude of the first channel input is constrained by A_{x_1} and the amplitude of the second input is constrained by A_{x_2}, the domain of $\mathbf{x}$ is a rectangular region. However, after applying the singular value decomposition, in the equivalent formulation, the region defining the input constraint turns out to be a parallelogram. Further, this region will be centered at origin (since the original rectangular region is symmetric around origin).

Define the following terms that characterize the new input constraint

$$a = \frac{\det(\mathbf{V})}{v_{22}}, \quad b = \frac{v_{12}}{v_{22}},$$

and

$$c = -\frac{\det(\mathbf{V})}{v_{21}}, \quad d = \frac{v_{11}}{v_{21}},$$

where v_{ij} is the ijth element of the matrix $\mathbf{V}$.

Then the feasible region of the equivalent channel in (5.10) is,

$$-\frac{1}{a}x + \frac{b}{a}y \leq A_{x_1},\ \frac{1}{a}x - \frac{b}{a}y \leq A_{x_1},$$

and

$$-\frac{1}{c}x + \frac{d}{c}y \leq A_{x_2},\ \frac{1}{c}x - \frac{d}{c}y \leq A_{x_2}.$$

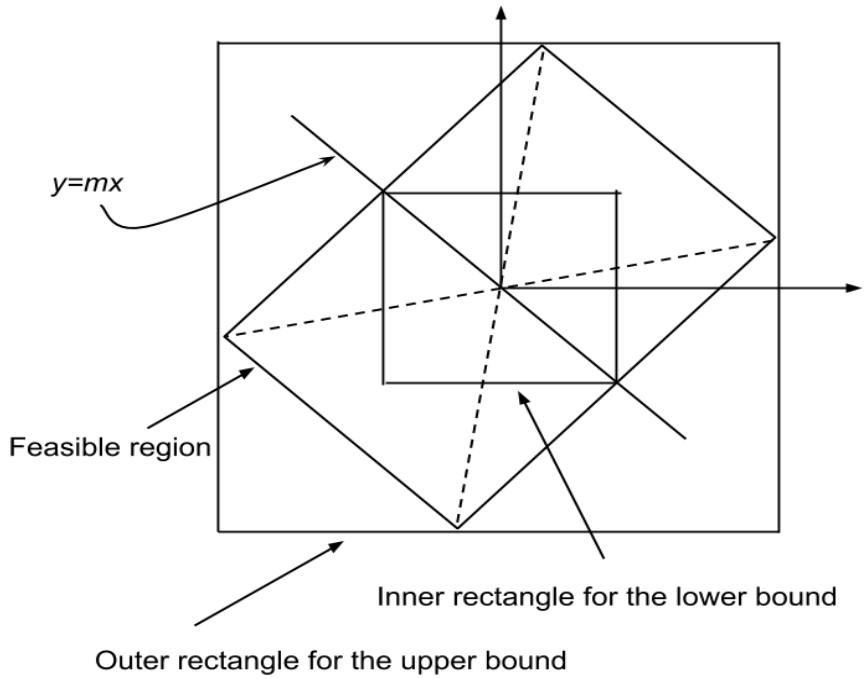

Figure 5.1: The actual feasible region and a smaller region represents the lower bound and an outer region represent the upper bound.

We derive upper and lower bounds on the capacity using this new formulation. We obtain the lower bound by looking for a smaller feasible region inside the parallelogram, i.e., we consider a rectangle inside, and we compute the corresponding mutual information between the input and output with the channel input vector constrained to be inside this rectangular region. For the upper bound, we follow a similar approach, i.e., we look for the the smallest rectangle that inscribes the parallelogram. This geometrical interpretation of the approach is illustrated in Fig. 5.1.

In both the lower and upper bounds, we choose to replace the feasible region with a rectangular one as the rectangular feasible region enables us to separate the two-dimensional problem into two one-dimensional problems whose solutions are readily available.

5.3.1 An Upper Bound on the Capacity of 2×2 MIMO Systems with Amplitude-Limited Inputs

A capacity upper bound is derived by solving the capacity optimization problem over the smallest rectangle that inscribes the original feasible region. This rectangle is constructed from the intersection points of every pair of lines forming the feasible region. The first intersection point is

$$x = \frac{bc}{d-b}A_{x_2} - \frac{ad}{d-b}A_{x_1},\ y = \frac{c}{d-b}A_{x_2} - \frac{a}{d-b}A_{x_1},$$

the second point is

$$x = -\frac{bc}{d-b}A_{x_2} - \frac{ad}{d-b}A_{x_1},\ y = -\frac{c}{d-b}A_{x_2} - \frac{a}{d-b}A_{x_1},$$

the third point is

$$x = \frac{bc}{d-b}A_{x_2} + \frac{ad}{d-b}A_{x_1},\ y = \frac{c}{d-b}A_{x_2} + \frac{a}{d-b}A_{x_1},$$

and the forth point is

$$x = -\frac{bc}{d-b}A_{x_2} + \frac{ad}{d-b}A_{x_1},\ y = -\frac{c}{d-b}A_{x_2} + \frac{a}{d-b}A_{x_1}.$$

Using the geometric interpretation of the feasible region, it is easy to show that in the equivalent formulation of the 2×2 MIMO system, the new amplitude limits on the two inputs

$$\Delta x_{upp} = \left|\frac{bc}{d-b}A_{x_2}\right| + \left|\frac{ad}{d-b}A_{x_1}\right|, \tag{5.11}$$

$$\Delta y_{upp} = \left|\frac{c}{d-b}A_{x_2}\right| + \left|\frac{a}{d-b}A_{x_1}\right|, \tag{5.12}$$

can be used to compute an upper bound on the channel capacity of the original MIMO system. Namely, the upper bound of the channel capacity is given by

$$C \leq C_0(\Delta x_{upp}) + C_0(\Delta y_{upp}), \tag{5.13}$$

where $C_0(A)$ is the capacity of the point-to-point AWGN channel for a given amplitude constraint A (computed using Smith's approach).

5.3.2 A Lower Bound on the Capacity of MIMO Systems with Amplitude-Limited Inputs

A lower bound on the capacity of the channel can be found by optimizing the mutual information over a smaller rectangular region inside the feasible region (parallelogram). To find such a rectangle, we determine the intersection of a straight line, $y = mx$, that passes through the origin (as the region is centered at the origin) and the boundary of the feasible region. In this case, it is easy to show that

$$\Delta x_{low} = \min\left(\left|\frac{aA_{x_1}}{1+bm}\right|, \left|\frac{aA_{x_1}}{1-bm}\right|, \left|\frac{cA_{x_2}}{1+dm}\right|, \left|\frac{cA_{x_2}}{1-dm}\right|\right), \tag{5.14}$$

$$\Delta y_{low} = \min\left(\left|\frac{amA_{x_1}}{1+bm}\right|, \left|\frac{amA_{x_1}}{1-bm}\right|, \left|\frac{cmA_{x_2}}{1+dm}\right|, \left|\frac{cmA_{x_2}}{1-dm}\right|\right), \tag{5.15}$$

for some arbitrary values for the slope m such that the set of points

$$\left\{(l\Delta x_{low}, k\Delta y_{low}) \in \mathcal{R} : l, k \in \{1, -1\}\right\},$$

where $\mathcal{R}$ is the feasible region. Thus, the lower bound on the channel capacity is given by

$$C \geq C_0(\Delta x_{low}) + C_0(\Delta y_{low}). \tag{5.16}$$

5.3.3 Bounds on the Capacity of General MIMO Systems with Amplitude-Limited Inputs

For the case of MIMO systems with larger number of transmit and receive elements, a similar approach can be followed to derive upper and lower bounds on the capacity of the channel with amplitude constraints. However, the feasible region of the capacity

optimization problem will not be a simple rectangle in the two-dimensional space as in the case of 2×2 systems. In other words, although numerical methods can be used to compute the resulting upper and lower bounds on the channel capacity for different noise levels, closed form expressions may not be easy to obtain.

These results can also be extended to the case of transmission over wireless bandpass channels for which the channel coefficients and the inputs can be taken as complex variables, and hence the inputs are complex variables. However, with MIMO systems, the dimensionality of the problem grows further. We do not consider this scenario as part of the current work for ease of explanation.

5.3.4 Capacity of 2×2 MIMO Systems with Amplitude-Limited and Power-Limited Inputs

Smith in [28] showed that for any amplitude-limited and power-limited point-to-point Gaussian channel, a unique capacity-achieving distribution exists and it is discrete. Again, extending these results to the case of MIMO systems is not feasible since there is no result corresponding to the Identity Theorem used in Smith's proof for multi-dimensional functions. However, we can follow a similar procedure to find upper and lower bounds on the capacity of MIMO systems with amplitude-limited inputs by relaxing the constraint on the amplitude and solving the capacity optimization problem over rectangular regions that inscribe and are inscribed by the original feasible region, respectively. We do not pursue this problem formulation any further in this work.

5.3.5 Asymptotic Bounds on the Capacity of the 2×2 MIMO Systems with Amplitude-Limited Inputs

In this section we study the asymptotic behavior of the upper and lower bounds on the capacity of MIMO systems at very high and low noise levels.

5.3.5.1 Very Low Noise Levels

For the point-to-point scalar Gaussian channel for very low noise variances, the entropy of the noise is very small compared to the entropy of the input. Thus, the following approximations are valid,

$$h(Y) \gg h(Y|X) \text{ and } h(X) \gg h(X|Y).$$

As a result,

$$h(X) = I(X;Y) + h(X|Y) = h(Y) - h(Y|X) + h(X|Y) \approx h(Y).$$

That is, the capacity can be approximated as

$$\begin{aligned} C &= \max I(X;Y), \\ &\approx \max h(X) - h(Y|X), \\ &= \log(2A) - \frac{1}{2}\log(2\pi e\sigma^2). \end{aligned}$$

Therefore, the capacity of the 2×2 MIMO system can be upper and lower bounded for low noise variances as

$$C \leq \log(4\Delta x_{upp}\Delta y_{upp}) - \frac{1}{2}\log(2\pi e\sigma_1^2) - \frac{1}{2}\log(2\pi e\sigma_2^2), \tag{5.17}$$

$$C \geq \log(4\Delta x_{low}\Delta y_{low}) - \frac{1}{2}\log(2\pi e\sigma_1^2) - \frac{1}{2}\log(2\pi e\sigma_2^2). \tag{5.18}$$

The lower bound on the capacity can be optimized by choosing the slope m (as defined in the previous section) that maximizes the mutual information between the input and the output. We have

$$\begin{aligned} C \geq & \max_m \log\left(4\left|\Delta x_{low}\Delta y_{low}\right|\right) \\ & -\frac{1}{2}\log(2\pi e\sigma_1^2) - \frac{1}{2}\log(2\pi e\sigma_2^2), \end{aligned} \tag{5.19}$$

such that the set of points

$$\{(l\Delta x_{low}, k\Delta y_{low}) \in \mathcal{R} : l, k \in \{1, -1\}\},$$

where Δx_{low}, Δy_{low}, and $\mathcal{R}$ are as defined in the previous section.

5.3.5.2 Very High Noise Levels

For very high noise variances, the optimal distribution is discrete and consists of only two mass points with the same probability [68]. The capacity of this discrete-time binary-input AWGN is well known [69], and the upper and lower bounds on the capacity are

$$C \leq g\left(\frac{\Delta x_{upp}}{\sigma_1}\right) + g\left(\frac{\Delta y_{upp}}{\sigma_2}\right), \tag{5.20}$$

$$C \geq g\left(\frac{\Delta x_{low}}{\sigma_1}\right) + g\left(\frac{\Delta y_{low}}{\sigma_2}\right), \tag{5.21}$$

where $g(x) = 1 - \int_{-\infty}^{\infty} \frac{1}{\sqrt{2\pi}} e^{-\frac{(u-x)^2}{2}} \log_2\left(1 + e^{-2ux}\right)\, du$.

5.3.5.3 The Gap Between the Upper and Lower Bounds

For very low noise variances, it is easy to see that the gap between the upper and lower bounds does not depend on the amplitude constraint if $A_{x_1} = A_{x_2}$. From (5.11) and (5.12), and if $A_{x_1} = A_{x_2} = A_0$ we have,

$$\Delta x_{upp} = G_{upp} A_0,\ \Delta y_{upp} = H_{upp} A_0,$$

where G_{upp} and H_{upp} are only function of the channel coefficients. Also from (5.14) and (5.15),

$$\Delta x_{low} = G_{low} A_0,\ \Delta y_{upp} = H_{low} A_0,$$

where G_{low} and H_{low} are only functions of the channel coefficients.

Thus, the gap between the upper and lower bounds ΔC can be written as

$$\begin{aligned} \Delta C &= \log\left(4 G_{upp} H_{upp} A_0^2\right) - \log\left(4 G_{low} H_{low} A_0^2\right), \\ &= \log\left(\frac{G_{upp} H_{upp}}{G_{low} H_{low}}\right), \end{aligned}$$

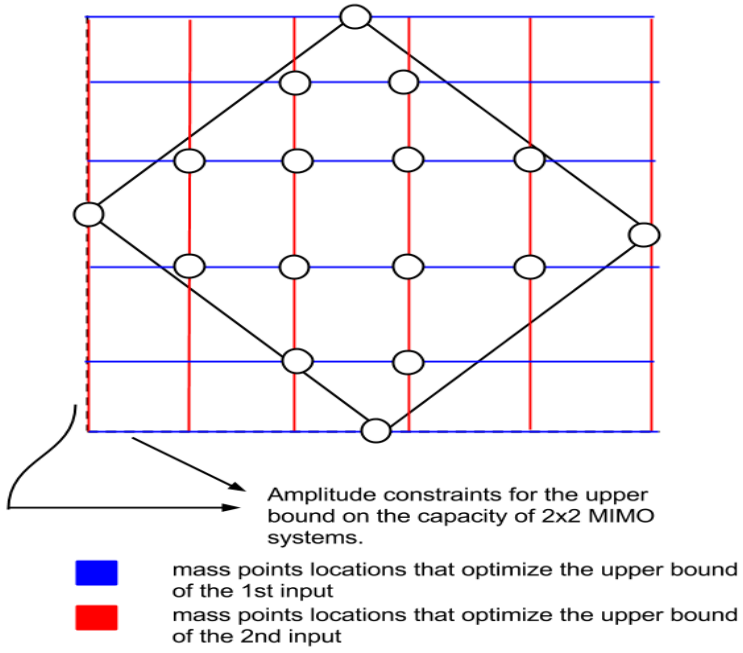

Figure 5.2: A suboptimal input distribution constructed from the cartesian product of the inputs distribution correspond to the upper bound.

which is independent of the amplitude constraints imposed on the inputs.

5.3.6 An Alternative Lower Bound on the Capacity

In this subsection, we demonstrate an alternative lower bound to the earlier results in the section 5.3.2. We note that the mutual information computed based on any arbitrarily chosen input distribution is a lower bound on the capacity, and we simply compute the mutual information for a particular input distribution. We consider a discrete distribution by constructing an input distribution from the cartesian product of the inputs distribution corresponding to the upper bound with mass points falling within the feasible region. An illustration is shown in Fig. 5.2. Examples on the resulting capacity lower bound with this approach will be given in Section 5.5.

5.4 Capacity of Independent Parallel Gaussian Channels with an Amplitude and Power-Limited Inputs

In this section, we turn our attention to a more tractable problem compared to the case of MIMO channels, namely to the parallel Gaussian channels, and we study the capacity of N independent parallel Gaussian channels with peak and average power-limited inputs. The capacity of parallel Gaussian channel under peak and average power constraints can be derived from Smith's results on the capacity of scalar Gaussian channels with amplitude-limited and power-limited inputs and has been reported previously in [34]. However, the solution for such problems relies on numerical calculations to find the optimal input distribution and the resulting capacity. Here, we deviate a bit by considering an analytical approximation to the capacity at low and low noise level regimes. In the following, we examine the asymptotic behavior of the capacity expressions in (5.6) at low and high noise levels.

5.4.1 Capacity of Parallel Gaussian Channels at Very High Noise Levels

At very high noise levels, the optimal input distribution that maximizes the mutual information between the input and the output (for amplitude-limited and power-limited inputs) is discrete with only two mass points and each one has a probability of one half [28]. Using the data processing inequality, one can easily argue that the capacity of each parallel channel is lower bounded by the capacity of a binary symmetric channel denoted by C_{BSC}. Recall that $C_{BSC} = 1 - H(p)$, where p is the cross-over probability which can be computed for the problem at hand as

$$p = Q\left(\sqrt{\frac{P}{\sigma^2}}\right), \tag{5.22}$$

where P is the average power at the transmitter side. We consider N parallel channels where the power assigned to each is $P_1, P_2, \cdots, P_N$, respectively. Thus, the capacity

of the channel is determined by the power assigned to each channel, and the capacity optimization problem boils down to a power assignment problem, i.e., choosing the optimal power for each channel so that the mutual information is maximized.

Since the input distribution for each channel input consists of two mass points with equal probabilities, we also have

$$P_i \leq A_i^2, \quad \forall i = 1, 2, \cdots, N. \tag{5.23}$$

Define a function $J(P_i)$, which is basically the binary entropy function, as

$$J(P_i) = -Q\left(\sqrt{\frac{P_i}{\sigma_i^2}}\right) \log\left(Q\left(\sqrt{\frac{P_i}{\sigma_i^2}}\right)\right) - \left(1 - Q\left(\sqrt{\frac{P_i}{\sigma_i^2}}\right)\right) \log\left(1 - Q\left(\sqrt{\frac{P_i}{\sigma_i^2}}\right)\right). \tag{5.24}$$

Then, the channel capacity of the parallel Gaussian channel is lower bounded by,

$$C \geq \max_{\substack{P_i,\ \forall i=1,2,\cdots,N,\ 0\leq P_i \leq A_i^2 \\ \mathbf{1}^T\mathbf{P} \leq P_0}} N - \sum_{i=1}^{N} J(P_i). \tag{5.25}$$

Solving this optimization problem results in the following power assignment policy (the proof is detailed in Appendix E) . Let us assume that the power assigned to the ith channel is P_i^*. Then, we consider three cases $P_i^* = 0$, $0 < P_i^* < A_i^2$, and $P_i = A_i^2$ separately, for $i = 1, 2, \cdots, N$, and solve for the candidate power assignments for the resulting $3^N - 2$ cases. For each case, considering only the non-zero power assignments with $P_i^* < A_i^2$, the water-filing parameter ν is chosen such that $P_i^* = g_i^{-1}(\nu)$, where $g_i(P_i)$ is defined as follows

$$g_i(P_i) = \frac{1}{2\sqrt{2\pi P_i \sigma_i^2}} \exp\left(-\frac{P_i}{2\sigma_i^2}\right) \log\left(\frac{1}{Q_i} - 1\right). \tag{5.26}$$

We also have $\sum_{i=1}^{N} P_i^* = P_0$. The optimal power assignment policy is chosen such that the KKT conditions are satisfied and the channel capacity is maximized.

There is an analogy between this solution and the classical water-filling solution used in assigning transmitted signal powers in the standard parallel Gaussian channel problem. The term "water-filling" arises from the similarity between the curve $g_i(P_i)$ and a bowl into which water (power) is poured, filling the bowl until there is no more power to use. The amount of water/energy in any subchannel is the depth of the water at the corresponding point in the bowl. There are some bowls that will be left empty. For the non-empty bowls a water (power) level is chosen such that there is no power and the mutual information is maximized.

5.4.2 Capacity of Parallel Gaussian Channels at Very Low Noise Levels

For a point-to-point scalar Gaussian channel for very low noise variances, the entropy of the noise is very small compared to the entropy of the input. Thus, the following approximations are valid [28],

$$h(Y) \gg h(Y|X) \text{ and } h(X) \gg h(X|Y).$$

That is, the capacity can be approximated as [28]

$$\begin{aligned} C &\triangleq \max_{f_X(x):\ |X|\leq A} I(X;Y), \\ &= \max_{f_X(x):\ |X|\leq A} h(Y) - h(Y|X), \\ &\approx \max_{f_X(x):\ |X|\leq A} h(X) - h(Y|X), \end{aligned}$$

where $f_X(x)$ is the input probability density function. Intuitively, at very low noise levels the output is not highly affected by the imposed noise and hence the entropy of the input does not change and instead of finding the input distribution that maximizes the output entropy, we solve a relaxed problem that aims to find the input distribution that maximizes the output entropy.

Lemma 5.4.1. *Consider a random variable X with a probability density function $f_X(x) \in \mathcal{F}_X$ where $|X| \leq A$, $\mathbf{E}[X^2] \leq P$, and $\mathcal{F}_X$ denotes the corresponding class*

of probability density functions such that $P(X > A) = 0$ *and* $P(X < -A) = 0$. *The probability density function that maximizes its entropy is* $f_X(x) = c_1 \exp(-c_2 x^2)$, *where* c_1 *and* c_2 *are the solutions of*

$$c_1 = \frac{1 - 2c_2 P}{2A \exp(-c_2 A^2)}, \tag{5.27}$$

and

$$\frac{1 - 2c_2 P}{2A \exp(-c_2 A^2)} \left[\sqrt{\frac{\pi}{c_2}} \operatorname{erf}(\sqrt{c_2} A) \right] = 1. \tag{5.28}$$

Proof. See Appendix F. □

The resulting differential entropy is given by

$$\begin{aligned} h(X) &= -\int_{-A}^{A} f(x) \log(f(x)) dx, & (5.29) \\ &= h(X) = -\log(c_1) + c_2 P. & (5.30) \end{aligned}$$

Finally, the mutual information between $(X_1, X_2, \cdots, X_N)$ and $(Y_1, Y_2, \cdots, Y_N)$ is approximated as

$$I(X_1, X_2, \cdots, X_N; Y_1, Y_2, \cdots, Y_N) \approx \sum_{i=1}^{N} h(X_i) - \sum_{i=1}^{N} \frac{1}{2} \log(2\pi e \sigma_i^2). \tag{5.31}$$

Similar to the previous subsection, the optimal power assignment for each channel can be performed through water-filling (details of the power assignment policy are given in Appendix G). For the ith channel, let us assume that the power assigned is P_i^*. Then, there are three possible cases, i.e., $P_i^* = 0$ or $P_i^* = A_i^2$ or $0 < P_i^* < A_i^2$. One can consider $3^N - 2$ cases separately, and when $0 < P_i < A_i^2$, the water-filing parameter ν is chosen such that $P_i^* = w_i^{-1}(\nu)$, where the function and $w_i(P_i)$ is the derivative of the objective function which is defined in Appendix G. The optimal power assignment policy is chosen by examining the necessary conditions for optimality and selecting the case with largest information rate.

We note an important difference between the power assignment policy derived for the low and low noise levels cases, the high noise levels policy depends on the noise variance of the channel besides the the amplitude constraints. However, the low noise levels policy does not depend on the noise variance, i.e., the same power assignment policy applies for the entire SNR range.

5.5 Numerical Examples

In this section, we present numerical examples that show the derived upper and lower bounds on the capacity of general MIMO systems for different channels and different input constraints. Along with the bounds of the capacity, we show the asymptotic bounds on the capacity of MIMO systems at low and high levels of noise variance. For the parallel Gaussian channels, we present an evaluation for the proposed bounds on the capacity of parallel Gaussian channels along with the exact capacity evaluated using the optimal power assignment (the optimal power is assigned through brute force approach). We also show an evaluation for the capacity using suboptimal power assigned using the policy derived at high and low noise variances as described in the previous section.

5.5.1 2×2 MIMO Systems

In this subsection, we present numerical examples that show the upper and lower bounds on the capacity of 2×2 MIMO systems for different channel coefficient matrices and different amplitude constraints. For the given channel coefficient matrices and amplitude constraints we use the results of the previous section to come up with new rectangular regions for the channel inputs, and then we numerically evaluate the mutual information as

$$\begin{aligned} I(\tilde{Y_1}, \tilde{Y_2}; \tilde{X_1}, \tilde{X_2}) &= I(\tilde{Y_1}; \tilde{X_1}) + I(\tilde{Y_2}; \tilde{X_2}), \\ &= h(\tilde{Y_1}) + h(\tilde{Y_2}) - D_1 - D_2, \end{aligned}$$

where $h(\centerdot)$ is the differential entropy, and $D_i = \frac{1}{2}\log(2\pi e\sigma_i^2)$ is the entropy of the Gaussian noise with variance equals to σ_i^2, $i = 1, 2$.

We consider two arbitrarily picked channel matrices given by

$$H_1 = \begin{bmatrix} 0.177 & 0.28 \\ 1 & 0.31 \end{bmatrix}, \quad H_2 = \begin{bmatrix} 0.997 & 0.295 \\ 1 & 0.232 \end{bmatrix}.$$

We assume that the amplitude constraints imposed on the inputs are identical, and both channels have the same noise variances.

Fig. 5.3 and Fig. 5.4 show the upper and lower bounds on the capacity and their asymptotic behavior for the two channels considered, we observe that the asymptotic characterizations of the bounds are tight with the bounds at low and high SNR, respectively. The gap between the upper and lower bounds indicate that there is more work to be done for a tighter characterization of the MIMO channel capacity with amplitude constraints. Fig. 5.5 shows the upper and lower bounds on the capacity of the second channel for different values of amplitude constraints. Clearly, when the amplitude constraint is increased, the capacity upper and lower bounds are also increased. Also, we observe that the gap between the upper and lower bounds does not depend on the amplitude constraint for very low noise variance values given that the same amplitude constraints are imposed on both antenna elements. As the value of the noise variance increases, i.e., the SNR decreases, the gap between the upper and lower bound decreases as the number of mass points for the optimal input distribution decreases (eventually it converges to only two mass points). Fig. 5.6 shows the upper and lower bounds derived from the approach described before a long with the alternative achievable lower bound at which we consider a suboptimal input distribution inspired by the optimal input distributions for the bounds, the alternative input distribution shows a better performance, yet the approach of constructing this

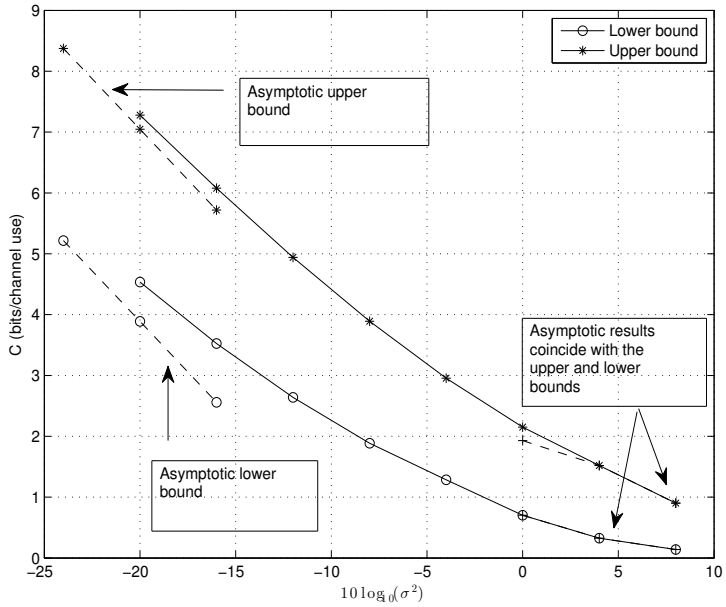

Figure 5.3: Upper and lower bounds on the capacity for H_1, along with the asymptotic capacity at low and high noise variances, with an amplitude constraint of 2 (for both inputs).

input distribution is heuristic.

5.5.2 Parallel Gaussian Channels

In this subsection, we present three numerical examples that demonstrate the behavior of the capacity and the bounds for different noise levels regimes. In the first example, we consider two parallel Gaussian channels where the peak power constraint on each channel is $|A_1| \leq 2$, and $|A_2| \leq 4$. The total power constraint is 4. We assume that the variance of the two parallel channels is the same. Fig. 5.7 shows the capacity of the two parallel Gaussian channel along with the upper and lower bounds derived in the Section 5.4. We also show the evaluation for the channel capacity using the low noise levels policy, high noise levels policy, and uniform power assignment, i.e., for each subchannel the optimal solution is computed using numerical techniques as in [28], given the particular power and amplitude limits. We note that low noise (high

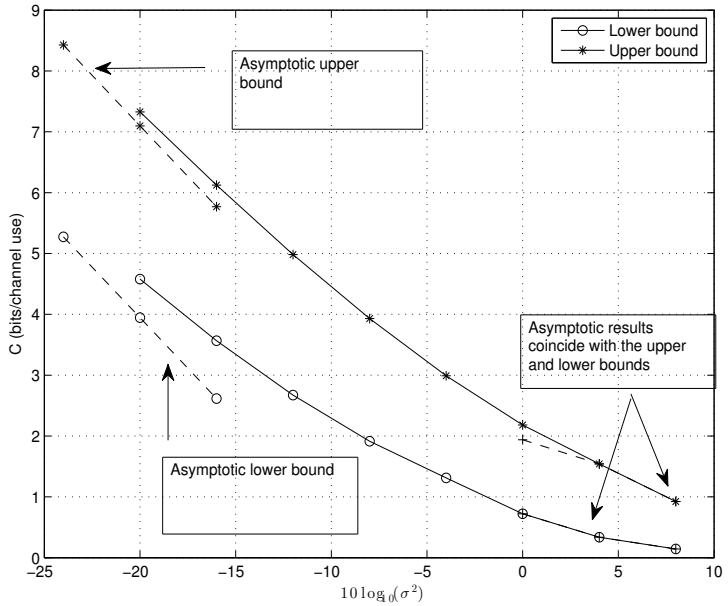

Figure 5.4: Upper and lower bounds on the capacity for H_2, along with the asymptotic capacity at low and high noise variances, with an amplitude constraint of 2 (for both inputs).

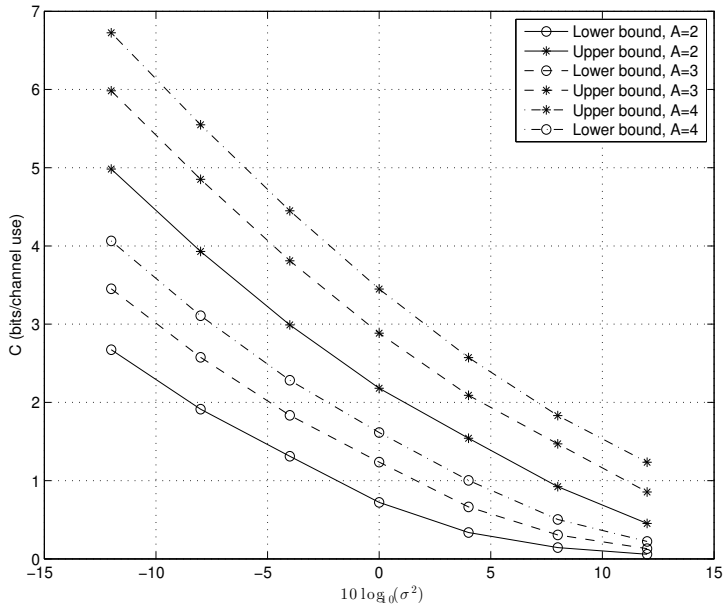

Figure 5.5: Illustration of capacity upper and lower bounds of the capacity of H_2 for different amplitude constraints on the inputs.

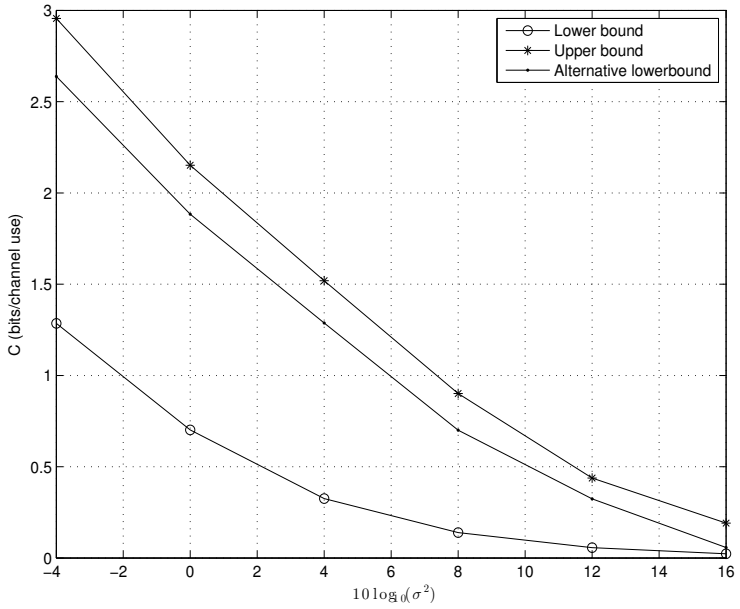

Figure 5.6: The upper and lower bounds on the capacity along with an alternative lower bound on the capacity of the MIMO channel.

noise) levels power assignment policy works better at low noise (high noise) levels as expected. For the second example we consider six parallel Gaussian channels with the total power constraint $P_0 = 15$ and with different amplitude constraints for each channel, i.e., $|A_1| \leq 0.1,\ |A_2| \leq 0.1,\ |A_3| \leq 1,\ |A_4| \leq 1,\ |A_5| \leq 10,\ |A_6| \leq 10$. Fig. 5.8 shows the capacity of the channel evaluated using power assignments resulting from the policy developed for high noise levels, the policy for the low noise variance case, and with uniform power assignments. From the figure we notice that at high noise levels there is a gap between the exact capacity and the the bound with the BSC approximation which is due to the fact that the BSC acts as a quantized version of the Gaussian channel (sometimes, it is called Gaussian channel with hard decision decoding [7]). The benefits of the proposed bounds appear when the number of parallel channels is very large as in that case computing the exact channel capacity is not viable as the brute force calculation of the optimal power assignments requires

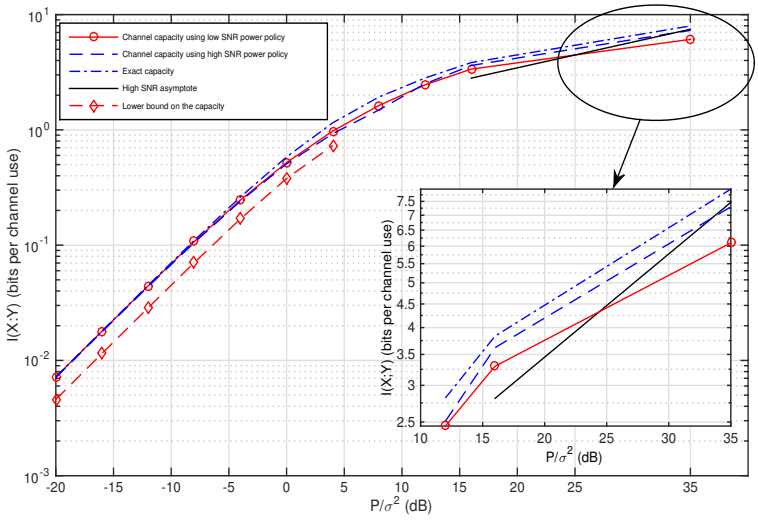

Figure 5.7: The channel capacity evaluated using low noise levels policy and high noise levels policy for two parallel Gaussian channel.

extensive computations. However, by using the proposed bounds we can characterize the channel capacity at different noise levels with a low computational complexity and at the same time obtain tight bounds.

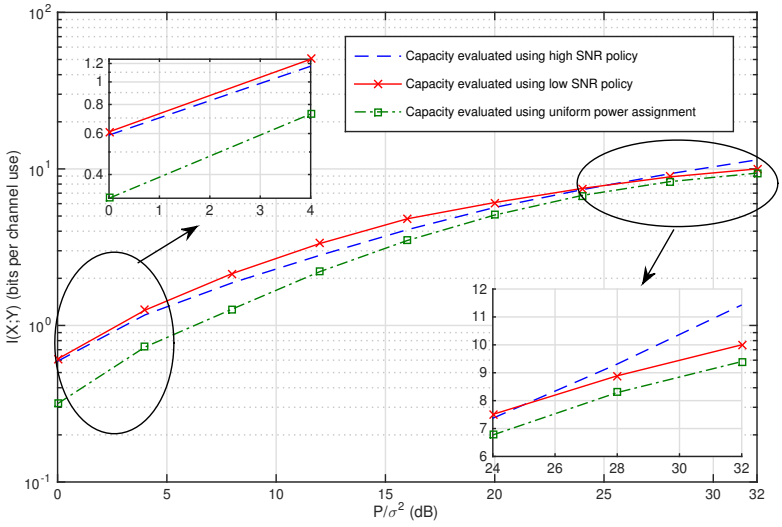

Figure 5.8: The channel capacity evaluated using low noise levels policy and high noise levels policy for six parallel Gaussian channel.

5.6 Chapter Summary

In this chapter, we studied the capacity of MIMO systems with amplitude-limited inputs. We computed analytical upper and lower bounds on the capacity of such systems. The upper bounds are derived by relaxing the feasible region of the capacity optimization problem. For the lower bound, we solve the problem by constraining the feasible region to a smaller one inscribed within the original. Furthermore, we study the capacity of parallel Gaussian channels, and provide an analytical characterization at low and high noise levels. In both cases, the corresponding optimal power assignment policy is derived by solving the capacity optimization problem by a suitable application of the KKT conditions. Several numerical examples are used to illustrate our findings on both MIMO and parallel Gaussian channels.

Chapter 6

CODING FOR CHANNELS WITH SIGNAL-DEPENDENT NOISE

In this chapter, we consider the problem of channel coding towards a further understanding of the proposed communication scheme in Chapter 2. The equivalent (approximate) channel model in (2.18) implies that the received signal parameters are contaminated by Gaussian noise with variance that depends on the transmitted signal. This model brings up new problems in coding to deal with impairments introduced by channels with signal-dependent additive noise. To address these problems, we consider two channel models. The first one is an AWGN channel but with noise variance that depends on the transmitted signal. The second one is a binary asymmetric channel (BAC) which serves as an approximation to the AWGN model.

There has been significant progress in designing channel codes for BACs in recent years. For instance, in [39], the authors introduce a new class of codes referred as group-theoretic codes, and they prove that this class of codes are able to correct one bit error that may occur during transmission. In [40], a new density evolution technique is developed for optimization of the low density parity check (LDPC) codes. In [41], the authors propose two methods for code construction; the first one is based on codebook expurgation where the goal is to alter the input distribution within the codebook such that the resulting input distribution for the channel becomes nonuniform and closer to the optimal one. The second construction method is based on introducing a mapper after a linear channel code. This mapper is from a non-binary linear block code into a binary codebook keeping in mind the same objective which is to have a biased (optimal) input distribution. We note that this is not the first time a mapper is introduced after a channel encoder; for example, the same idea has been used before in [38], where a non-linear mapper is introduced after

LDPC encoding to make the input distribution closer to the optimal one. In [42], the authors present new constructions of codes for asymmetric channels for both binary and nonbinary alphabets, based on methods of generalized code concatenation.

In our study, we focus on certain class of block-codes called ultra-small codes, which feature codebooks with small number of messages and codewords with short block lengths. These codes appear in many communication scenarios as viable solutions, e.g., in the initiation of communication links in which we have a small number of messages to be transmitted, and also for applications that are so sensitive to delay that cannot tolerate transmission of long blocks.

The literature is not rich in the context of ultra-small codes. For instance, [43, 44] introduce a family of ultra-small block codes called flip and weak-flip codes. The approach is to design optimal codes (optimal in the sense that they minimize the average error probability) for the BSC, BAC, and Z-channels. The authors propose a new approach toward code design, specifically, they design codes using a column-wise representation by collecting combinations of columns from a set of alternatives called candidate columns. The authors are able to design optimal codes when the number of messages is limited to four or five. Also, they provide performance assessments for the case where the number of messages is four or five, however, designing larger codes and providing performance assessments when the dimension grows seems intractable.

Towards the goal of code design, we first propose a new upper bound on the error probability of a coded system based on Bonferroni-type inequalities by considering the error probability resulting from the intersection of two and three pairwise error events. We apply the proposed bound for three different channel models and employ it to design codes for one of the Z-channel. The channel models considered here are the usual AWGN channels, additive Gaussian noise channels for which the

noise variance depends on the transmitted signal, binary-input binary-output asymmetric channels, and as a special case the Z-channel. The interest in BACs is due to the fact that it is a more general model than the BSC, and it acts as an approximation to the equivalent system model we provide in Chapter 2. We note that the proposed upper bound performs as good as one of the best upper bounds that exists in the literature [70] for the examples considered.

One of the main benefits of this new proposed upper bound is that it helps in providing performance assessments for the class of codes that we are interested in. To be more specific, we note that although the error probability of short codes seems to be tractable due to their small size, we still cannot provide closed form expressions for it when the code sizes are increased even slightly. On the other hand, we are able to compute tight approximations for the error probability for scenarios where an exact error probability expression is not achievable. We also are able to use the proposed upper bound to design codes for Z-channels by defining a new metric that we call the weighted sum Hamming distance as directly motivated by the derived bounds.

The chapter is organized as follows. In Section 6.1, we propose an upper bound on the probability of error of a coded system. We then we show how this upper bound can be applied for the AWGN case in Section 6.2, for the signal-dependent Gaussian noise channel in Section 6.3, BAC in Section 6.4, and Z-channel in Section 6.5. In Section 6.6, we propose a new metric for code design, and detail the code design procedure for Z-channels. In Section 6.7, we present several numerical examples to illustrate the use of the proposed upper bounds and the performance of the newly designed codes. Finally, we summarize the chapter in Section 6.8.

6.1 Upper Bound on the Error Probability

In this section, we derive an upper bound on the error probability of a coded system based on Bonferroni type inequalities. The objective is to communicate M equally likely messages, $\mathbf{x}_0, \mathbf{x}_1, \cdots, \mathbf{x}_{M-1}$, of dimension N, i.e., M messages are picked from the codebook $\mathcal{C}$ with dimensions (M, N), we assume that $\mathbf{x}_0, \mathbf{x}_1, \cdots, \mathbf{x}_{M-1}$ are binary modulates, i.e., "0" is mapped to "-1" and "1" is mapped to "1". At the receiver side we assume that a maximum likelihood (ML) decoder is used such that

$$\hat{\mathbf{x}} = \arg \max_{\mathbf{x}_u \in \mathcal{C}} P(\mathbf{y}|\mathbf{x}_u). \tag{6.1}$$

The probability of error given that $\mathbf{x}_u$ is transmitted is given by

$$P(\varepsilon|\mathbf{x}_u) = \Pr\left[\left(\bigcup_{\mathbf{x}_i \in \mathcal{C}, i \neq u} \varepsilon_{iu}\right) \middle| \mathbf{x}_u\right], \tag{6.2}$$

where ε_{iu} is the pairwise error event defined as

$$\varepsilon_{iu} = \{P(\mathbf{y}|\mathbf{x}_i) \geq P(\mathbf{y}|\mathbf{x}_u)\}, \quad \forall \mathbf{x}_i, \mathbf{x}_u \in \mathcal{C}, i \neq u, \tag{6.3}$$

and

$$\varepsilon = \bigcup_{i \neq u} \varepsilon_{iu}, \quad \forall \mathbf{x}_i, \mathbf{x}_u \in \mathcal{C}. \tag{6.4}$$

The average error probability is then given by

$$P(\varepsilon) = \frac{1}{M} \sum_{u=0}^{M-1} P(\varepsilon|\mathbf{x}_u). \tag{6.5}$$

A classical upper bound on the error probability is the union bound that bounds the error probability by summing up the pairwise error probabilities such that

$$P(\varepsilon|\mathbf{x}_u) \leq \sum_{\substack{j=0 \\ j \neq u}}^{M-1} P\left(\varepsilon_{ju}|\mathbf{x}_u\right). \tag{6.6}$$

A lower bound on the error probability that is based on Bonferroni type inequalities is given by

$$P(\varepsilon|\mathbf{x}_u) \geq \sum_{\substack{i=0 \\ i\neq u}}^{M-1} P(\varepsilon_{iu}) - \sum_{\substack{k=0 \\ k\neq u}}^{M-1} \sum_{i=0}^{k-1} P(\varepsilon_{iu} \cap \varepsilon_{ku}). \tag{6.7}$$

In order to come up with a tighter upper bound than the union bound, we utilize intersections of triplet error events as well. The resulting bound can be expressed as follows

$$P(\varepsilon|\mathbf{x}_u) \leq \sum_{\substack{i=0 \\ i\neq u}}^{M-1} P(\varepsilon_{iu}) - \sum_{\substack{k=0 \\ k\neq u}}^{M-1} \sum_{i=0}^{k-1} P(\varepsilon_{iu} \cap \varepsilon_{ku}) + \sum_{\substack{j=0 \\ j\neq u}}^{M-1} \sum_{k=0}^{j-1} \sum_{i=0}^{k-1} P(\varepsilon_{iu} \cap \varepsilon_{ku} \cap \varepsilon_{ju}). \tag{6.8}$$

The average error probability is then upper bounded as,

$$\begin{aligned} P(\varepsilon) \quad \leq \quad & \frac{1}{M} \sum_{u=0}^{M-1} \sum_{\substack{i=0 \\ i\neq u}}^{M-1} P(\varepsilon_{iu}) - \frac{1}{M} \sum_{u=0}^{M-1} \sum_{\substack{k=0 \\ k\neq u}}^{M-1} \sum_{i=0}^{k-1} P(\varepsilon_{iu} \cap \varepsilon_{ku}) \\ & + \frac{1}{M} \sum_{u=0}^{M-1} \sum_{\substack{j=0 \\ j\neq u}}^{M-1} \sum_{k=0}^{j-1} \sum_{i=0}^{k-1} P(\varepsilon_{iu} \cap \varepsilon_{ku} \cap \varepsilon_{ju}). \end{aligned}$$

This new upper bound is tight compared to the union bound. Also, numerical examples will show that in some cases it is extremely close to the exact bit error rates estimated using Monte Carlo simulations.

6.2 Upper Bounds for Additive White Gaussian Noise Channels

In this section, we apply the proposed upper bound to the case of information transfer over AWGN channels. The received signal $\mathbf{y}$ is given by

$$\mathbf{y} = \mathbf{x} + \mathbf{n}, \tag{6.9}$$

where $\mathbf{x}$ is the transmitted codeword, and $\mathbf{n} = [n_0, n_1, \cdots, n_{N-1}]$ is an AWGN vector. The elements of this vector are independent of $\mathbf{x}$, and each other such that $n_i \sim \mathcal{N}(0, N_0/2)$. In the AWGN case, the ML decoder boils down to

$$\hat{\mathbf{x}} = \arg \min_{\mathbf{x}_u \in \mathcal{C}} ||\mathbf{y} - \mathbf{x}_u||. \tag{6.10}$$

The pairwise error event in this case is

$$\varepsilon_{iu} = \{||\mathbf{y} - \mathbf{x}_i|| < ||\mathbf{y} - \mathbf{x}_u||\}, \tag{6.11}$$

and the pairwise error probability is [7]

$$P(\epsilon_{iu}|\mathbf{x}_u) = Q\left(\frac{||\mathbf{x}_u - \mathbf{x}_i||}{\sqrt{2N_0}}\right). \tag{6.12}$$

For the sake of convenience, we refer to [71] for the probability of the intersection of two pairwise error events. Here, we derive the probability of intersection of triplet error events defined as

$$P(\epsilon_{iu} \cap \epsilon_{ju} \cap \epsilon_{ku}|\mathbf{x}_u) = \Pr[||\mathbf{y}-\mathbf{x}_i|| < ||\mathbf{y}-\mathbf{x}_u||, ||\mathbf{y}-\mathbf{x}_j|| < ||\mathbf{y}-\mathbf{x}_u||, ||\mathbf{y}-\mathbf{x}_k|| < ||\mathbf{y}-\mathbf{x}_u|| \; |\mathbf{x}_u] \tag{6.13}$$

which reduces to

$$\Pr\left[X_i \geq \frac{d_{iu}}{\sqrt{2N_0}}, X_j \geq \frac{d_{ju}}{\sqrt{2N_0}}, X_k \geq \frac{d_{ku}}{\sqrt{2N_0}}\right] \tag{6.14}$$

where d_{iu} is the Euclidean distance between the codeword $\mathbf{x}_i$ and $\mathbf{x}_u$, and

$$X_i = \frac{\sqrt{2}}{\sqrt{N_0}||\mathbf{x}_i - \mathbf{x}_u||} < \mathbf{n}, \mathbf{x}_i - \mathbf{x}_u > . \tag{6.15}$$

We define the mutual correlation coefficients $\rho_{ij}, \rho_{ik}, \rho_{jk}$ as

$$\rho_{ij} = E[X_i X_j] = \frac{< \mathbf{x}_i - \mathbf{x}_u, \mathbf{x}_j - \mathbf{x}_u >}{||\mathbf{x}_i - \mathbf{x}_u||||\mathbf{x}_j - \mathbf{x}_u||}, \tag{6.16}$$

$$\rho_{ik} = E[X_i X_k] = \frac{< \mathbf{x}_i - \mathbf{x}_u, \mathbf{x}_k - \mathbf{x}_u >}{||\mathbf{x}_i - \mathbf{x}_u||||\mathbf{x}_k - \mathbf{x}_u||}, \tag{6.17}$$

$$\rho_{jk} = E[X_j X_k] = \frac{< \mathbf{x}_j - \mathbf{x}_u, \mathbf{x}_k - \mathbf{x}_u >}{||\mathbf{x}_j - \mathbf{x}_u||||\mathbf{x}_k - \mathbf{x}_u||}, \tag{6.18}$$

where $< \mathbf{x}, \mathbf{y} >$ is the dot product between the vectors $\mathbf{x}$ and $\mathbf{y}$ which is defined as

$$< \mathbf{x}, \mathbf{y} > \triangleq \sum_{i=0}^{N-1} \mathbf{x}(i)\mathbf{y}(i), \tag{6.19}$$

where $\mathbf{x}(i)$, $\mathbf{y}(i)$ are the i-th element of the vectors $\mathbf{x}$ and $\mathbf{y}$, respectively. The correlation matrix $\boldsymbol{\rho}$ is defined as

$$\boldsymbol{\rho} = \begin{bmatrix} 1 & \rho_{ij} & \rho_{ik} \\ \rho_{ji} & 1 & \rho_{jk} \\ \rho_{ki} & \rho_{kj} & 1 \end{bmatrix}. \tag{6.20}$$

The probability of the intersection of triplet error events is then

$$\begin{aligned} &P(\epsilon_{ui} \cap \epsilon_{uj} \cap \epsilon_{uk} | \mathbf{x}_u) \\ &= \frac{1}{\sqrt{(2\pi)^3 |\boldsymbol{\rho}|}} \int_{d_{ui}/\sqrt{2N_0}}^{\infty} \int_{d_{uj}/\sqrt{2N_0}}^{\infty} \int_{d_{uk}/\sqrt{2N_0}}^{\infty} \exp\left(-\frac{1}{2} [x\ y\ z] \boldsymbol{\rho}^{-1} [x\ y\ z]^T \right) dx\, dy\, dz \end{aligned} \tag{6.21}$$

where $|\boldsymbol{\rho}|$ is the determinant of the correlation matrix $\boldsymbol{\rho}$

$$|\boldsymbol{\rho}| = 1 - \rho_{jk}^2 - \rho_{ik}^2 - \rho_{ij}^2 + 2\rho_{ij}\rho_{ik}\rho_{jk}, \tag{6.22}$$

and

$$\boldsymbol{\rho}^{-1} = \frac{1}{|\boldsymbol{\rho}|} \begin{bmatrix} 1 - \rho_{jk}^2 & \rho_{ik}\rho_{jk} - \rho_{ij} & \rho_{ij}\rho_{jk} - \rho_{ik} \\ \rho_{jk}\rho_{ki} - \rho_{ij} & 1 - \rho_{ik}^2 & \rho_{ik}\rho_{ij} - \rho_{jk} \\ \rho_{ij}\rho_{jk} - \rho_{ik} & \rho_{ij}\rho_{ik} - \rho_{kj} & 1 - \rho_{ij}^2 \end{bmatrix}. \tag{6.23}$$

The integral above can be equivalently be written as

$$\begin{aligned} &P(\epsilon_{ui} \cap \epsilon_{uj} \cap \epsilon_{uk} | \mathbf{x}_u) \\ &= \frac{1}{\sqrt{(2\pi)^3 |\boldsymbol{\rho}|}} \int_{d_{ui}/\sqrt{2N_0}}^{\infty} \int_{d_{uj}/\sqrt{2N_0}}^{\infty} \int_{d_{uk}/\sqrt{2N_0}}^{\infty} \exp\Bigg(-\frac{1}{2|\boldsymbol{\rho}|} \Big((1-\rho_{jk}^2)x^2 + (1-\rho_{ik}^2)y^2 + (1-\rho_{ij}^2)z^2 \\ &\qquad + 2(\rho_{jk}\rho_{ik} - \rho_{ij})xy + 2(\rho_{ij}\rho_{jk} - \rho_{ik})xz + 2(\rho_{ij}\rho_{ik} - \rho_{jk})yz \Big) \Bigg) dx\, dy\, dz. \end{aligned} \tag{6.24}$$

Direct calculation of the bound given above requires calculation of the triple integral for all codeword triplets, and calculation of the double integral for all codeword pairs. To overcome this computational difficulty, an enumeration can be done for the codebook by counting the number of triplets corresponding to the same correlation matrix which is similar to defining a weight enumerating function for a code.

6.3 Upper Bounds for Signal-Dependent Gaussian Noise Channels

In this section, we apply the proposed upper bound in Section 6.1 to the case of Gaussian channels with additive noise whose variance depends on the transmitted signal. In our model, the received signal $\mathbf{y}$ is given by

$$\mathbf{y} = \mathbf{x} + \mathbf{n}(\mathbf{x}), \tag{6.25}$$

where $\mathbf{x}$ is the transmitted modulated codeword, and $\mathbf{n} = [n_0, n_1, \cdots, n_{N-1}]$ is an AWGN vector. The elements of this vector has a Gaussian distribution such that the variance corresponding to transmission of zeros is different than the variance corresponding to transmission of ones; namely $n_i \sim \mathcal{N}(0, N_0^{(i)}(\mathbf{x})/2)$ where $N_0^{(i)} \in \{N_0^{(0)}, N_0^{(1)}\}$ and

$$N_0^{(i)}(\mathbf{x}) = \begin{cases} N_0^{(0)} & \text{if } \mathbf{x}(i) = -1, \\ N_0^{(1)} & \text{if } \mathbf{x}(i) = 1. \end{cases} \tag{6.26}$$

The maximum likelihood decoder in that case is more difficult to analyze. Hence, we consider a suboptimal minimum distance decoder which results in an upper bound on the error probability. Namely, using

$$\hat{\mathbf{x}} = \arg\min_{\mathbf{x}_u \in \mathcal{C}} ||\mathbf{y} - \mathbf{x}_u||, \tag{6.27}$$

as the decoding rule, we can derive an error rate bound. The pairwise error event defined as

$$\varepsilon_{iu} = \{||\mathbf{y} - \mathbf{x}_i|| < ||\mathbf{y} - \mathbf{x}_u||\}, \tag{6.28}$$

has the probability

$$P(\epsilon_{iu}|\mathbf{x}_u) = Q\left(\frac{||\mathbf{x}_u - \mathbf{x}_i||^2}{\sqrt{2\hat{N}_0^{(ij)}}}\right), \tag{6.29}$$

where $\hat{N_0}^{(ij)}(\mathbf{x}_u) = \sum_{m=0}^{N-1} N_0^{(m)}(\mathbf{x}_u)(\mathbf{x}_i(m) - \mathbf{x}_u(m))^2$. For the probability of intersection of two pairwise error events, we have

$$P(\epsilon_{iu} \cap \epsilon_{ju}|\mathbf{x}_u) = \Pr[||\mathbf{y} - \mathbf{x}_i|| < ||\mathbf{y} - \mathbf{x}_u||, ||\mathbf{y} - \mathbf{x}_j|| < ||\mathbf{y} - \mathbf{x}_u|| \ |\mathbf{x}_u] \tag{6.30}$$

which reduces to

$$\Pr\left[X_i \geq \frac{d_{iu}^2}{2}, X_j \geq \frac{d_{ju}^2}{2}|\mathbf{x}_u\right] \tag{6.31}$$

where d_{iu} is the Euclidean distance between the codeword $\mathbf{x}_i$ and $\mathbf{x}_u$, and

$$X_i =< \mathbf{n}, \mathbf{x}_i - \mathbf{x}_u > . \tag{6.32}$$

We define the mutual correlation coefficients $\rho_{ij}, \rho_{ik}, \rho_{jk}$ as

$$\rho_{ij} = E[X_i X_j] = \frac{\hat{N_0}^{(iju)}}{\sqrt{\hat{N_0}^{(iu)} \hat{N_0}^{(ju)}}}, \tag{6.33}$$

where $\hat{N_0}^{(iju)} = \sum_{m=0}^{N-1} N_0^{(m)}(\mathbf{x}_u)(\mathbf{x}_i(m) - \mathbf{x}_u(m))(\mathbf{x}_j(m) - \mathbf{x}_u(m))$. We then obtain

$$P(\epsilon_{ui} \cap \epsilon_{uj}|\mathbf{x}_u) = \frac{1}{2\pi\sqrt{1-\rho_{ij}}} \int_{d_{ui}/\sqrt{2\hat{N_0}^{(iu)}}}^{\infty} \int_{d_{uj}/\sqrt{2\hat{N_0}^{(ju)}}}^{\infty} \exp\left(-\frac{(x^2 - 2\rho_{ij}xy + y^2)}{2(1-\rho_{ij}^2)}\right) dx\, dy. \tag{6.34}$$

We now derive the probability of intersection of triplet error events that is defined as

$$P(\epsilon_{iu} \cap \epsilon_{ju} \cap \epsilon_{ku}|\mathbf{x}_u) = \Pr[||\mathbf{y} - \mathbf{x}_i|| < ||\mathbf{y} - \mathbf{x}_u||, ||\mathbf{y} - \mathbf{x}_j|| < ||\mathbf{y} - \mathbf{x}_u||, ||\mathbf{y} - \mathbf{x}_k|| < ||\mathbf{y} - \mathbf{x}_u|| \ |\mathbf{x}_u] \tag{6.35}$$

which reduces to

$$P(\epsilon_{iu} \cap \epsilon_{ju} \cap \epsilon_{ku}|\mathbf{x}_u) = \Pr\left[X_i \geq \frac{d_{iu}^2}{2}, X_j \geq \frac{d_{ju}^2}{2}, X_k \geq \frac{d_{ku}^2}{2}|\mathbf{x}_u\right]. \tag{6.36}$$

We define the mutual correlation coefficients $\rho_{ij}, \rho_{ik}, \rho_{jk}$ as

$$\rho_{ij} = E[X_i X_j] = \frac{\hat{N_0}^{(iju)}}{\sqrt{\hat{N_0}^{(iu)} \hat{N_0}^{(ju)}}}, \tag{6.37}$$

$$\rho_{ik} = E[X_i X_k] = \frac{\hat{N_0}^{(iku)}}{\sqrt{\hat{N_0}^{(iu)} \hat{N_0}^{(ku)}}}, \tag{6.38}$$

$$\rho_{jk} = E[X_j X_k] = \frac{\hat{N}_0^{(jku)}}{\sqrt{\hat{N}_0^{(ju)} \hat{N}_0^{(ku)}}}, \tag{6.39}$$

and construct the correlation matrix $\boldsymbol{\rho}$ as

$$\boldsymbol{\rho} = \begin{bmatrix} 1 & \rho_{ij} & \rho_{ik} \\ \rho_{ji} & 1 & \rho_{jk} \\ \rho_{ki} & \rho_{kj} & 1 \end{bmatrix}. \tag{6.40}$$

Then, the probability of intersection of triplet error events can be computed as

$$\begin{aligned} &P(\epsilon_{ui} \cap \epsilon_{uj} \cap \epsilon_{uk} | \mathbf{x}_u) \\ &\quad = \frac{1}{\sqrt{(2\pi)^3 |\boldsymbol{\rho}|}} \int_{d_{ui}/\sqrt{2N_0}}^{\infty} \int_{d_{uj}/\sqrt{2N_0}}^{\infty} \int_{d_{uk}/\sqrt{2N_0}}^{\infty} \exp\left(-\frac{1}{2} [x\ y\ z] \boldsymbol{\rho}^{-1} [x\ y\ z]^T \right) dx\, dy\, dz. \end{aligned} \tag{6.41}$$

This can be equivalently be written as

$$\begin{aligned} &P(\epsilon_{ui} \cap \epsilon_{uj} \cap \epsilon_{uk} | \mathbf{x}_u) \\ &= \frac{1}{\sqrt{(2\pi)^3 |\boldsymbol{\rho}|}} \int_{d_{ui}/\sqrt{2\hat{N}_0^{(iu)}}}^{\infty} \int_{d_{uj}/\sqrt{2\hat{N}_0^{(ju)}}}^{\infty} \int_{d_{uk}/\sqrt{2\hat{N}_0^{(ku)}}}^{\infty} \exp\Bigg(-\frac{1}{2|\boldsymbol{\rho}|} \Big((1-\rho_{jk}^2)x^2 + (1-\rho_{ik}^2)y^2 + (1-\rho_{ij}^2)z^2 \\ &\qquad + 2(\rho_{jk}\rho_{ik} - \rho_{ij})xy + 2(\rho_{ij}\rho_{jk} - \rho_{ik})xz + 2(\rho_{ij}\rho_{ik} - \rho_{jk})yz \Big) \Bigg) dx\, dy\, dz. \end{aligned} \tag{6.42}$$

As discussed in the case of AWGN channels, code enumeration is required in order to reduce the computational complexity of the proposed upper bound for evaluation purposes.

6.4 Upper Bounds for Binary Asymmetric Channels

In this section, we apply the upper bound derived in Section 6.1 to the BAC case. Consider the general BAC with cross-over probabilities ϵ_0 and ϵ_1, the conditional probability of the received vector $\mathbf{y}$ given that the codeword $\mathbf{x}$ sent is

$$P_{Y|X}(\mathbf{y}|\mathbf{x}) = (1-\epsilon_0)^{d_{00}(\mathbf{x},\mathbf{y})} . \epsilon_0^{d_{01}(\mathbf{x},\mathbf{y})} . \epsilon_1^{d_{10}(\mathbf{x},\mathbf{y})} . (1-\epsilon_1)^{d_{11}(\mathbf{x},\mathbf{y})}. \tag{6.43}$$

where we define $d_{\alpha\beta}(\mathbf{x}, \mathbf{y})$ to be the number of positions m at which $x_m = \alpha$ and $y_m = \beta$. So, $d_{10}(\mathbf{x}, \mathbf{y})$ denotes the number of locations at which $\mathbf{x} = 1$ and $\mathbf{y} = 0$

while $d_{11}(\mathbf{x},\mathbf{y})$ is the number of locations at which $\mathbf{x}=1$ and $\mathbf{y}=1$. We define D_i as

$$D_i = (1-\epsilon_0)^{d_{00}(\mathbf{x}_i,\mathbf{y})}.\epsilon_0^{d_{01}(\mathbf{x}_i,\mathbf{y})}.\epsilon_1^{d_{10}(\mathbf{x}_i,\mathbf{y})}.(1-\epsilon_1)^{d_{11}(\mathbf{x}_i,\mathbf{y})} \tag{6.44}$$

and D_u as

$$D_u = (1-\epsilon_0)^{d_{00}(\mathbf{x}_u,\mathbf{y})}.\epsilon_0^{d_{01}(\mathbf{x}_u,\mathbf{y})}.\epsilon_1^{d_{10}(\mathbf{x}_u,\mathbf{y})}.(1-\epsilon_1)^{d_{11}(\mathbf{x}_u,\mathbf{y})}. \tag{6.45}$$

The pairwise error event ε_{iu} is

$$\varepsilon_{iu} = \{D_u \leq D_i\}. \tag{6.46}$$

We note that the event $\{D_u = D_i\}$ is considered as an error event which results in an upper bound on the probability of error. The pairwise error probability can then be written as

$$P(\varepsilon_{iu}|\mathbf{x}_u) = \sum_{\mathbf{y}} I\{D_u \leq D_i\}P(\mathbf{y}), \tag{6.47}$$

where

$$I(\text{statement}) = \begin{cases} 1 & \text{if statement is true,} \\ 0 & \text{if statement is false.} \end{cases} \tag{6.48}$$

The probability of intersection of two error events is given by

$$P(\varepsilon_{iu} \cap \varepsilon_{ju}|\mathbf{x}_u) = \sum_{\mathbf{y}} I\{D_u \leq D_i\}I\{D_u \leq D_j\}P(\mathbf{y}), \tag{6.49}$$

and the probability of intersection of triplet error events is

$$P(\varepsilon_{iu} \cap \varepsilon_{ju} \cap \varepsilon_{ku}|\mathbf{x}_u) = \sum_{\mathbf{y}} I\{D_u \leq D_i\}I\{D_u \leq D_j\}I\{D_u \leq D_k\}P(\mathbf{y}). \tag{6.50}$$

As a result, the average error probability is bounded by

$$\begin{aligned} P(\varepsilon) \quad \leq \quad & \frac{1}{M}\sum_u \sum_{i\neq u} \sum_{\mathbf{y}} I\{D_u \leq D_i\}P(\mathbf{y}) \\ & -\frac{1}{M}\sum_u \sum_{i,j\neq u} \sum_{\mathbf{y}} I\{D_u \leq D_i\}I\{D_u \leq D_j\}P(\mathbf{y}) \\ & +\frac{1}{M}\sum_u \sum_{i,j,k\neq u} \sum_{\mathbf{y}} I\{D_u \leq D_i\}I\{D_u \leq D_j\}I\{D_u \leq D_k\}P(\mathbf{y}). \end{aligned} \tag{6.51}$$

$$\tag{6.52}$$

6.5 Upper Bounds for the Z-Channel

A special case of the BAC is the Z-channel where one of the cross-over probabilities is zero. We consider the model shown in Figure 6.1.

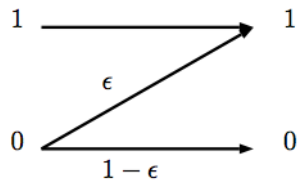

Figure 6.1: Z-channel.

The conditional probability of the received vector given the sent codeword can now be written as

$$P_{Y|X}(\mathbf{y}|\mathbf{x}) = (1-\epsilon)^{d_{00}(\mathbf{x},\mathbf{y})}.\epsilon^{d_{01}(\mathbf{x},\mathbf{y})}, \tag{6.53}$$

where $\mathbf{y}$ is the received codeword, $\mathbf{x} = [x_0, x_1, \ldots, x_{N-1}]$ is the transmitted codeword. The ML decoder is given by

$$g(\mathbf{y}) \triangleq \arg \max_{1 \le i \le M} P_{Y|X}(\mathbf{y}|\mathbf{x}_i). \tag{6.54}$$

We define the pairwise error probability as the probability of transmitting the codeword $\mathbf{x}_i$ and decoding it as $\mathbf{x}_j$, i.e.,

$$\begin{aligned} \Pr(\mathbf{x}_i \to \mathbf{x}_j|\mathbf{x}_i) &\triangleq \Pr[\tilde{g}(\mathbf{y}) = j|\mathbf{x} = \mathbf{x}_i], \\ &= \sum_{\mathbf{y}} P(\mathbf{y}|\mathbf{x}_i) I(g(\mathbf{y}) = j, j \neq i), \end{aligned}$$

where $\tilde{g}(\mathbf{y}) \triangleq \arg \max_{k=[i,j]} P_{Y|X}(\mathbf{y}|\mathbf{x}_k)$ is the decoding rule for the codebook with two-codewords only. To compute the pairwise error probability, we need to compute the conditional output probability $P(\mathbf{y}|\mathbf{x}_i)$ and the indicator function $I(g(\mathbf{y}) = j)$. For

the conditional output error probability, we can write

$$\begin{aligned} P(\mathbf{y}|\mathbf{x}_i) &= (1-\epsilon)^{d_{00}(\mathbf{x}_i,\mathbf{y})}.\epsilon^{d_{01}(\mathbf{x}_i,\mathbf{y})}, \\ &= (1-\epsilon)^{n-w_H(\mathbf{y})}.\epsilon^{w_H(\mathbf{y})-w_H(\mathbf{x}_i)}, \\ &= (1-\epsilon)^{n}\epsilon^{-w_H(\mathbf{x}_i)}\left(\frac{\epsilon}{1-\epsilon}\right)^{w_H(\mathbf{y})}, \end{aligned}$$

where $w_H(\mathbf{x})$ indicates the weight of the codeword $\mathbf{x}$ defined as $w_H(\mathbf{x}) = \sum_{m=0}^{N-1} \mathbf{x}(m)$. For the indicator function, we write

$$\begin{aligned} I(\tilde{g}(\mathbf{y}) = j) &= I\left(P_{Y|X}(\mathbf{y}|\mathbf{x}_j)) \geq P_{Y|X}(\mathbf{y}|\mathbf{x}_i)\right), \\ &= I\left((1-\epsilon)^{d_{00}(\mathbf{x}_j,\mathbf{y})}.\epsilon^{d_{01}(\mathbf{x}_j,\mathbf{y})} \geq (1-\epsilon)^{d_{00}(\mathbf{x}_i,\mathbf{y})}.\epsilon^{d_{01}(\mathbf{x}_i,\mathbf{y})}\right). \end{aligned}$$

To simplify the notations, we denote $d_{00}(\mathbf{x}_j, \mathbf{y})$ as $d_{00}^{(j)}$, $d_{01}(\mathbf{x}_j, \mathbf{y})$ as $d_{01}^{(j)}$, and $d_{11}(\mathbf{x}_j, \mathbf{y})$ as $d_{11}^{(j)}$. Hence, the indicator function is

$$I(\tilde{g}(\mathbf{y}) = j) = I\left((1-\epsilon)^{d_{00}^{(j)}-d_{00}^{(i)}}.\epsilon^{d_{01}^{(j)}-d_{01}^{(i)}} \geq 1\right), \tag{6.55}$$

and the pairwise error probability is given by

$$P(\mathbf{x}_i \to \mathbf{x}_j|\mathbf{x}_i) = (1-\epsilon)^{n}\epsilon^{-w_H(\mathbf{x}_i)} \sum_{\mathbf{y}} \left(\frac{\epsilon}{1-\epsilon}\right)^{w_H(\mathbf{y})} I\left((1-\epsilon)^{d_{00}^{(j)}-d_{00}^{(i)}}.\epsilon^{d_{01}^{(j)}-d_{01}^{(i)}} \geq 1\right). \tag{6.56}$$

The upper bound is then computed by evaluation (6.52) for the probability of intersection of two error events and the intersection of triplet error events.

6.6 Code Design

In this section, we first propose a further simplification on the pairwise error probability expression in (6.56) which results in a more insightful expression for the pairwise probability that is helpful to derive a new metric for code design.

We consider the pairwise error probability. For the code pair $\mathbf{x}_i$ and $\mathbf{x}_j$ where $\mathbf{x}_i$ is the transmitted codeword over the Z-channel, the cardinality of the received

signal set $\mathcal{Y}$ is $2^{N-w_H(\mathbf{x}_i)}$ (since the "1"s will not change but the "0"s may be altered during the transmission over the channel). There are two sets of zeros in the codeword $\mathbf{x}_i$, namely $\mathcal{S}_{00} = \{m|\mathbf{x}_i(m) = 0, \mathbf{x}_j(m) = 0\}$ and $\mathcal{S}_{01} = \{m|\mathbf{x}_i(m) = 0, \mathbf{x}_j(m) = 1\}$, where $\mathbf{x}_i(m)$ and $\mathbf{x}_j(m)$ are the mth bit in the codewords $\mathbf{x}_i$ and $\mathbf{x}_j$, respectively. For any transmitted codeword $\mathbf{x}_i$ there are $N - w_H(\mathbf{x}_i)$ locations at which the zeros will be altered to one due to a channel error. These changes will not correspond to any error (the received message $\mathbf{y}$ cannot be decoded as $\mathbf{x}_j$) as long as $|\mathcal{S}_{01}| < d_{01}(\mathbf{x}_i, \mathbf{x}_j)$, this condition can also be written as $|\mathcal{S}_{01}| < d_{10}(\mathbf{x}_j, \mathbf{x}_i)$.

The indicator function can be rewritten as a function of the codeword pair as follows: let us assume that there are k errors, and these k errors occur at the location of zeros in the set $\mathcal{S}_{00}$. As a result,

$$\begin{aligned} d_{00}(\mathbf{x}_i, y) &= N - w_H(\mathbf{x}_i) - k, \\ d_{01}(\mathbf{x}_i, y) &= k, \\ d_{00}(\mathbf{x}_j, y) &= d_{00}(\mathbf{x}_j, \mathbf{x}_i) - k, \\ d_{01}(\mathbf{x}_j, y) &= d_{01}(\mathbf{x}_j, \mathbf{x}_i) + k. \end{aligned}$$

Then, the weight of the received codeword $\mathbf{y}$ is $w_H(\mathbf{y}) = k + d_{10}(\mathbf{x}_j, \mathbf{x}_i)$. Hence the indicator function can be written as

$$\begin{aligned} I\{D_j \geq D_i\} &= I\left((1-\epsilon)^{d_{00}^{(j)} - d_{00}^{(i)}} \epsilon^{d_{01}^{(j)} - d_{01}^{(i)}} \geq 1\right), \\ &= I\left((1-\epsilon)^{d_{00}(\mathbf{x}_j, \mathbf{x}_i) - N + w_H(\mathbf{x}_i) - 2k} \epsilon^{d_{01}(\mathbf{x}_j, \mathbf{x}_i)} \geq 1\right). \end{aligned}$$

Now, the probability of receiving $\mathbf{y}$ given that $\mathbf{x}_i$ is transmitted can be written as

$$\begin{aligned} P(\mathbf{y}|\mathbf{x}_i) &= (1-\epsilon)^N \epsilon^{-w_H(\mathbf{x}_i)} \left(\frac{\epsilon}{1-\epsilon}\right)^{w_(\mathbf{y})}, \\ &= (1-\epsilon)^N \epsilon^{-w_H(\mathbf{x}_i)} \left(\frac{\epsilon}{1-\epsilon}\right)^{d_{10}(\mathbf{x}_j, \mathbf{x}_i)} \left(\frac{\epsilon}{1-\epsilon}\right)^{k} \left(\frac{\epsilon}{1-\epsilon}\right)^{w_(\mathbf{x}_i)}, \\ &= (1-\epsilon)^{N - w_H(\mathbf{x}_i)} \left(\frac{\epsilon}{1-\epsilon}\right)^{d_{10}(\mathbf{x}_j, \mathbf{x}_i)} \left(\frac{\epsilon}{1-\epsilon}\right)^{k}. \end{aligned}$$

Code Parameter	Weight
d_{01}	$\log(1-\epsilon)$
d_{10}	$\log(\epsilon)-\log(1-\epsilon)$
d_{00}	$\log(1-\epsilon)$

Table 6.1: Code parameters and their associated weights.

Hence, the pairwise error probability is

$$P(\mathbf{x}_i \to \mathbf{x}_j|\mathbf{x}_i) = (1-\epsilon)^{N-w_H(\mathbf{x}_i)} \left(\frac{\epsilon}{1-\epsilon}\right)^{d_{10}(\mathbf{x}_j,\mathbf{x}_i)} \tag{6.57}$$

$$I\left((1-\epsilon)^{d_{00}(\mathbf{x}_j,\mathbf{x}_i)-N+w_H(\mathbf{x}_i)-2k}\epsilon^{d_{01}(\mathbf{x}_j,\mathbf{x}_i)} \geq 1\right)$$

$$\sum_{k=0}^{d_{00}(\mathbf{x}_j,\mathbf{x}_i)} \left(\frac{\epsilon}{1-\epsilon}\right)^{k} \begin{pmatrix} d_{00}(\mathbf{x}_j,\mathbf{x}_i) \\ k \end{pmatrix}. \tag{6.58}$$

We note that the indicator function, and hence the pairwise error probability depends on three parameters, i.e., $d_{00}(\mathbf{x}_j,\mathbf{x}_i)$, $d_{01}(\mathbf{x}_j,\mathbf{x}_i)$, and $d_{10}(\mathbf{x}_j,\mathbf{x}_i)$.

Based on the simplification of the pairwise error probability expression, we propose to use a new metric that characterizes a certain codebook, called the weighted sum Hamming distance between the code pairs defined as

$$d_\alpha(i,j) \triangleq w_0 d_{01}(\mathbf{x}_j,\mathbf{x}_i) + w_1 d_{10}(\mathbf{x}_j,\mathbf{x}_i) + w_2 d_{00}(\mathbf{x}_j,\mathbf{x}_i) \tag{6.59}$$

in the design process. Suitable values for w_0, w_1, and w_2 need to be chosen depending on the contribution of the parameters $d_{01}(\mathbf{x}_j,\mathbf{x}_i)$, $d_{10}(\mathbf{x}_j,\mathbf{x}_i)$, and $d_{00}(\mathbf{x}_j,\mathbf{x}_i)$ to the error probability expression which can be obtained by further investigating (6.58). These weights are summarized in Table 6.1.

For the purpose of designing practical codes, we assume that we have a collection of codewords $\mathcal{C}$ and the objective is to choose the optimal subset of codewords $\mathcal{C}_0$; the optimality here is from the error probability point of view. From (6.58) it is obvious that lower probability of error is associated with lower values for $d_\alpha(i,j)$

dominates the error probability and hence the objective is to choose the set of codewords that maximize the minimum weighted sum Hamming distance, i.e., the code design principle is

$$\mathcal{C}_0 = \arg\max_{\mathcal{C}} \min_{\text{code pairs}} d_\alpha(i,j). \tag{6.60}$$

6.7 Numerical Examples

In this section, we present several numerical examples that illustrate the use of the proposed upper bound for Gaussian and binary channels in the previous sections. We also show some examples of newly designed codes, study their performance, and we compare our proposed code design process with one of the new design approaches for ultrasmall codes developed in [43].

6.7.1 Proposed Upper Bound on the Probability of Error

We now present numerical examples of the proposed error rate upper bound along with some of the known bounds in the literature. Figure 6.2 shows the newly derived upper bound along with the one in [70] and the union bound for transmission over an AWGN channel. The bit error probability is computed for codebook with four codewords and the length of each codeword is taken as 15. The codewords used are

$$C_1 = \begin{bmatrix} 0 & 0 & 0 & 0 & 0 & 0 & 0 & 0 & 0 & 0 & 0 & 0 & 0 & 0 & 0 \\ 0 & 0 & 0 & 0 & 0 & 1 & 1 & 1 & 1 & 1 & 1 & 1 & 1 & 1 & 1 \\ 1 & 1 & 1 & 1 & 1 & 0 & 0 & 0 & 0 & 0 & 1 & 1 & 1 & 1 & 1 \\ 1 & 1 & 1 & 1 & 1 & 1 & 1 & 1 & 1 & 1 & 0 & 0 & 0 & 0 & 0 \end{bmatrix}. \tag{6.61}$$

We observe that the performance of the proposed upper bound is extremely close to the exact bit error rate estimated using Monte Carlo simulations.

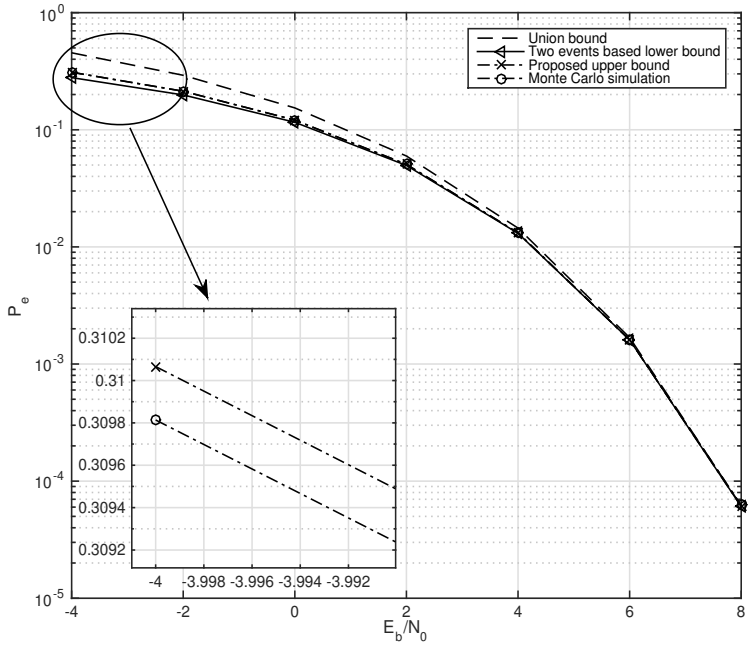

Figure 6.2: Bounds on the probability of error for the code in (6.61) over an AWGN channel.

Figure 6.3 compares the same bounds on the error probability for a larger codebook that consists of eight codewords with length 15 given by

$$C_2 = \begin{bmatrix} 0 & 0 & 0 & 0 & 0 & 0 & 0 & 0 & 0 & 0 & 0 & 0 & 0 & 0 & 0 \\ 0 & 0 & 0 & 0 & 0 & 1 & 1 & 1 & 1 & 1 & 1 & 1 & 1 & 0 & 0 \\ 1 & 1 & 1 & 1 & 1 & 0 & 0 & 0 & 0 & 0 & 1 & 1 & 1 & 1 & 1 \\ 1 & 1 & 1 & 1 & 1 & 1 & 1 & 1 & 1 & 1 & 0 & 0 & 0 & 0 & 0 \\ 0 & 0 & 0 & 0 & 0 & 1 & 1 & 1 & 1 & 1 & 0 & 0 & 0 & 0 & 0 \\ 1 & 1 & 1 & 1 & 1 & 0 & 0 & 0 & 0 & 0 & 0 & 1 & 0 & 0 & 1 \\ 0 & 0 & 0 & 0 & 0 & 1 & 1 & 1 & 1 & 1 & 1 & 1 & 1 & 1 & 1 \\ 1 & 1 & 1 & 1 & 1 & 0 & 0 & 0 & 0 & 0 & 0 & 0 & 0 & 0 & 0 \end{bmatrix}. \tag{6.62}$$

We observe that the proposed upper bound performs much better than the union bound and as good as the upper bound in [70]. The figure also shows that at high SNRs, the proposed upper bound is excellent. Despite not being very tight at low

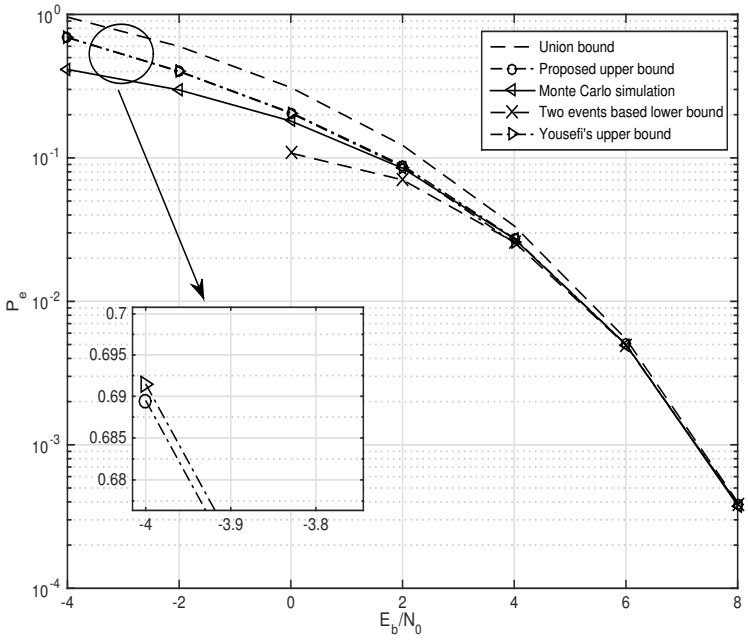

Figure 6.3: Bounds on the probability of error for the code in (6.62) over an AWGN channel.

SNRs, the bound still closely characterizes the probability of error much more closely than the classical union bound.

Figure 6.4 shows the performance of the proposed upper bound for transmission over a Z-channel with parameter ϵ. The codebook that is used to compute this bound consists of four codewords given in (6.61). We observe that the proposed upper bound performs better than the union bound and it is extremely close to the exact probability of error values estimated via Monte Carlo simulations. The figure shows that when the cross-over probability is low, the upper bound is tight. Moreover, when the cross-over probability is high (when there are more frequent channel errors), the proposed upper bound performs very well, i.e., the difference between the upper bound and the estimated error probability (using Monte Carlo simulation) is quite small.

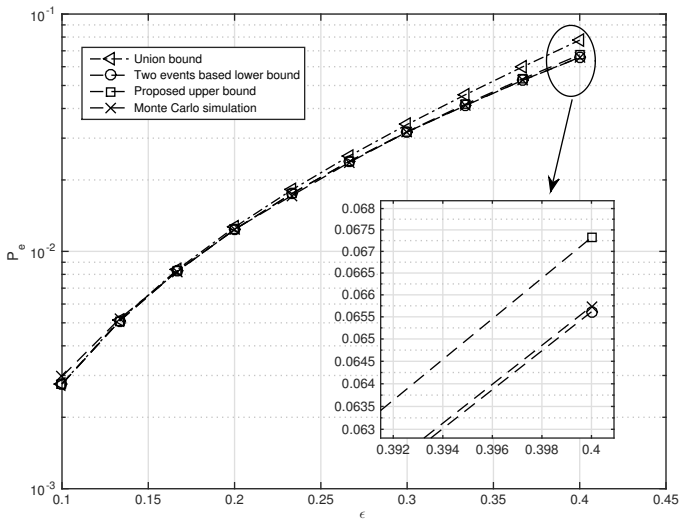

Figure 6.4: Bounds on the probability of error for the code in (6.61) over BAC.

6.7.2 Code Design

We now give a code design example. Using the proposed method we are able to design non-standard sized codes. We design codes of length 15 with the number of messages in each code being four, six, and eight messages, respectively. For comparison, we compute the error probability associated with the designed codes and some codes picked arbitrarily from the pool of codewords we are choosing from. The designed codes are given below in (6.63), (6.64), and (6.65):

$$C_{4 \text{ codewords}} = \begin{bmatrix} 0 & 0 & 0 & 0 & 0 & 0 & 0 & 0 & 0 & 0 & 0 & 0 & 0 & 0 & 0 \\ 0 & 0 & 0 & 0 & 0 & 1 & 1 & 1 & 1 & 1 & 1 & 1 & 1 & 1 & 1 \\ 1 & 1 & 1 & 1 & 1 & 0 & 0 & 0 & 0 & 0 & 1 & 1 & 1 & 1 & 1 \\ 1 & 1 & 1 & 1 & 1 & 1 & 1 & 1 & 1 & 1 & 0 & 0 & 0 & 0 & 0 \end{bmatrix}, \tag{6.63}$$

$$C_{6 \text{ codewords}} = \begin{bmatrix} 0 & 0 & 0 & 0 & 0 & 0 & 0 & 0 & 0 & 0 & 0 & 0 & 0 & 0 & 0 & 0 \\ 1 & 1 & 1 & 1 & 1 & 1 & 1 & 1 & 1 & 1 & 1 & 1 & 1 & 1 & 1 & 1 \\ 1 & 1 & 1 & 1 & 1 & 1 & 1 & 0 & 0 & 0 & 0 & 0 & 0 & 0 & 0 & 0 \\ 0 & 0 & 0 & 0 & 0 & 0 & 0 & 1 & 1 & 1 & 1 & 1 & 1 & 1 & 1 & 1 \\ 0 & 1 & 0 & 1 & 0 & 1 & 0 & 1 & 0 & 1 & 0 & 1 & 0 & 1 & 0 & 1 \\ 1 & 0 & 1 & 0 & 1 & 0 & 1 & 0 & 1 & 0 & 1 & 0 & 1 & 0 & 1 & 0 \end{bmatrix}, \tag{6.64}$$

$$C_{8 \text{ codewords}} = \begin{bmatrix} 0 & 0 & 0 & 0 & 0 & 0 & 0 & 0 & 0 & 0 & 0 & 0 & 0 & 0 & 0 & 0 \\ 1 & 1 & 1 & 1 & 1 & 1 & 1 & 1 & 1 & 1 & 1 & 1 & 1 & 1 & 1 & 1 \\ 1 & 1 & 1 & 1 & 0 & 0 & 0 & 0 & 0 & 0 & 0 & 0 & 1 & 1 & 1 & 1 \\ 0 & 0 & 0 & 0 & 1 & 1 & 0 & 1 & 0 & 1 & 0 & 1 & 1 & 0 & 0 & 0 \\ 1 & 1 & 1 & 1 & 1 & 1 & 1 & 0 & 0 & 0 & 0 & 0 & 0 & 0 & 0 & 0 \\ 0 & 1 & 1 & 1 & 1 & 1 & 1 & 1 & 1 & 1 & 1 & 1 & 0 & 0 & 0 & 0 \\ 0 & 0 & 0 & 0 & 0 & 0 & 0 & 1 & 1 & 1 & 1 & 1 & 1 & 1 & 1 & 1 \\ 0 & 1 & 0 & 1 & 0 & 1 & 0 & 1 & 0 & 1 & 0 & 1 & 0 & 1 & 0 & 1 \end{bmatrix}. \tag{6.65}$$

The resulting performance comparisons between our designs and some other codes are made in Figures 6.5, 6.6, and 6.7, respectively. The figures show that the newly designed codes over perform significantly better than others picked arbitrarily among possible codebooks.

Let us recall that the main objective of our study is to design codes for additive channels with signal-dependent noise. Motivated by this, we now use one of the newly designed codes for the Z-channel on a Gaussian channel with additive noise whose variance depends on the transmitted signal. We assume that the power spectral density of the noise is $N_0^{(0)}$ for "0" and $N_0^{(1)}$ for "1", we assume that the between these variances $\frac{N_0^{(1)}}{N_0^{(0)}} = 2$. Figure 6.8 shows a comparison between the performance of the newly designed code and another one constructed from four codewords of a

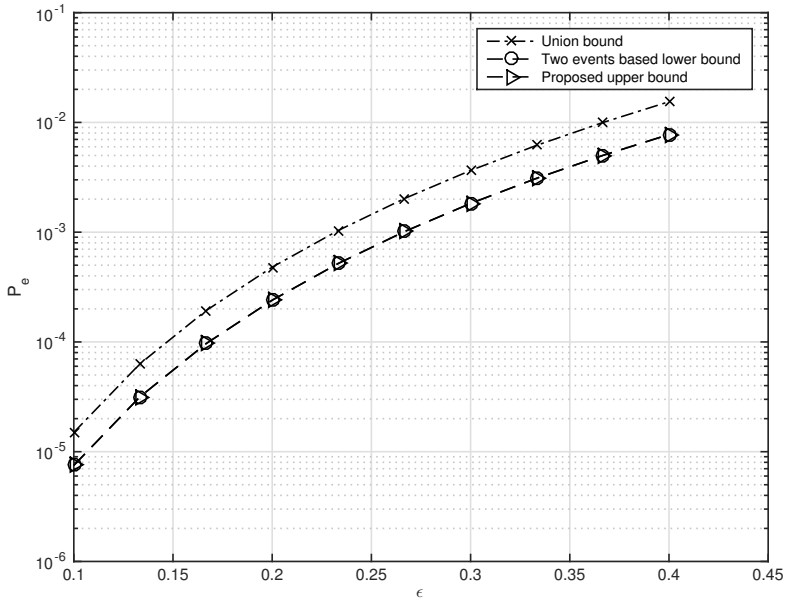

Figure 6.5: Bounds on the probability of error for the code in (6.63) over a BAC.

$(15, 11)$ Hamming code. The codebook used for comparison purposes is

$$C' = \begin{bmatrix} 1 & 1 & 0 & 0 & 0 & 1 & 0 & 0 & 1 & 0 & 1 & 1 & 0 & 0 & 1 \\ 1 & 0 & 1 & 1 & 0 & 1 & 1 & 0 & 1 & 1 & 0 & 1 & 1 & 0 & 1 \\ 1 & 1 & 1 & 1 & 1 & 0 & 0 & 0 & 0 & 1 & 1 & 1 & 1 & 0 & 0 \\ 0 & 1 & 0 & 0 & 0 & 1 & 1 & 1 & 1 & 1 & 1 & 0 & 1 & 1 & 1 \end{bmatrix}. \tag{6.66}$$

The figure shows that the newly designed codes over signal-dependent Gaussian noise channels perform better than other codes designed for BSCs. This preliminary results suggests that signal dependent noise channels require new design rules to capture their different behavior. To accomplish this, one may obtain a new metric adapted for these channels by studying carefully the error probability bound.

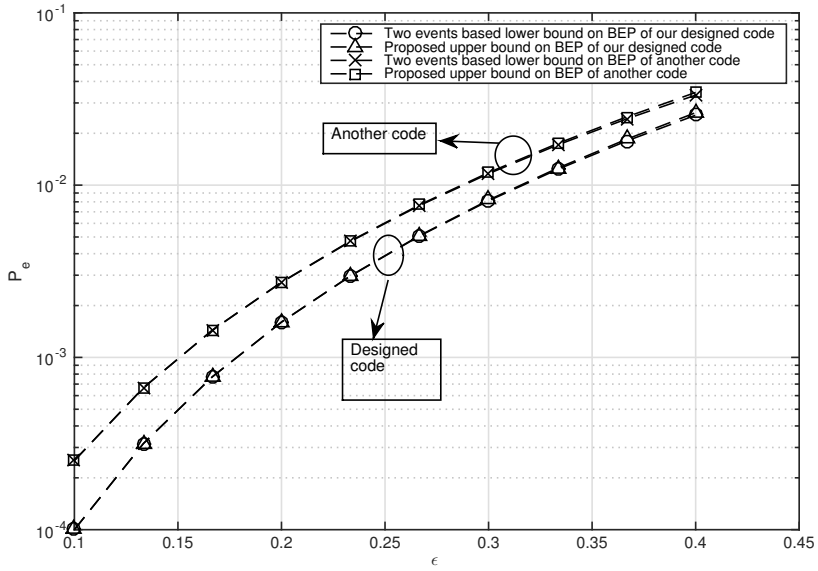

Figure 6.6: Bounds on the probability of error for the code in (6.64) over a BAC.

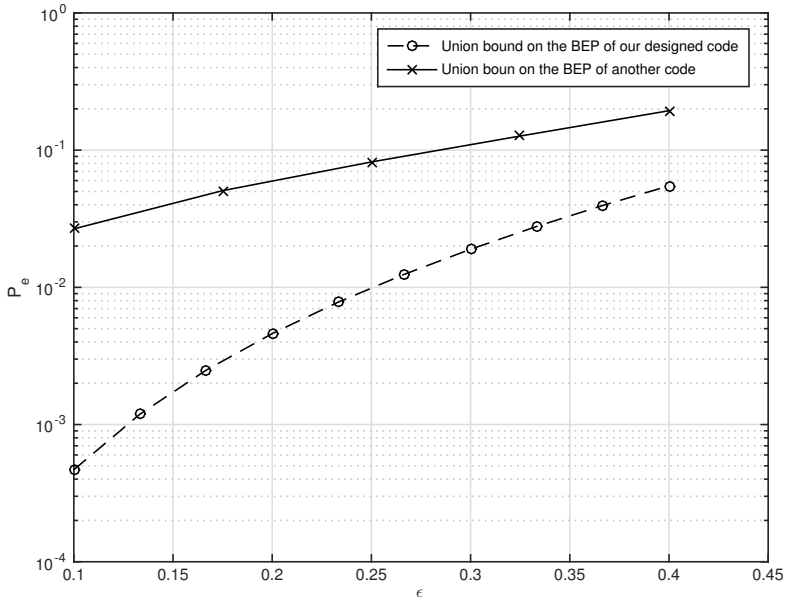

Figure 6.7: Bounds on the probability of error for the code in (6.65) over a BAC.

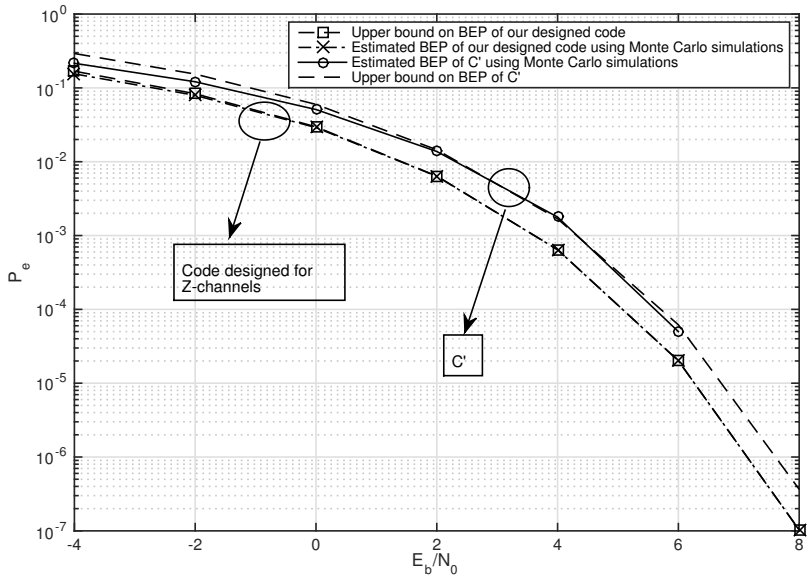

Figure 6.8: Performance comparison between the designed codes for a Z-channel, and C' with codewords picked from a $(15, 11)$ Hamming code for transmission over Gaussian channels with additive noise whose variance depends on the transmitted signal.

6.8 Chapter Summary

In this chapter, we have studied the code design problem for signal-dependent Gaussian noise channels. We proposed a tight upper bound on the error probability, and applied it on AWGN, the signal-dependent Gaussian noise, binary asymmetric and Z-channels. We then employed them for designing codes over the Z-channel by defining a new metric, namely, the weighted sum Hamming distance. We demonstrated via examples the tightness of the bounds and showed that the newly designed codes offer superior performance for different channels.

Chapter 7

SUMMARY AND CONCLUSIONS

We have proposed a new communications scheme where signature signals are used to carry digital data. One possible application for this communications scheme is in UWA communications. With this motivation, we have applied the proposed scheme by using biomimetic sound signals as the signature signals. We have utilized analytical models for the mammalian sounds specified by certain signal parameters, and to complete the design, we have developed a two-stage decoder to reduce the computational complexity. The decoder aims to find estimates of the parameters of the transmitted signal, and demaps them into information bits. We have also derived an approximate system model to facilitate its analysis. Furthermore, we have illustrated the viability of the proposed scheme via experimental data recorded at the recent KAM11 experiment.

We have also performed an information theoretic study of the equivalent approximate system model implied by the proposed communications scheme. The equivalent system model suggests that the channel can be modeled as an AWGN channel with amplitude-limited inputs and signal-dependent noise. With this motivation, we have studied capacity of single-antenna communications with amplitude-limited inputs. We have also explored the capacity of arbitrary fading channels with amplitude-limited inputs when the channel state information is available at the receiver. We have shown that the capacity achieving distribution is discrete. To accomplish this, we proved that the conditional mutual information function is a continuous, strictly concave, and weakly differentiable function of the input distribution. Then, the capacity optimization turns out to be a convex optimization problem. Hence, there is a unique optimal distribution that maximizes the conditional mutual information func-

tion. We have used techniques from complex analysis and measure theory to show the discreteness of the capacity-achieving distribution. We have also considered Gaussian channels with signal-dependent noise and amplitude-limited inputs, and shown that for arbitrary but well-behaved noise variance functions, the capacity-achieving distribution is discrete with a finite number of mass points.

Furthermore, we have studied the capacity of the multi-antenna systems and parallel Gaussian channels under peak and average power constraints. For the MIMO systems, computing the capacity is not viable using the existing techniques since the Identity Theorem is available only for one-dimensional functions, and there is no equivalent form for the multi-dimensional case. Therefore, we have derived upper and lower bounds on the capacity. We have derived these bounds by solving the capacity optimization problem over different feasible regions than the original one. For the upper bound, we have relaxed the capacity optimization problem by assuming inputs over a large region that inscribes the feasible region, and for the lower bound we have constrained the capacity optimization problem by assuming inputs over a smaller region inside the feasible one. We have also proposed an alternative upper bound by inspecting other suboptimal input distributions. For parallel Gaussian channels with peak and average power constraints, we have derived analytical bounds on the capacity for low and high noise variances, and utilized these asymptotic results to obtain an information theoretic characterization for the entire SNR range.

Finally, we have considered the practical channel coding problem for the equivalent system model studied in Chapter 2. We have considered two channel models; Gaussian channels with additive noise whose variance depends on the transmitted signal, and binary-input binary-output asymmetric channels that serve as approximations. In our study, we have considered ultra-small block codes. We have developed

a new upper bound on the error probability based on Bonferroni type inequalities by considering the doublet and triplet pairwise error events. Furthermore, we have developed an error probability expression for Z-channels that leads to a universal metric for code design. This new metric, called weighted sum Hamming distance, results in characterizing the codebooks without the need of extensive computations of the error probabilities. We have employed this metric to design new codes and illustrated their performance via several examples.

As possible extensions of the work in this dissertation, we cite several different directions. For the proposed communication scheme, in order to improve the performance of the decoder, a more advanced receiver can be designed. This new receiver may incorporate a joint channel estimator and parameter vector decoder. The receiver can also be designed to compensate for the UWA channel effects such as Doppler scaling.

In our work, we considered fading channels and signal dependent noise for amplitude-limited channels for which the additive noise is Gaussian. A possible extension is for channels that are not necessarily Gaussian. Under certain conditions on the noise probability density functions similar results on the channel capacity may be obtained.

Another possible extension is in the subject of code design. In this dissertation, we have considered code design for Z-channels by proposing a new performance metric. A similar metric can be developed for signal-dependent Gaussian channels to design codes by examining the derived error rate bounds closely. We speculate that it could be possible to design codes that perform better in signal-dependent Gaussian channels than the conventional codes designed for AWGN channels or BSCs.

REFERENCES

[1] A. ElMoslimany, M. Zhou, T. M. Duman, and A. Papandreou-Suppappola, "A new signaling scheme for Underwater Acoustic communications," in *IEEE Oceans*, September 2013, pp. 1–5.

[2] W. S. Hodgkiss, H. C. Song, G. Dean, M. Badiey, and A. Song, "Kauai Acomms MURI 2011 (KAM11) Experiment Trip Report," Tech. Rep., August 2011.

[3] R. Wood, "Detection and capacity limits in magnetic media noise," *IEEE Transactions on Magnetics*, vol. 34, no. 4, pp. 1848–1850, Jul 1998.

[4] M. Stojanovic and J. Preisig, "Underwater acoustic communication channels: Propagation models and statistical characterization," *IEEE Communications Magazine*, vol. 47, no. 1, pp. 84–89, January 2009.

[5] M. Stojanovic, "Recent advances in high-speed underwater acoustic communications," *IEEE Journal of Oceanic Engineering*, vol. 21, no. 2, pp. 125–136, April 1996.

[6] M. Suzuki, T. Sasaki, and T. Tsuchiya, "Digital acoustic image transmission system for deep-sea research submersible," in *IEEE OCEANS*, vol. 2, 1992, pp. 567–570.

[7] J. G. Proakis and M. Salehi, *Digital Communications*, 5th ed. New York, NY: McGraw-Hill, 2008, p. 1150.

[8] M. Stojanovic, J. A. Catipovic, and J. G. Proakis, "Phase-coherent digital communications for underwater acoustic channels," *IEEE Journal of Oceanic Engineering*, vol. 19, no. 1, pp. 100–111, January 1994.

[9] S. Haykin, *Adaptive filter theory (ISE).* Prentice Hall, 2003.

[10] M. Stojanovic, "Low complexity OFDM detector for underwater acoustic channels," in *IEEE Oceans*, September 2006, pp. 1–6.

[11] ——, "OFDM for underwater acoustic communications: Adaptive synchronization and sparse channel estimation," in *IEEE International Conference on Acoustics, Speech and Signal Processing (ICASSP)*, April 2008, pp. 5288–5291.

[12] K. Tu, D. Fertonani, T. M. Duman, M. Stojanovic, J. G. Proakis, and P. Hursky, "Mitigation of intercarrier interference for OFDM over time-varying underwater acoustic channels," *IEEE Journal of Oceanic Engineering*, vol. 36, no. 2, pp. 156–171, April 2011.

[13] K. Tu, T. M. Duman, M. Stojanovic, and J. G. Proakis, "Multiple-resampling receiver design for OFDM over Doppler-distorted underwater acoustic channels," *IEEE Journal of Oceanic Engineering*, vol. 38, pp. 333–346, April 2013.

[14] S. Roy, T. M. Duman, V. K. McDonald, and J. G. Proakis, "High-rate communication for underwater acoustic channels using multiple transmitters and space-time coding: receiver structures and experimental results," *IEEE Journal of Oceanic Engineering*, vol. 32, no. 3, pp. 663–688, July 2007.

[15] S. Roy, T. M. Duman, and V. K. McDonald, "Error rate improvement in underwater MIMO communications using sparse partial response equalization," *IEEE Journal of Oceanic Engineering*, vol. 34, no. 2, pp. 181–201, September 2009.

[16] M. Stojanovic, "MIMO OFDM over underwater acoustic channels," in *Conference Record of the Forty-Third Asilomar Conference on Signals, Systems and Computers*, November 2009, pp. 605–609.

[17] Y. Emre, V. Kandasamy, T. M. Duman, P. Hursky, and S. Roy, "Multi-input multi-output OFDM for shallow-water UWA communications (invited paper)," in *Proceedings of ACOUSTICS 2008*, July 2008.

[18] D. Rouseff, D. R. Jackson, W. L. J. Fox, C. D. Jones, J. A. Ritcey, and D. R. Dowling, "Underwater acoustic communication by passive-phase conjugation: Theory and experimental results," *IEEE Journal of Oceanic Engineering*, vol. 26, no. 4, pp. 821–831, October 2001.

[19] J. Gomes and V. Barroso, "A matched field processing approach to underwater acoustic communication," in *IEEE Oceans*, vol. 2, September 1999, pp. 991–995.

[20] W. A. Kuperman, W. S. Hodgkiss, H. C. Song, T. Akal, C. Ferla, and D. R. Jackson, "Phase conjugation in the ocean: Experimental demonstration of an acoustic time-reversal mirror," *The journal of the Acoustical Society of America*, vol. 103, pp. 25–40, August 1997.

[21] G. F. Edelmann, H. C. Song, S. Kim, W. S. Hodgkiss, W. A. Kuperman, and T. Akal, "Underwater acoustic communications using time reversal," *IEEE Journal of Oceanic Engineering*, vol. 30, no. 4, pp. 852–864, October 2005.

[22] J. A. Flynn, J. A. Ritcey, D. Rouseff, and W. L. J. Fox, "Multichannel equalization by decision-directed passive phase conjugation: Experimental results," *IEEE Journal of Oceanic Engineering*, vol. 29, no. 3, pp. 824–836, July 2004.

[23] H. C. Song, "Time reversal communication in a time-varying sparse channel," *The Journal of the Acoustical Society of America*, vol. 130, no. 4, pp. EL161–EL166, October 2011.

[24] H. C. Song, W. S. Hodgkiss, W. A. Kuperman, T. Akal, and M. Stevenson, "Multiuser communications using passive time reversal," *IEEE Journal of Oceanic Engineering*, vol. 32, no. 4, pp. 915–926, October 2007.

[25] H. C. Song, J. S. Kim, W. S. Hodgkiss, W. A. Kuperman, and M. Stevenson, "High-rate multiuser communications in shallow water," *The Journal of the Acoustical Society of America*, vol. 128, pp. 2920–2925, November 2010.

[26] S. Liu, G. Qiao, and A. Ismail, "Covert underwater acoustic communication using dolphin sounds," *The Journal of the Acoustical Society of America*, vol. 133, no. 4, pp. EL300–EL306, April 2013.

[27] S. Liu, G. Qiao, A. Ismail, B. Liu, and L. Zhang, "Covert underwater acoustic communication using whale noise masking on DSSS signal," in *IEEE Oceans*, June 2013, pp. 1–6.

[28] J. G. Smith, "The information capacity of amplitude and variance-constrained scalar Gaussian channels," *Information and Control*, vol. 18, no. 3, pp. 203–219, 1971.

[29] A. Tchamkerten, "On the discreteness of capacity-achieving distributions," *IEEE Transactions on Information Theory*, vol. 50, no. 11, pp. 2773–2778, October 2004.

[30] S. Shamai and I. Bar-David, "The capacity of average and peak-power-limited quadrature Gaussian channels," *IEEE Transactions on Information Theory*, vol. 41, no. 4, pp. 1060–1071, July 1995.

[31] I. C. Abou-Faycal, M. D. Trott, and S. Shamai, "The capacity of discrete-time memoryless Rayleigh-fading channels," *IEEE Transactions on Information Theory*, vol. 47, no. 4, pp. 1290–1301, May 2001.

[32] M. Katz and S. Shamai, "On the capacity-achieving distribution of the discrete-time noncoherent and partially coherent AWGN channels," *IEEE Transactions on Information Theory*, vol. 50, no. 10, pp. 2257–2270, Oct. 2004.

[33] M. C. Gursoy, H. V. Poor, and S. Verdú, "The noncoherent Rician fading channel-part I: structure of the capacity-achieving input," *IEEE Transactions on Wireless Communications*, vol. 4, no. 5, pp. 2193–2206, Sept. 2005.

[34] T. H. Chan, S. Hranilovic, and F. R. Kschischang, "Capacity-achieving probability measure for conditionally gaussian channels with bounded inputs," *IEEE Transactions on Information Theory*, vol. 51, no. 6, pp. 2073–2088, May 2005.

[35] B. Mamandipoor, K. Moshksar, and A. K. Khandani, "On the sum-capacity of Gaussian MAC with peak constraint," in *IEEE International Symposium on Information Theory Proceedings*, July 2012, pp. 26–30.

[36] O. Ozel and S. Ulukus, "On the capacity region of the Gaussian MAC with batteryless energy harvesting transmitters," in *IEEE Global Communications Conference*, December 2012, pp. 2385–2390.

[37] A. Lapidoth, S. M. Moser, and M. A. Wigger, "On the capacity of free-space optical intensity channels," *IEEE Transactions on Information Theory*, vol. 55, no. 10, pp. 4449–4461, October 2009.

[38] N. Marina, "LDPC codes for binary asymmetric channels," in *IEEE International Conference on Telecommunications*, June 2008, pp. 1–7.

[39] S. D. Constantin and T. Rao, "On the theory of binary asymmetric error correcting codes," *Information and Control*, vol. 40, no. 1, pp. 20–36, Janurary 1979.

[40] C.-C. Wang, S. R. Kulkarni, and H. V. Poor, "Density evolution for asymmetric memoryless channels," *IEEE Transactions on Information Theory*, vol. 51, no. 12, pp. 4216–4236, December 2005.

[41] R. Gabrys and L. Dolecek, "Coding for the binary asymmetric channel," in *IEEE International Conference on Computing, Networking and Communications*, February 2012, pp. 461–465.

[42] M. Grassl, P. Shor, G. Smith, J. Smolin, and B. Zeng, "New constructions of codes for asymmetric channels via concatenation," in *IEEE International Symposium on Information Theory Proceedings*, July 2012, pp. 751–755.

[43] P.-N. Chen, H.-Y. Lin, and S. Moser, "Optimal ultrasmall block-codes for binary discrete memoryless channels," *IEEE Transactions on Information Theory*, vol. 59, no. 11, pp. 7346–7378, November 2013.

[44] ——, "Weak flip codes and applications to optimal code design on the binary erasure channel," in *Annual Allerton Conference on Communication, Control, and Computing*, October 2012, pp. 160–167.

[45] T. C. Yang and W. Yang, "Low probability of detection underwater acoustic communications using direct-sequence spread spectrum," *The Journal of the Acoustical Society of America*, vol. 124, no. 6, pp. 3632–3647, December 2008.

[46] J. Ling, H. He, J. Li, W. Roberts, and P. Stoica, "Covert underwater acoustic communications," *The Journal of the Acoustical Society of America*, vol. 128, no. 5, pp. 2898–2909, November 2010.

[47] J. Severson, "Modeling and frequency tracking of marine mammal whistle calls," Master's thesis, Massachusetts Institute of Technology, 2009.

[48] A. Papandreou-Suppappola and S. B. Suppappola, "Sonar echo ranging using signals with non-linear time-frequency characteristics," *IEEE Signal Processing Letters*, vol. 11, pp. 393–396, March 2004.

[49] ——, "Analysis and classification of time-varying signals with multiple time-frequency structures," *IEEE Signal Processing Letters*, vol. 9, pp. 92–95, March 2002.

[50] S. M. Kay, *Fundamentals of Statistical Signal Processing: Estimation Theory*, 1st ed., ser. Prentice-Hall signal processing series. Upper-Saddle River, NJ: Prentice-Hall PTR, 1993, vol. 1, p. 625.

[51] H. V. Poor, *An Introduction to Signal Detection and Estimation*, 2nd ed. New York, NY: Springer-Verlag, 1988, pp. 182–183.

[52] W. Li and J. C. Preisig, "Estimation of rapidly time-varying sparse channels," *IEEE Journal of Oceanic Engineering*, vol. 32, no. 4, pp. 927–939, October 2007.

[53] C. R. Berger, S. Zhou, J. C. Preisig, and P. Willett, "Sparse channel estimation for multicarrier underwater acoustic communication: From subspace methods to compressed sensing," *IEEE Transactions on Signal Processing*, vol. 58, no. 3, pp. 1708–1721, May 2010.

[54] S. J. Wright, R. D. Nowak, and M. A. T. Figueiredo, "Sparse reconstruction by separable approximation," *IEEE Transactions on Signal Processing*, vol. 57, no. 7, pp. 2479–2493, July 2009.

[55] R. M. Gray, *Entropy and Information Theory*. Springer, 1990.

[56] M. S. Pinsker, *Information and Information Stability of Random Variables and Processes*. Izv. Akad. Nauk, 1960.

[57] B. Ash, Robert, *Information Theory*. Dover, New York, 1965.

[58] R. M. Dudley, *Real Analysis and Probability*. Cambridge University Press, 2002, vol. 74.

[59] S. Boyd and L. Vandenberghe, *Convex Optimization*. Cambridge University Press, 2009.

[60] R. G. Gallager, *Information Theory and Reliable Communication*. New York, NY: John Wiley & Sons, 1968.

[61] J. G. Smith, "On the information capacity of peak and average power constrained Gaussian channels," Ph.D. dissertation, Department of Electrical Engineering, University of California, Berkeley, California, 1969.

[62] L. C. Barbosa, "A model for magnetic recording channels with signal dependent noise," *IEEE Transactions on Magnetics*, vol. 31, no. 2, pp. 1062–1064, 1995.

[63] T. Oenning and J. Moon, "Modeling the Lorentzian magnetic recording channel with transition noise," *IEEE Transactions on Magnetics*, vol. 37, no. 1, pp. 583–591, 2001.

[64] P. Webb, R. McIntyre, and J. Conradi, "Properties of avalanche photodiodes," *RCA review*, vol. 35, pp. 234–278, 1974.

[65] M. N. Khan and W. G. Cowley, "Signal dependent Gaussian noise model for FSO communications," in *IEEE Australian Communications Theory Workshop (AusCTW),*, 2011, pp. 142–147.

[66] S. M. Moser, "Capacity results of an optical intensity channel with input-dependent gaussian noise," *IEEE Transactions on Information Theory*, vol. 58, no. 1, pp. 207–223, Janurary 2012.

[67] K. Knopp and F. Bagemihl, *Theory of functions*. Courier Corporation, 1996, vol. 1.

[68] M. Raginsky, "On the information capacity of Gaussian channels under small peak power constraints," in *Annual Allerton Conference on Communication, Control, and Computing*, September 2008, pp. 286–293.

[69] T. M. Duman and A. Ghrayeb, *Coding for MIMO Communication Systems*. John Wiley & Sons, 2007.

[70] S. Yousefi and A. K. Khandani, "A new upper bound on the ML decoding error probability of linear binary block codes in AWGN interference," *IEEE Transactions on Information Theory*, vol. 50, no. 12, pp. 3026–3036, 2004.

[71] G. E. Séguin, "A lower bound on the error probability for signals in white Gaussian noise," *IEEE Transactions on Information Theory*, vol. 44, no. 7, pp. 3168–3175, 1998.

[72] R. Weinstock, *Calculus of variations: with applications to physics and engineering*. Courier Corporation, 1952.

APPENDIX A

FISHER INFORMATION MATRIX FOR MLE OF SIGNAL PARAMETERS TRANSMITTED ON AWGN

For a given value of the transmitted sequence length M (treated as known in the sequel) we have,

$$\begin{aligned} x[n] &= s[n] + w[n] \\ &= A\sqrt{\nu[n]}\cos\left(2\pi c\xi[n]\right) + w[n], \qquad n = 0, 1, \ldots, M-1. \end{aligned} \tag{A.1}$$

we define the likelihood function for the parameters θ as

$$\ln p = \ln p(\mathbf{x};\theta) = -\frac{M}{2}\ln(2\pi\sigma^2) - \frac{1}{2\sigma^2}\sum_{n=0}^{M-1}\left(x[n] - Ar[n]\right)^2. \tag{A.2}$$

The ijth element of the Fisher information matrix [50] is defined as

$$\left[I\left(\theta\right)\right]_{ij} = -\mathbf{E}\left[\frac{\partial \ln p}{\partial\theta_i}\frac{\partial \ln p}{\partial\theta_j}\right]. \tag{A.3}$$

From (A.2) we can write the following,

$$\frac{\partial \ln p}{\partial A} = \frac{1}{\sigma^2}\sum_{n=0}^{M-1}\left(x[n] - Ar[n]\right)r[n], \tag{A.4}$$

$$\frac{\partial \ln p}{\partial c} = \frac{1}{\sigma^2}\sum_{n=0}^{M-1}\left(x[n] - Ar[n]\right)A\frac{\partial r[n]}{\partial c}, \tag{A.5}$$

$$\frac{\partial^2 \ln p}{\partial^2 A} = -\frac{1}{\sigma^2}\sum_{n=0}^{M-1}\left(r[n]\right)^2, \tag{A.6}$$

$$\frac{\partial^2 \ln p}{\partial^2 c} = \frac{1}{\sigma^2}\sum_{n=0}^{M-1}\left(-A^2\left(\frac{\partial r[n]}{\partial c}\right)^2 + \left(x[n] - Ar[n]\right)A\frac{\partial^2 r[n]}{\partial^2 c}\right), \tag{A.7}$$

$$\frac{\partial^2 \ln p}{\partial A\partial c} = \frac{1}{\sigma^2}\sum_{n=0}^{M-1}\left(-A\left(\frac{\partial r[n]}{\partial c}\right)r[n] + \left(x[n] - Ar[n]\right)\frac{\partial r[n]}{\partial c}\right), \tag{A.8}$$

$$\frac{dr[n]}{dc} = -2\pi\xi[n]\sqrt{\nu[n]}\sin\left(2\pi c\xi[n]\right), \tag{A.9}$$

and, since $\mathrm{E}\left[\left(x[n] - Ar[n]\right)\right] = 0$, we obtain

$$\begin{aligned} \left[I\left(\theta\right)\right]_{11} &= -\mathrm{E}\left[\frac{\partial^2 \ln p}{\partial^2 A}\right] \\ &= \frac{1}{\sigma^2}\sum_{n=0}^{M-1} r^2[n], \end{aligned}$$

$$
\begin{aligned}
\left[I\left(\theta\right)\right]_{12} &= -\mathrm{E}\left[\frac{\partial^2 \ln p}{\partial A \partial c}\right] \\
&= \frac{1}{\sigma^2}\sum_{n=0}^{M-1}\left(Ar[n]\frac{\partial r[n]}{\partial c}\right),
\end{aligned}
$$

$$
\left[I\left(\theta\right)\right]_{21} = \left[I\left(\theta\right)\right]_{12},
$$

$$
\begin{aligned}
\left[I\left(\theta\right)\right]_{22} &= -\mathrm{E}\left[\frac{\partial^2 \ln p}{\partial^2 c}\right] \\
&= \frac{1}{\sigma^2}\sum_{n=0}^{M-1}\left(A\frac{\partial r[n]}{\partial c}\right)^2.
\end{aligned}
$$

APPENDIX B

FISHER INFORMATION MATRIX FOR MLE OF SIGNAL PARAMETERS TRANSMITTED ON MULTIPATH CHANNELS

Given the transmitted sequence length M we have,

$$x[n] = \begin{cases} \sum_{l=0}^{L-1} h_l[n]s[n-l] + w[n] & \text{if } n = 0, 1, \ldots, M-1, \ldots, M+L-2 \\ w[n] & \text{if } n = M+L-1, \ldots, N-1, \end{cases} \tag{B.1}$$

similar to the AWGN case, the likelihood function for the vector θ for a given M is

$$\ln p(\mathbf{x}; \theta) = -\frac{M}{2} \ln(2\pi\sigma^2) - \frac{1}{2\sigma^2} \sum_{n=0}^{M-1} (x[n] - Au[n])^2. \tag{B.2}$$

Also,

$$\frac{\partial \ln p}{\partial A} = \frac{1}{\sigma^2} \sum_{n=0}^{M-1} (x[n] - Au[n])\, u[n], \tag{B.3}$$

$$\frac{\partial \ln p}{\partial c} = \frac{1}{\sigma^2} \sum_{n=0}^{M-1} (x[n] - Au[n])\, A \frac{\partial u[n]}{\partial c}, \tag{B.4}$$

$$\frac{\partial^2 \ln p}{\partial^2 A} = -\frac{1}{\sigma^2} \sum_{n=0}^{M-1} u^2[n], \tag{B.5}$$

$$\frac{\partial^2 \ln p}{\partial^2 c} = \frac{1}{\sigma^2} \sum_{n=0}^{M-1} -A^2 \left(\frac{\partial r}{\partial c}\right)^2 + (x[n] - Au[n])\, A \frac{\partial^2 u[n]}{\partial^2 c}, \tag{B.6}$$

$$\frac{\partial^2 \ln p}{\partial A \partial c} = \frac{1}{\sigma^2} \sum_{n=0}^{M-1} -A \left(\frac{\partial u[n]}{\partial c}\right) u[n] + (x[n] - Au[n]) \frac{\partial u[n]}{\partial c}, \tag{B.7}$$

$$\frac{du[n]}{dc} = -2\pi \sum_{l=0}^{L-1} h_l[n]\xi[n-l]\sqrt{\nu[n-l]} \sin\left(2\pi c \xi[n-l]\right), \tag{B.8}$$

and, since $\mathrm{E}\left[(x[n] - Au[n])\right] = 0$, we obtain Thus, the elements of the Fisher information matrix are,

$$\begin{aligned} \left[I\left(\psi\right)\right]_{11} &= -\mathrm{E}\left[\frac{\partial^2 \ln p}{\partial^2 A}\right] \\ &= \frac{1}{\sigma^2} \sum_{n=0}^{M-1} u^2[n]. \end{aligned}$$

$$\begin{aligned}
\left[I\left(\psi\right)\right]_{12} &= -\mathrm{E}\left[\frac{\partial^2 \ln p}{\partial A \partial c}\right] \\
&= \frac{1}{\sigma^2}\sum_{n=0}^{M-1}\left(Au[n]\frac{\partial u[n]}{\partial c}\right).
\end{aligned}$$

$$\left[I\left(\psi\right)\right]_{21} = \left[I\left(\psi\right)\right]_{12}.$$

$$\begin{aligned}
\left[I\left(\psi\right)\right]_{22} &= -\mathrm{E}\left[\frac{\partial^2 \ln p}{\partial^2 c}\right] \\
&= \frac{1}{\sigma^2}\sum_{n=0}^{M-1}\left(A\frac{\partial u[n]}{\partial c}\right)^2.
\end{aligned}$$

APPENDIX C

THE MARGINAL ENTROPY IS EXTENDABLE TO THE COMPLEX DOMAIN

The marginal entropy density $h(x; F_X)$ is, for arbitrary $F_X \in \mathcal{F}$,

$$h(x; F_x) = -\int_{-\infty}^{\infty} P_N(y-x, x) \log f_Y(y; F_x) dy, \quad \forall x \in [-A, A]. \tag{C.1}$$

First, we assume that the function $\log(\sigma^2(z))$ can be extended to the entire complex plane $\mathbb{C}$ excluding the branch cuts of $\log(\sigma^2(z))$, i.e.,

$$\sigma_n^2(z) + \sigma_z^2 = \sigma_r^2 + j\sigma_i^2. \tag{C.2}$$

That is, $\forall\ z\ \in \mathbb{C}$, i.e., $z = a + jb$, $|\sigma^2(z)| < \infty$, $|\sigma_r^2| < \infty$, and $|\sigma_i^2| < \infty$.

The function $h(x; F_X)$ can be extended to the entire complex plane $\mathbb{C}$ by showing that $\forall\ z$ s.t. $|z| < \infty$

$$\begin{aligned}
|h(z; F_X)| &\leq \int_{-\infty}^{\infty} |P_N(y-z, z)|\, |\log(P_Y(y; F_X))|\, dy, \\
&= \frac{1}{\sqrt{2\pi|\sigma_z^2 + \sigma_n^2(z)|}} \int_{-\infty}^{\infty} \left| \exp\left(-\frac{(y-a-jb)^2}{2\sigma_r^2 + j2\sigma_i^2} \right) \right| |\log(f_Y(y; F_X))| dy, \\
&= \frac{1}{\sqrt{2\pi|\sigma_z^2 + \sigma_n^2(z)|}} \int_{-\infty}^{\infty} \left| \exp\left(-\frac{1}{2} \frac{\left((y-a)^2 + b^2 - 2jb(y-a)\right)\left(\sigma_r^2 - j\sigma_i^2\right)}{(\sigma_r^2)^2 + (\sigma_i^2)^2} \right) \right| \\
&\qquad |\log(f_Y(y; F_X))| dy, \\
&= \frac{\eta}{\sqrt{2\pi|\sigma_z^2 + \sigma_n^2(z)|}} \int_{-\infty}^{\infty} \left| \exp\left(-\frac{(y-\zeta)^2}{\epsilon} \right) \right| \log(f_Y(y; F_X))| dy, \\
&\leq \frac{\eta}{\sqrt{2\pi|\sigma_z^2 + \sigma_n^2(z)|}} \int_{-\infty}^{\infty} \left| \exp\left(-\frac{(y-\zeta)^2}{\epsilon} \right) \right| [-\log(\gamma(y)) + 2|\log k|] dy, \\
&< \infty,
\end{aligned}$$

where η, ζ, and ϵ are function of $a, b, \sigma_r^2, \sigma_i^2$. The last step follows since we can show the finiteness of the integration as in [35]. Thus, $h(z; F_X)$ can be extended to the complex domain.

APPENDIX D

THE MARGINAL ENTROPY IS AN ANALYTIC FUNCTION ON THE COMPLEX PLANE

In this appendix, we show that the marginal entropy is an analytic function under some restrictions on the noise variance. We assume that the noise variance function $\log(\sigma^2(x))$ can be extended to an open connected set in the complex plane containing the real line. We also assume that the function $\log(\sigma^2(z))$ is analytic over some open connected set on the complex domain excluding some branch cuts .

First, we show that the function $h(z; F_X)$ is continuous on any domain $\mathcal{D}_\delta$. If we can show that there is an integrable function $g : \mathbb{R} \to [0, \infty)$ such that $|P_N(y - z_n, z_n) \log(P_Y(y; F_X))| \leq g(y)$ for any $y \in \mathbb{R}$, and $\int_{-\infty}^{\infty} g(y)dy < \infty$ then we can invoke the Dominated Convergence Theorem to conclude the continuity of $P_N(y - z_n, z_n)$. But we have

$$|P_N(y - z_n, z_n) \log(f_Y(y; F_X))| < |P_N(y - z_n, z_n)| \, |\log(f_Y(y; F_X))| \, . \tag{D.1}$$

Let $\{z_n\}_{n\geq 1}$ be a sequence of complex numbers in $\mathcal{D}_\delta$ converging to $z \in \mathcal{D}_\delta$. Let $z_n = \eta_n + \xi_n$ such that $|\xi_n| \leq \delta$. First, let us write the noise variance as.

$$\sigma_n^2(z_n) + \sigma_z^2 = \sigma_r^2(z_n) + j\sigma_i^2(z_n), \tag{D.2}$$

hence

$$\begin{aligned} \left|\sigma_n^2(z_n) + \sigma_z^2\right| &= (\sigma_r^2(z_n))^2 + (\sigma_i^2(z_n))^2, \\ &\geq (\sigma_r^2(z_n))^2, \\ &= M(\delta). \end{aligned}$$

Now, we have

$$\begin{aligned}
|P_N(y-z_n,z_n)| &= \left|\frac{1}{\sqrt{2\pi(\sigma_z^2+\sigma_n^2(z_n))}}\exp\left(-\frac{(y-z_n)^2}{2(\sigma_z^2+\sigma_n^2(z_n))}\right)\right|,\\
&\leq \left|\frac{1}{\sqrt{2\pi(\sigma_z^2+\sigma_n^2(z_n))}}\right|\left|\exp\left(-\frac{(y-z_n)^2}{2(\sigma_z^2+\sigma_n^2(z_n))}\right)\right|,\\
&\leq \frac{1}{\sqrt{M(\delta)}}\left|\exp\left(-\frac{(y-\eta_n-j\xi_n)^2}{2(\sigma_r^2(z_n)+j\sigma_i^2(z_n))}\right)\right|,\\
&\leq \frac{1}{\sqrt{M(\delta)}}\exp\left(\frac{\xi_n^2\sigma_r^2(z_n)}{2(\sigma_r^2(z_n)+j\sigma_i^2(z_n))}\right),\\
&\leq \frac{1}{\sqrt{M(\delta)}}\exp\left(\frac{\xi^2}{2}\right),\\
&\leq \frac{1}{\sqrt{M(\delta)}}\exp\left(\frac{\delta^2}{2}\right),
\end{aligned}$$

which results in

$$|P_N(y-z_n,z_n)|\,|\log(f_Y(y;F_X))| \leq \frac{1}{\sqrt{M(\delta)}}\exp\left(\frac{\delta^2}{2}\right)\left[-2\log(\gamma(y))+2|\log(k_1)|\right]. \tag{D.3}$$

We can then invoke the Dominated Convergence Theorem to conclude the continuity of $h(z;F_X)$ for any domain $\mathcal{D}_\delta$.

To show that the function $h(z;F_X)$ is analytic on the complex plane, it is sufficient to show that this function is analytic for any $z\in\mathbb{C}$ such that $|z|<\infty$. We assume that the function $\sigma^2(z)$ is analytic, then it is clear the function $P_N(y-z,z)$ is analytic as well. Thus, by invoking Morera's Theorem we have

$$\begin{aligned}
\oint_\omega h(z;F_X)dz &= -\oint_\omega\int_{-\infty}^{\infty} P_N(y-z,z)\log(P_Y(y;F_X))dydz,\\
&\overset{(a)}{=} \int_{-\infty}^{\infty}\log(P_Y(y;F_X))\oint_\omega P_N(y-z,z)dydz,\\
&= 0,
\end{aligned}$$

where the order of integration in (a) is changed using Fubini's Theorem. In order to apply Fubini's Theorem we need to show the finiteness of the whole integration.

Recall that the inner integration is the entropy density $h(z; F_X)$ which was shown to be finite in Appendix C. Now let us define M_ω as

$$M_\omega = \max_{z \in \omega} |h(z; F_X)| , \tag{D.4}$$

and hence

$$\begin{aligned}
\left| \oint_\omega h(z; F_X) dz \right| &= \left| \oint_\omega \int_{-\infty}^{\infty} P_N(y - z, z) \log(f_Y(y; F_X)) dy dz \right| , \\
&\leq \oint_\omega \int_{-\infty}^{\infty} |P_N(y - z, z) \log(f_Y(y; F_X))| \, dy dz, \\
&\leq \oint_\omega M_\omega dz, \\
&\leq M_\omega l_\omega, \\
&< \infty,
\end{aligned}$$

where l_ω is the length of ω which is finite as ω is a closed contour.

APPENDIX E

OPTIMAL POWER ASSIGNMENT FOR THE PARALLEL GAUSSIAN CHANNELS FOR HIGH NOISE LEVELS

In this subsection, we obtain the optimal power assignment for the N parallel Gaussian channels for high noise levels. The channel capacity is the sum of the capacity of the individual channels, i.e., we can write (5.25) as

$$C \geq \max_{\substack{P_i, \ \forall i = 1,2,\cdots,N \\ \mathbf{1}^T\mathbf{P} \leq P_0 \\ 0 \leq P_i \leq A_i^2}} N - \sum_{i=1}^{N} J(P_i). \tag{E.1}$$

We first assume that $P_0 < \sum_{i=1}^{N} A_i^2$, since for $P_0 \geq \sum_{i=1}^{N} A_i^2$, it is straightforward to see that the optimal power assignment policy is $P_i = A_i^2, \quad \forall i = 1, 2, \cdots, N$. For notational simplicity, we define Q_i as

$$Q_i \triangleq Q\left(\sqrt{\frac{P_i}{\sigma_i^2}}\right) \quad \forall i = 1, 2, \cdots, N, \tag{E.2}$$

and $J(P_i)$ as

$$J(P_i) = -Q_i \log Q_i - (1 - Q_i)\log(1 - Q_i) \quad \forall i = 1, 2, \cdots, N. \tag{E.3}$$

Clearly, for the optimal power assignment $\sum_{i=1}^{N} P_i = P_0$. Hence, the Lagrangian of the optimization problem as a minimization of negative of the RHS in (E.1) is

$$L(P_i, \lambda, \nu) = -N + \sum_{i=1}^{N} J(P_i) + \sum_{i=1}^{N} \lambda_i(P_i - A_i^2) - \sum_{i=1}^{N} \lambda_i' P_i + \nu(\mathbf{1}^T\mathbf{P} - P_0). \tag{E.4}$$

The derivative of the entropy term with respect to the power assigned to the channel is

$$\frac{dJ(P_i)}{dP_i} = Q_i' \log\left(\frac{1}{Q_i} - 1\right) \quad \forall i = 1, 2, \cdots, N, \tag{E.5}$$

where

$$\frac{dQ_i}{dP_i} = \frac{-1}{2\sqrt{2\pi P_i \sigma_i^2}} \exp\left(-\frac{P_i}{2\sigma_i^2}\right) \quad \forall i = 1, 2, \cdots, N. \tag{E.6}$$

From the KKT conditions, necessary conditions for optimality are

$$\begin{gathered} \mathbf{1}^T\mathbf{P} = P_0, \quad \lambda_i \geq 0, \quad P_i \geq 0, \quad \lambda_i(P_i - A_i^2) = 0, \quad \lambda_i' \geq 0, \quad \lambda_i' P_i = 0, \\ \nu(\mathbf{1}^T\mathbf{P} - P_0) = 0, \quad \frac{-1}{2\sqrt{2\pi P_i \sigma_i^2}} \exp\left(-\frac{P_i}{2\sigma_i^2}\right) \log\left(\frac{1}{Q_i} - 1\right) + \lambda_i - \lambda_i' + \nu = 0, \quad i = 1, \cdots, N. \end{gathered} \tag{E.7}$$

For simplicity, we define the function $g(P_i)$ as

$$g_i(P_i) = \frac{1}{2\sqrt{2\pi P_i \sigma_i^2}} \exp\left(-\frac{P_i}{2\sigma_i^2}\right) \log\left(\frac{1}{Q_i} - 1\right), \tag{E.8}$$

and write the last condition as

$$g_i(P_i) + \lambda_i - \lambda_i' + \nu = 0, \quad i = 1, \cdots, N. \tag{E.9}$$

We note that

$$\lim_{P_i \to 0} g_i(P_i) = \frac{1}{\pi \sigma_i^2}, \tag{E.10}$$

and

$$\lim_{P_i \to \infty} g_i(P_i) = 0. \tag{E.11}$$

Moreover, it is easy to show that the function $g_i(P_i)$ is monotonically decreasing. Let us assume that the power assigned to the ith channel is P_i^*. Then, there are three possible power assignments, i.e., $P_i^* = 0$ or $P_i^* = A_i^2$ or $0 < P_i^* < A_i^2$. Thus, we have $3^N - 2$ cases to consider (we exclude $P_i^* = 0 \ \ \forall i = 1, 2, \cdots, N$ and $P_i^* = A_i^2 \ \ \forall i = 1, 2, \cdots, N$). For the non-zero power assignments if $P_i^* < A_i^2$, we have $P_i^* = g_i^{-1}(\nu)$.

APPENDIX F

ASYMPTOTIC CAPACITY ACHIEVING DISTRIBUTION OF PEAK AND AVERAGE POWER CONSTRAINED GAUSSIAN CHANNEL IS CONTINUOUS WITH A TRUNCATED GAUSSIAN-LIKE PDF

For a random variable X with a probability density function $f(x)$, $|X| \leq A$ almost surely, and $\mathbf{E}[X^2] \leq P$, we are interested in the probability density function that maximizes the entropy $h(X)$, i.e., we want to

$$\begin{aligned} \text{maximize} \qquad & h(X) = -\int_{-A}^{A} f(x) log(f(x)) dx, \\ \text{subject to} \qquad & \mathbf{E}[X^2] \leq P, \quad \int_{-A}^{A} f(x) dx = 1. \end{aligned} \tag{F.1}$$

The Lagrangian can be written as,

$$u(x,f(x)) = \int_{-A}^{A} f(x) log(f(x))\, dx + \lambda_1 \int_{-A}^{A} f(x)\left(x^2 - P\right) dx + \lambda_2 \int_{-A}^{A} \left(f(x) - \tfrac{1}{2A}\right) dx, \tag{F.2}$$

where λ_1 and λ_2 are the Lagrange multipliers where $\lambda_1 \geq 0$. We can rewrite $u(x, f(x))$ as

$$u(x, f(x)) = \int_{-A}^{A} g(x, f(x))\, dx, \tag{F.3}$$

and

$$g(x, f(x)) = f(x) \log(f(x)) + \lambda_1 x^2 f(x) - \lambda_1 P f(x) + \lambda_2 f(x) - \frac{\lambda_2}{2A}. \tag{F.4}$$

Using the Euler-Lagrange equation from calculus of variations [72], i.e.,

$$\frac{\partial g(x, f(x))}{\partial f(x)} = 0, \tag{F.5}$$

results in

$$\log(f(x)) + 1 + \lambda_1 x^2 - \lambda_1 P + \lambda_2 = 0, \quad \text{for } x \in [-A, A]. \tag{F.6}$$

Then, for the optimal probability density function we obtain

$$f(x) = \exp(-\lambda_1 x^2 + \lambda_1 P - \lambda_2 - 1), \tag{F.7}$$

$$= c_1 \exp(-c_2 x^2), \tag{F.8}$$

for some constants c_1, c_2. We have (since $f(x)$ is a probability density function) $c_1 \int_{-A}^{A} \exp(-c_2 x^2) dx = 1$ and $c_1 \int_{-A}^{A} x^2 \exp(-c_2 x^2) dx = P$, hence we can solve for c_1 and c_2 using

$$c_1 = \frac{1 - 2c_2 P}{2A \exp(-c_2 A^2)}, \tag{F.9}$$

and

$$c_1 \left[\sqrt{\frac{\pi}{c_2}} \text{erf}\left(\sqrt{c_2} A\right) \right] = 1, \tag{F.10}$$

where the error function $\text{erf}(\cdot)$ is defined as $\text{erf}(x) \triangleq \frac{2}{\sqrt{\pi}} \int_0^x \exp(-t^2) dt$. By combining (F.9) and (F.10), the solution for c_2 can be obtained from

$$\frac{1 - 2c_2 P}{2A \exp(-c_2 A^2)} \left[\sqrt{\frac{\pi}{c_2}} \text{erf}\left(\sqrt{c_2} A\right) \right] = 1. \tag{F.11}$$

We can then use in (F.9) to solve for c_1.

APPENDIX G

OPTIMAL POWER ASSIGNMENT FOR THE PARALLEL GAUSSIAN CHANNELS AT LOW NOISE LEVELS

We have shown in Appendix D that the input distribution $f_X(x)$ that maximizes the input entropy $h(X)$ is given by (F.8), (F.9), and (F.11). The corresponding differential entropy is given by

$$h(X) = -\log(c_1) + c_2 P. \tag{G.1}$$

Using (F.9), the entropy of X can be written as

$$h(X) = -\log(1 - 2c_2 P) + \log(2A) - c_2 A^2 + c_2 P, \tag{G.2}$$

where c_2 satisfies (F.11). For simplicity, we refer to the single constant c_2 as c_i for the ith channel in the following.

To find the optimal power assignment at low noise levels, we solve the following capacity optimization problem (assuming that $\sum_{i=1}^{N} A_i^2 \geq P_0$).

$$\max_{\substack{P_i, \quad \forall i = 1, 2, \cdots, N \\ \mathbf{1}^T \mathbf{P} = P_0 \\ 0 \leq P_i \leq A_i^2}} \sum_{i=1}^{N} -\log(1 - 2c_i P_i) + \log(2A_i) - c_i A_i^2 + c_i P_i - \frac{1}{2} \sum_{i=1}^{N} \log(2\pi e \sigma_i^2). \tag{G.3}$$

The Lagrangian of the optimization problem is

$$L(P_i, \omega, \nu) = \sum_{i=1}^{N} \log(1 - 2c_i P_i) - \log(2A_i) + c_i A_i^2 - c_i P_i - \sum_{i=1}^{N} \omega_i' P_i + \sum_{i=1}^{N} \omega_i (P_i - A_i^2) + \nu(\mathbf{1}^T \mathbf{P} - P_0). \tag{G.4}$$

The derivative of the Lagrangian is given by

$$\frac{dL(P_i, \omega, \nu)}{dP_i} = -\frac{2c_i}{1 - 2c_i P_i} - \frac{2P_i \frac{dc_i}{dP_i}}{1 - 2c_i P_i} + A_i^2 \frac{dc_i}{dP_i} - P_i \frac{dc_i}{dP_i} - c_i - \omega_i' + \omega_i + \nu \tag{G.5}$$

where $\frac{dc_i}{dP_i}$ can be found by from (F.11) as

$$\frac{dc_i}{dP_i} = \frac{\pi c_i \left(\operatorname{erf}\left(\sqrt{c_i} A_i\right)\right)^2}{-\frac{\pi}{c_i}\left(\operatorname{erf}\left(\sqrt{c_i} A_i\right)\right)^2 + A_i^3 \sqrt{\pi c_i} \operatorname{erf}\left(\sqrt{c_i} A_i\right) \exp(-c_i A_i^2) + \frac{A_i}{2} \sqrt{\frac{\pi}{c_i}} \operatorname{erf}\left(\sqrt{c_i} A_i\right) \exp(-c_i A_i^2) + A_i^2 \exp(-2c_i A_i^2)}. \tag{G.6}$$

Let us denote $\frac{dc_i}{dP_i}$ by $r(c_i)$. Therefore, we can replace $g(c_i, P_i)$ by $r(c_i)$. Thus,

$$\frac{dL(P_i, \omega, \nu)}{dP_i} = \frac{-2c_i}{1 - 2c_i P_i} - \frac{2P_i r(c_i)}{1 - 2c_i P_i} - A_i^2 r(c_i) + P_i r(c_i) + c_i + -\omega_i' + \omega_i + \nu. \tag{G.7}$$

By applying the KKT conditions, we obtain the following necessary conditions for optimality

$$\omega_i \geq 0,\ \omega_i' \geq 0,\ P_i \geq 0,\ \omega_i' P_i = 0,\ \omega_i(P_i - A_i^2) = 0 \quad i = 1, 2, \cdots, N,\ \ \nu(\mathbf{1}^T\mathbf{P} - P_0) = 0, \tag{G.8}$$

and

$$\frac{dL(P_i, \omega, \nu)}{dP_i} = \frac{-2c_i}{1 - 2c_i P_i} - \frac{2P_i r(c_i)}{1 - 2c_i P_i} - A_i^2 r(c_i) + P_i r(c_i) + c_i - \omega_i' + \omega_i + \nu = 0. \tag{G.9}$$

For simplicity we define the function $w_i(P_i)$ as

$$w_i(P_i) = \frac{2c_i}{1 - 2u^{-1}(P_i)P_i} + \frac{2P_i r(u^{-1}(P_i))}{1 - 2P_i u^{-1}(P_i)} + A_i^2 r(u^{-1}(P_i)) - P_i r(u^{-1}(P_i)) + u^{-1}(P_i). \tag{G.10}$$

For the ith channel, lets assume that the power assigned to this channel is P_i^*. Then, there are three possible power assignments, i.e., $P_i^* = 0$ or $P_i^* = A_i^2$ or $0 < P_i^* < A_i^2$. For the non-zero power assignments, we have $P_i^* = w_i^{-1}(\nu)$, and $\sum_{i=1}^{N} P_i^* = P_0$. The optimal power assignment policy is chosen such that the KKT conditions are satisfied and the channel capacity is maximized [1].

[1] We note that the KKT conditions in this case are necessary but not sufficient.